UNIVERSITY OF CAPE TOWN

FACULTY OF ENGINEERING AND BUILT ENVIRONMENT

Department of Civil Engineering

A Laboratory Investigation on the Shear Strength Characteristics of Soil Reinforced with Recycled Linear Low-Density Polyethylene

Geotechnical Engineering Group

Student: Lita Nolutshungu

Supervisor: Associate Professor D. Kalumba

A thesis submitted in partial fulfilment of the requirement for award of the degree of Master of Science in Civil Engineering / Geotechnical Engineering at the University of Cape town

Feb 2018

PLAGIARISM DECLARATION

1. Plagiarism is to use another's work and to pretend that it is one's own. I know that plagiarism is wrong.

2. I have used the Harvard convention for citation and referencing. Each significant contribution to and quotation in this report from the work or works of the other people has been attributed and has been cited and referenced.

3. This thesis is my own work.

4. I have not allowed and will not allow anyone to copy my work with the intention of passing it off as his or her own work.

Signature: Signed by candidate ………………………………………… Date: 22 October 2018 ……………………………

Student Name: Lita Nolutshungu ………………………………………

DEDICATION

To Kai for his patience, understanding, unconditional love and support…

ACKNOWLEDGEMENTS

I wish to thank the Almighty God for his countless blessings.

My most sincere gratitude for my supervisor, Associate Professor Denis Kalumba, whose support, guidance, constructive criticism and encouragement not only enabled the completion of this research, but also provided opportunity and an environment conducive to me exploring my long term goals.

Undertaking post-graduate studies would not be possible without the financial support and mentorship received from Aurecon South Africa (Pty) Ltd. A special mention to Mr Albertus Geldenhuys, Mr Andries Claasens and Mr Trevor Pape for the guidance and appreciation of the many challenges faced through this research journey.

Many thanks to the following people:

- University of Cape Town laboratory staff, especially Nooredien Hassen, Elvino Witbooi, Tahir Mukaddam and Charles Nicholas.
- Atlantic Plastics Recycling (Cape Town) for providing the material required for this research and the tour of the facility provided by Mr Steven Cheetham.
- The geotechnical group, which included Vincent Oderah, Byron Mawer, Angela Lekea, Dercio Chim Jin, Sam Wegener, Samuel Jjukko, Johnny Oriokot, Dennis Kiptoo, Paul Wanyama, Joanne Ongodia, Yogen Pudaruth, Steven Seymour, Tracey Hill, Motheo Ntsolo, Paul Mavundla, Sanelisiwe Buthelezi, Laxmee Sobhee and Ruben Aza-Gnandji for making the post-graduate journey enjoyable.
- Temba and Nontando Nolutshungu for their unconditional love, support and understanding.
- My friends Sibulele Mvana, Koleka Nolutshungu, Faridah Chebet and Thandekile Dlova for their support and patience.

.

Lita Nolutshungu

ABSTRACT

Since the development of plastics in the 1930's, plastics have increasingly become widely used for packaging in the commercial market place. With this application being for immediate disposal, the amount of plastic waste generated presents a challenge in the disposal thereof. The risks associated with non-biodegradable products on humans and animal life, pressure on existing landfills and the increasing costs thereof have necessitated the development of alternative options for waste management over the years. Research has resulted in various forms of treatments and recycling processes adopted and implemented as environmentally and economically viable solutions. The use of this recycled material in various applications, such as soil reinforcement addresses the need for engineering solutions with a multifaceted approach which strike a balance between environment, economy and equity. This has been the driving force behind research on the use of alternative materials in engineering design.

This study aimed to present an investigation into the use of recycled Linear Low-Density (LLDPE) as reinforcement in Cape Flats sand. To understand the implication of the main aim of the investigation, a review of literature on soil reinforcement theory, various forms of reinforcement material and previous studies was conducted. The selected material for testing was in the form of pellets and flakes produced during the recycling process. Triaxial tests were done on samples where the concentration of the inclusions and compaction effort was varied.

The test data presented showed that both pellets and flakes affected the shear strength by plotting Mohr's circles and the relationship between shear stress and normal stress, which revealed changes in the shear strength parameters. The friction angle was increased by 3.35% at an optimum pellet concentration of 5%. Inclusion of the flakes, however, resulted in a maximum improvement in cohesion of 295% at 0.25% concentration.

A discussion on the stress- strain relationship gave an indication on the effect on the stiffness. This showed that the peak shear stress was reached at higher strains when the flakes and pellets were included, compared to the unreinforced sand. Improvements by up to 25% were recorded from the initial 6% strain at peak shear stress of unreinforced sand.

In concluding the study, Slide7.0 was used to conduct a 2D finite element analysis using Bishop's method to analyse the practical application of LLDPE flakes and pellets for slope stability. The optimum shear strength parameters were used in the model, which resulted in an improved global factor of safety meeting the minimum requirement of 1.25 (South African Institution of Civil Engineers,Geotechnical Division 1993).

TABLE OF CONTENTS

LIST OF FIGURES

LIST OF TABLES

NOTATIONS

Symbol	Unit	Description
ϕ	^{o}	Angle of internal friction
σ	-	Standard deviation
σ_1 or σ_v	kPa	Major principal stress
σ_3 or σ_h	kPa	Minor principal stress
σ_d	kPa	Deviator stress
σ_f	kPa	Normal stress at failure
$\sigma_{f,ult}$	kPa	Ultimate tensile strength of individual fibre
τ_f	kPa	Shear stress at failure
ρ	%	Desired percentage of reinforcement
A	m^2	Area of soil in shear
A_f	m^2	Fibre area
c	kPa	Cohesion
n	-	Sample size
N	-	Population size
S	kPa	Shear strength of unreinforced soil
S_{eq}	kPa	Equivalent shear strength

Symbol	Unit	Description
$S_{eq,p}$	kPa	Equivalent shear strength, governed by pullout
$S_{eq,t}$	kPa	Equivalent shear strength, governed by tensile breakage
t	kPa	Fibre induced tension
t_p	kPa	mobilised tensile strength
t_p	kPa	Fibre-induced distribution tension, failure governed by pullout
t_t	kPa	Fibre-induced distribution tension, failure governed by tensile breakage
w_f	grams	Weight of fibres
W_s	grams	Dry weight of soil
Z	-	Z-score

ABBREVIATIONS

Abbreviation		Description
BPA	-	Bisphenol A
CU	-	Consolidated Undrained
EPS	-	Expanded Polystyrene
HCE	-	High Compaction Effort
HDPE	-	High Density Polyethylene
LCE	-	Low Compaction Effort
LDPE	-	Low Density Polyethylene
LLDPE	-	Linear Low Density Polyethylene
OMC	-	Optimum Moisture Content
PE	-	Polyethylene
PET	-	Polyethylene Terephthalate
PVC	-	Polyvinyl Chloride
PP	-	Polypropylene
PS	-	Polystyrene
SEM	-	Scanning Electron Microscope
UCS	-	Unconfined Compression Strength
UCT	-	University of Cape Town
USCS	-	Unified Soil Classification Systems

1 INTRODUCTION

1.1 Background

Plastics are corrosion-resistant and inexpensive materials whose durability, electrical insulation properties, and potential for diverse applications were used for a variety of products which brought about advances in medical and technological fields, but also presented environmental and waste management problems (Thompson, Moore et al. 2009, Andrady, Neal 2009, Yarsley, Couzens 1945). During the manufacturing process, additives are included to improve the performance of the plastic. These include thermal and ultraviolet stabilisers, plasticizers for pliability, carbon ans silica to reinforce the material, flame retardants and colourings, some of which are potentially toxic and have negative and in some cases life-threatening impact on animals and humans (Koch, Calafat 2009, Meeker, Sathyanarayana et al. 2009, Oehlmann, Schulte-Oehlmann et al. 2009, Talsness, Andrade et al. 2009).

Plastics present a problem for wildlife through entanglement and/or ingestion. According to Gregory (2009), Derraik (2002) and Laist (1997) over 260 species of marine animals have been affected by this, resulting in negative impacts on movement and feeding, a reduction in the number of offspring, lacerations and death. Furthermore, due to their buoyancy, plastic waste accumulates on the sea surface and is sometimes washed ashore as debris on shorelines (Yamashita & Tanimura 2007, Barnes 2002; Gregory 1978) and consequently ingested by seabirds (Ryan, Moore et al. 2009, Van Franeker et al. 2005).

Therefore, practical re-employment of pre-used plastic (as opposed to disposal) would not only have environmental benefits when used in large quantities but could offer a sustainable alternative for soil reinforcement. The use of this material has strongly influenced geotechnical practice primarily in the application of geosynthetics, piping and waterproofing for underground structures. Beyond this, the application of plastics as an alternative material for ground improvement through soil reinforcement is of interest primarily due to the availability of polypropylene plastic bottles, polyethylene plastic bags and plastic packaging materials that are currently filling up disposal sites. Various studies (Wanyama 2017, Pradhan, Kar et al. 2012, Sobhee 2010, O'Rourke, Druschel et al. 1990) have been conducted to investigate the effect of the different types of plastics on the engineering behaviour of soils where the incorporation of these plastics as reinforcement in soil would be expected to increase shearing resistance.

1.2 Problem statement

Soil stability is an area that geotechnical engineers must investigate and provide solutions for potential challenges prior to the construction of any structure. This involves understanding the engineering properties of the soil and knowing which improvement techniques best suit the required outcome. The solution is based on the prediction of load-deformation characteristics and should balance cost and practicality of implementation. Soil reinforcement is one of the techniques that can improve the engineering properties of soil. A possibility for reinforcement is the use of plastic, incorporated in the soil (Babu, Chouksey 2011, Zaimoglu, Yetimoglu 2012, Tang, Shi et al. 2007, Ranjan, Vasan et al. 1994).

According to the Department of Environmental Affairs (2012) South Africa generated approximately 108 million tonnes of waste in 2011. Only 10% of this was recycled and 98 million tonnes of this waste was disposed of at landfills. In 2014, a total of 1.4 million tons of plastic was converted. With this amount in plastic waste, South Africa’s landfills are rapidly getting full and running out of airspace. In an attempt to reduce waste, 20% of the 1.4 million was recycled (Plastics SA, 2015), which eased the pressure on existing landfills. This goes long way to reduction of the greenhouse gases that are created by waste decomposition, as well as pollution created by the chemicals produced when garbage breaks down (leachate) and the chemicals used in the treatment of landfills. The reuse of plastic will address both the need to identify alternative materials for soil reinforcement, as well as alleviate an ongoing environmental challenge.

1.3 Justification

Shear strength evaluation is necessary in soil stability problems such as the provision of adequate slope for embankments, determining the load a soil can carry safely and determining bearing capacity for footings and foundations.

Various studies have been conducted to investigate the effect of using plastics on the engineering behaviour of soils (Benson, Khire 1994, Akbulut, Arasan et al. 2007, Babu, Chouksey 2011, Kalumba, Chebet 2013). They involved various types of plastics such as high-density polyethylene (HDPE), polypropylene (PP) and polyethylene terephthalate (PET). It was found that, in general, the inclusion of these plastics in soils increased the shear and compressive strength of soil. As much as these studies were comprehensive, they were limited to a specific type with little or no reference to other categories or forms of plastics. The purpose of this thesis therefore was to present a comprehensive investigation into the effect of using recycled low-density polyethylene plastic, thereby contributing to the advancement of economic soil reinforcement methods.

1.4 Aim and objectives

The aim of this study was to investigate the effect of randomly distributed inclusions of recycled linear low-density polyethylene (LLDPE) on the shear strength characteristics of soils.

The specific objectives were:

1) Study the effect of varying concentrations of recycled LLDPE on the shear strength of sand
2) Investigate the effect of varying compaction energy on the density of soils containing LLDPE inclusions
3) Make recommendations on the potential use of recycled LLDPE as reinforcement

1.5 Scope and limitations of the study

The study evaluated the shear strength parameters of Cape Flats sand reinforced with recycled LLDPE. These parameters were obtained through triaxial testing on unreinforced soil and soil reinforced with LLDPE at different concentrations and compaction efforts. Moisture effects on the shear strength parameters were excluded from the study by using dry soil. The primary reason is that the plastic material used did not absorb water and thus the physical and mechanical properties were not affected at room temperature under which the laboratory experiments were conducted.

1.6 Thesis outline

Chapter 1 introduces and provides the background and justification for carrying out the research. In chapter 2, reinforcement theory is discussed followed by a review of plastics in Chapter 3. This includes details on the different types of plastics and the recycling process. Chapter 4 presents previous studies that have been undertaken. Chapter 5 details the methodology, including characterization of the materials used in the study. The results and analysis thereof are stated in chapter 6, including practical considerations. The thesis ends with conclusions and recommendations for future research in chapter 7.

2 SOIL REINFORCEMENT

2.1 Introduction

This chapter contains information obtained from literature which is relevant to this study. It starts with a background of soil reinforcement, provides insight on the theory of reinforcement and the factors that affect the performance of reinforcement. Further to this, the different types and forms of reinforcement, as well as placement thereof, are presented in the review.

2.2 Background

It has always been a challenge for civil engineers to find ways to improve the properties of soil. The principles in reinforced soils have been used for many centuries for soils with poor mechanical properties (Swami 2010). The improvement can be done through soil stabilisation and/or soil reinforcement. Soil stabilisation is the process of mixing a binding agent, such as lime, cement or bitumen, to bind the soil particles. This process improves the engineering properties of soils but reduce permeability and compressibility. Soil reinforcement, on the other hand, is the inclusion of reinforcing elements (such as strips, bars or fabrics) of certain materials, such as metal, wood, polymer and plastic, to improve the mechanical properties of soils. The various methods of soil reinforcement are classified as illustrated in Figure 2-1.

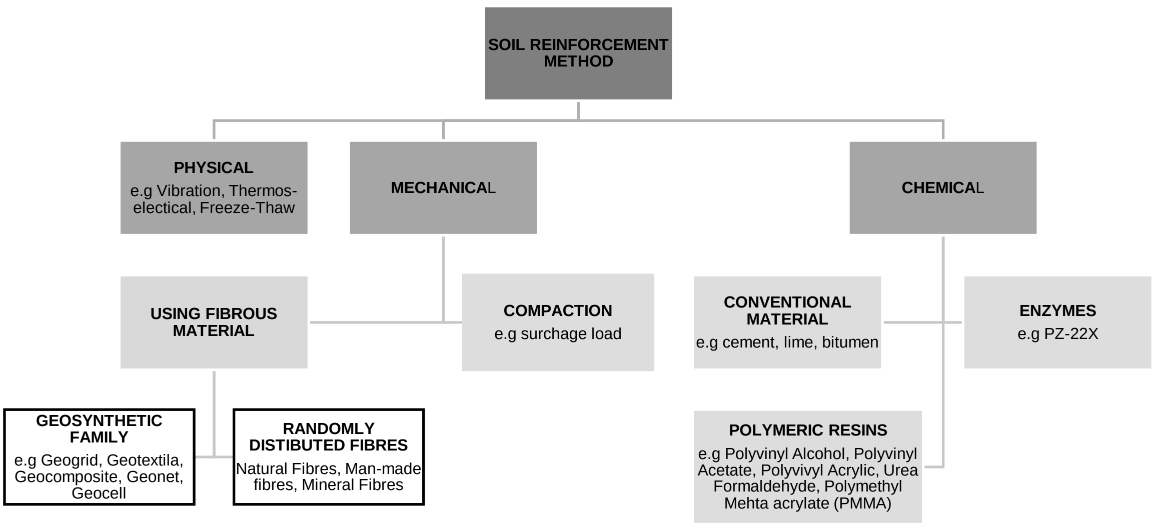

Figure 2-1: Different methods of soil reinforcement adapted from Hejazi et al. (2012)

2.3 Soil reinforcement theory

Earth materials, such as sand and silts, are made up of particles which are not cemented and reinforcement is made of elements which are elongated. The inclusion of these reinforcing members causes soils to exhibit some cohesion. This cohesion is as a result of the friction between the reinforcing element and the soil particles. These frictional forces transmitted between the particles and reinforcement result in true cohesion in the whole mass and increased resistance which may be due to soil particles locking into the reinforcing element in certain cases (Vidal 1969). Furthermore, as a load is introduced to a reinforced mass of soil, tensile forces are introduced to the reinforcement. This results in an increased friction angle. In reinforcement with high tensile resistance, the increase in friction angle is enhanced. The tensile force is the resultant of the two components. The first is a normal force which acts perpendicular to the shear plane, increasing the confining stress resulting in increased shear resistance and volume change as the soil grains are compressed towards each other. The second component of the tensile force is tangential to the failure plane, which offers direct resistance to a shearing force (Gray, Ohashi 1983).

Looking at a mass of reinforced soil as a whole, it exhibits cohesion in all directions (Vidal 1969). The implication herein is that design and placing of reinforcement are important as they determine resistance against shearing and sliding. Most importantly, the stresses developed in the reinforcement depend on the total contact between the soil particles and the reinforcement. It is important therefore to establish proper contact between the reinforcement and soil particles, as illustrated in Figure 2-2.

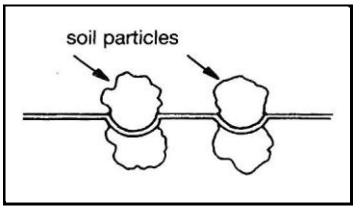

Figure 2-2: Schematic diagram of contact between soil particles and reinforcement (Gray, Ohashi 1983)

The contact between soil particles and reinforcement is important because reinforcements should intersect potential failure surfaces in the soil in order to be effective (Miraftab, Lickfold 2008). This is so that the reinforcement is placed so that the friction, which is the main cause of the reinforcing action, is generated with minimal or no sliding effect between the soil and reinforcement.

2.4 Classification of reinforcement materials

Two types of reinforcing materials exist. These are extensible reinforcement and inextensible reinforcement (Bonaparte, Holtz et al. 1987, Pokharel 1995). The role and function, as well as the expected stress-strain behaviour, of each type is detailed in Table 2-1.

Table 2-1: Role, function and behaviour of the two classes of reinforcement (McGown, Andrawes et al. 1978, Swami 2010)

Type of reinforcement	Role and function	Stress-strain behaviour
Extensible	Increases ductility (extensibility) and results in smaller losses after maximum strength is attained compared to unreinforced soil	Inclusion cannot rupture, regardless of strength and imposed loads. i.e. inclusions have greater strain resistance compared to maximum tensile strains in soils without inclusions
Inextensible	Increase shear resistance of soil, inhibits deformations. Catastrophic failure and collapse of soil can occur if reinforcement breaks.	The possibility of rupture exists with this type of reinforcement, dependent on the ultimate strength of the inclusions. This means that this type of reinforcement may have rupture strains less than the maximum tensile strain in the soil with no inclusions.

2.5 Factors affecting behaviour and performance of reinforced soil

When reinforcement is included in soil it changes the normal pattern of strain that would develop if the soil were not reinforced and limits the formation of rupture surfaces throughout the soil. This results in improved stiffness and strength, as exhibited in Figure 2-3.

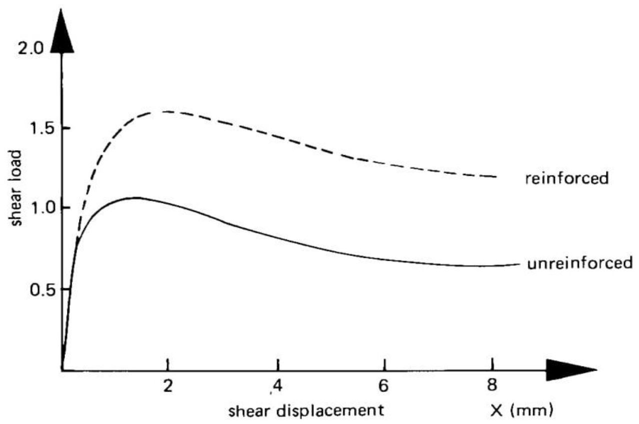

Figure 2-3: Load displacement results reflecting higher shear loads for reinforced soil (Jewell 1980)

Although there is an improvement in strength, there are certain factors relating to the reinforcement material that influence the behaviour and performance of reinforced soil.

2.5.1 Form and surface properties

The most common forms of reinforcement are bars, strips/sheets, grids and anchors as shown in Figure 2-4 (a) to (d), respectively.

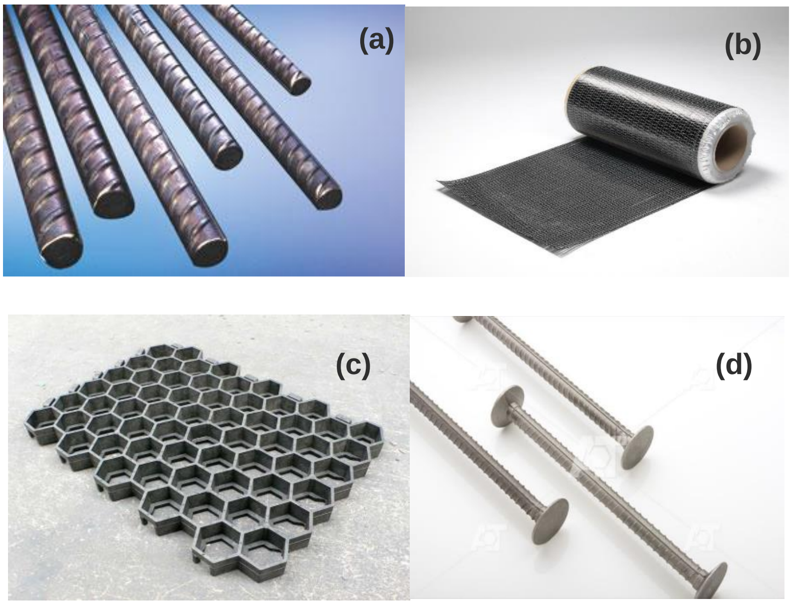

Figure 2-4:Reinforcement (a) steel bars (Liberty Onesteel Reinforcing 2016), (b) carbon fibre sheet (S&P Reinforcement International 1999), (c) recycled plastic grid (Kedel 2014) and (d) anchors (Ankertechniek 2016)

In order for the reinforcement to improve the performance of the soil it must be shaped such that any deformations in the soil would produce strain in the reinforcement. With the introduction of loads on soil, there is heavy reliance on friction for the development of bonds between the reinforcement and the soil. The frictional resistance available for bars and strip/sheet is illustrated by Figure 2-5.

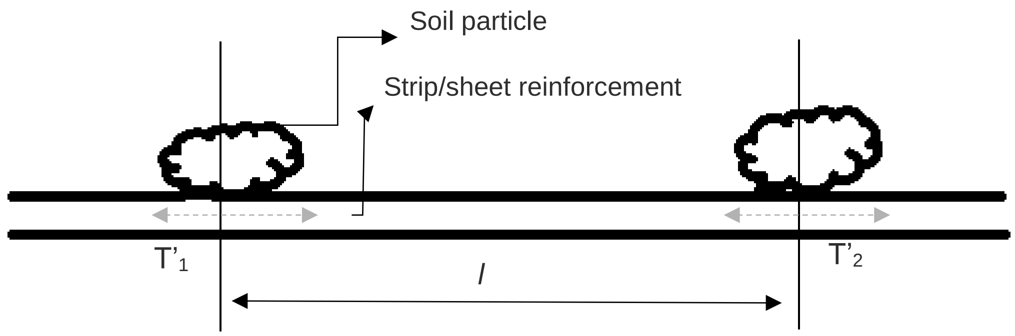

Figure 2-5: Adhesion development on strip/sheet reinforcement adapted from Jones (1996)

The adhesion/bond developed (T_{ad}) is the difference of the tension between the two soil particles (T'_1-T'_2). Using a strip/sheet with length *l*, width *B* and under normal stress σ_v, the force acting on the reinforcement can be represented as $\sigma_v lB$ (stress x area). With this occurring on both sides and the coefficient of friction between the soil and reinforcement represented by μ, the tensile force generated in the strip/sheet is represented by:

$$T_{ad} = 2 \times \sigma_v lB\mu \quad [2\text{-}1]$$

Therefore, to avoid slippage, the coefficient of friction should exceed the tensile force generated in the strip/sheet (Jones 1996):

i.e. $\mu > \frac{T_{ad}}{2\times\sigma_v lB}$ [2-2]

This is a critical property for these types of reinforcements as the higher the coefficient of friction, the more efficient the reinforcement (Jones 1996, Schlosser, Elias 1978). This implies that a rough surface would perform significantly better than reinforcement with a smooth surface, as seen in Figure 2-6.

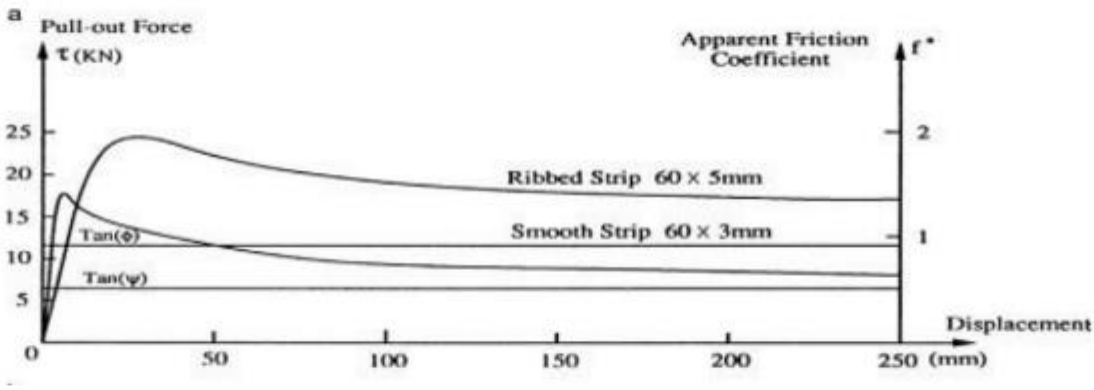

Figure 2-6:Influence of reinforcement surface (Schlosser, Elias 1978)

With the tension introduced in the reinforcement, the stiffness has influence in the performance and has been shown to be of particular importance where reinforcements are used as tension membranes over soft soils (Jones, Zakaria 1994). Figure 2-7 illustrates the difference by comparing the stress-strain response of extensible (stiff) and inextensible (very low stiffness) reinforcement. The use of inextensible reinforcements results in a linear relationship. However, extensible reinforcement reflects a maximum load capacity which is related to the peak shear strength of the unreinforced soil. The inclusion of this reinforcement thus results in improved strength at the same strain.

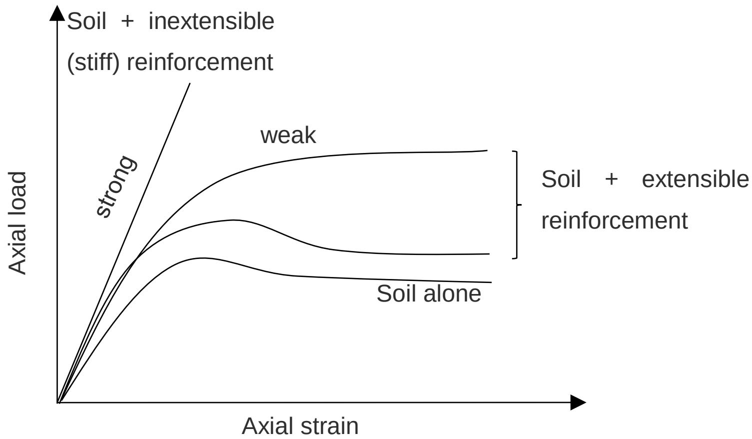

Figure 2-7: Load-strain relationship of soil and soil reinforced with extensible and inextensible material (McGown, Andrawes et al. 1978)

In the case of the grid, the bond is provided through the interlocking of the soil (or the development of an abutment in anchors) and as a result tests for the pull-out (slippage) resistance have been conducted by researchers (Koerner 1986, Hayashi, Yamanouchi et al. 1985, Johnston 1985, Rowe, Ho et al. 1985, Farrag, Acar et al. 1993, Ingold 1983, Jewell 1980).

The application of a pull-out force being transmitted from one end to the other end of a geogrid results in displacement of the grid junctions. Quantitative data measuring the pull-out resistance and displacement of each junction in sand was used by Ochiai et al. (1996) to analyse the interaction and mechanism of the reinforced mass. Resistance was determined using the applied pull-out force (F_i) and the junction displacements (X_i). The strain in the grid was calculated using the following equation:

$$\varepsilon_{i,i+1} = \frac{X_i - X_{i+1}}{d} \quad [2\text{-}3]$$

Where: i is the ith grid junction

$i+1$ is the adjacent junction

d is the distance between two adjacent junctions

Plotting the pull-out force ($F_{i,i+1}$) against the strain ($\varepsilon_{i,i+1}$) at each junction yielded an index curve as shown in Figure 2-8(a) which show that equal increases in the applied force result in incremental increases in the strain. This test was done on geogrids with different width of ratios (B/B_o) of 1.0, 0.7 and 0.4, where:

B = geogrid width

B_o = pull-out box width.

The pull-out force (used to determine resistance) was then plotted against the displacement for each width ratio as depicted in Figure 2-8 (b) which indicates the influence of width in geogrids. A smaller grid width, resulting in a lower width ratio, requires a higher pull-out force for the same displacement. This means that the pull-out resistance increases with grid width, which is consistent with results obtained by Jewell (1980).

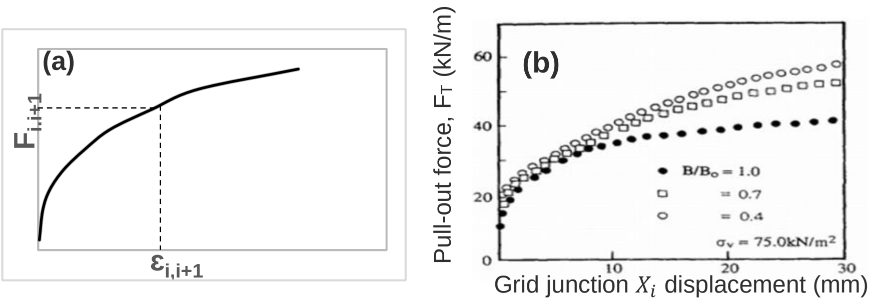

Figure 2-8: (a) Force and strain index curve (b) Geogrid width influence on performance; (Ochiai, Otani et al. 1996)

This highlights the importance of dimensions in the effectiveness of reinforcements, which applies for strips as well. Results obtained by Bacot et al. (1978) in investigating the effects of strip width and length showed that the relationship between width and the coefficient of friction is exponential, shown in Figure 2-9 (a), as opposed to linear with length (Figure 2-9(b)).

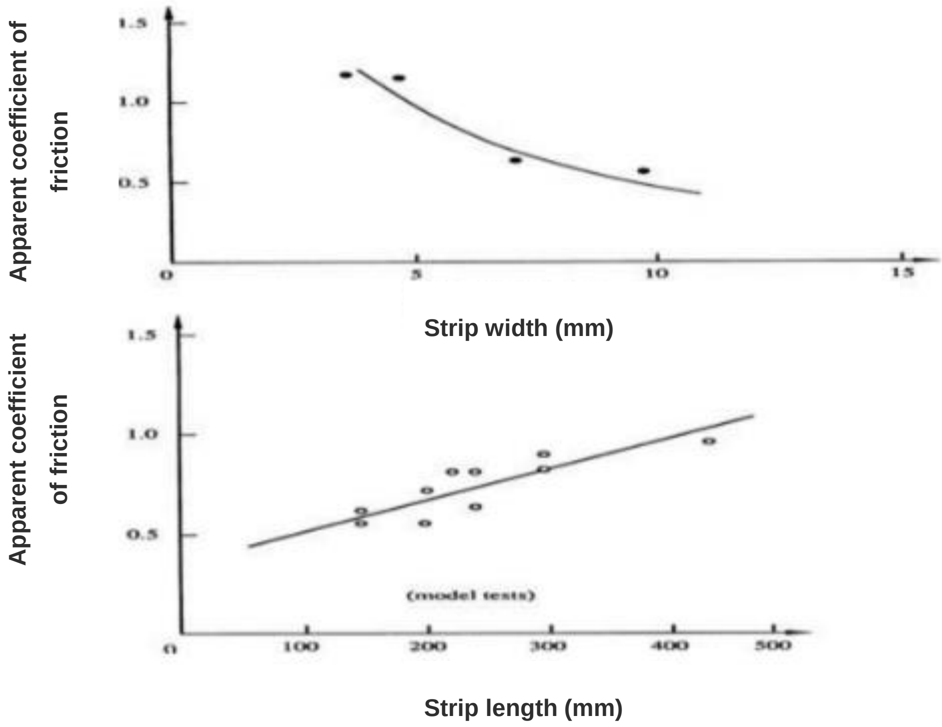

Figure 2-9: Variation of apparent coefficient of friction with (a) strip width and (b) strip length (Bacot, Iltis et al. 1978)

2.5.2 Placement and Distribution

Ideally, reinforcement should be positioned in the location of maximum tensile strain (Jones 1996, Jewell 1980), which requires establishing all potential failure mechanisms and planes, together with the associated strain fields. Changing this direction, to that of compressive strain, would reduce effectiveness as tensile reinforcement and change it to compressive strain reinforcement. If the orientation is along the zero extension direction, the strength may revert to the same as though it were not reinforced (Palmeira, Milligan 1989, Jewell 1980). This is illustrated in Figure 2-10, where $\theta°$ is the orientation of the reinforcement.

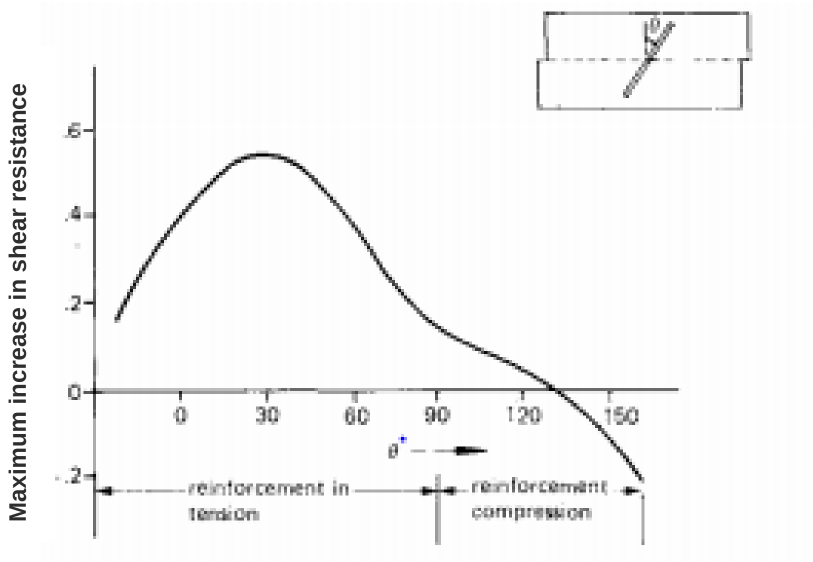

Figure 2-10: Effect of orientation on shear strength (Jewell 1980)

This is mainly applicable to designing structures. When working with soils predetermination of the failure plane is not always possible and it may therefore be best to reinforce the soil as an entire mass, as opposed to localised reinforcement. This can be done systematically or by random mixing of the soil with strips and/or fibres (Shukla, Sivakugan et al. 2009), which can be done during the construction phase (Jewell, Pedley 1990). Figure 2-11 is a graphical illustration of systematic placement of reinforcement.

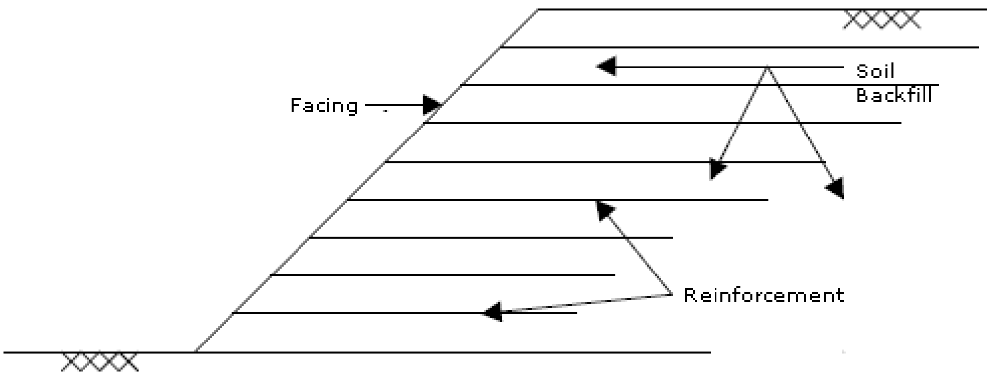

Figure 2-11: Systematic reinforcement of soil slope (Landtek Design Build Inc 2015)

This method of placement is mostly used for inextensible reinforcement material such as steel but can be used in placing of geosynthetic material for reinforcing embankments (Saran 2010). A disadvantage of this method of placement is the introduction of planes of weakness, evidence of which has found in the rupture of geosynthetics in a direction parallel to the shear plane (Koerner 2012).

The random placement method involves random mixing of reinforcement in a certain proportion to the soil and then compacted to the desired density. The advantage to this method of placement is that the end result is a relatively homogenous soil-fibre composite. With this high probability in homogeneity, the isotropy of the soil is maintained compared to systematic placement which introduces potential failure planes (Maher, Gray 1990, Saran 2010). Polypropylene fibres and their appearance when randomly mixed with soil are shown in Figure 2-12.

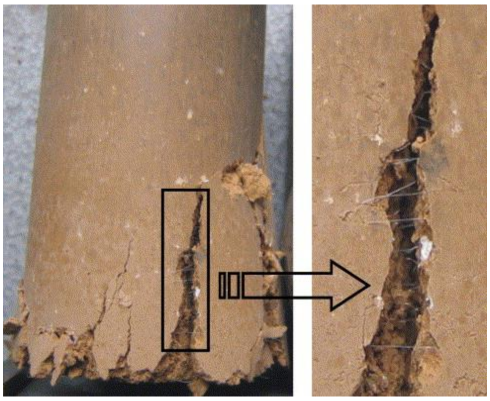

Figure 2-12: Soil reinforced with randomly distributed polypropylene fibres (Tang, Shi et al. 2007)

Further to this, spacing is another factor that influences reinforcement effectiveness. Smith (1977) and Jewel (1980) established through laboratory testing that the spacing between reinforcing elements affects the performance of individual members. It was found that as the spacing reduces, so does the increase in shear strength contributed by each member as shown in Figure 2-13. This is however, dependent on the ratio of spacing to the length of the reinforcement extending away from the soil failure plane, represented by S and L_R respectively (Jones, Zakaria 1994). A desired ratio is where the length of the reinforcement is longer than the spacing. In other words, a critical ratio of $S/L \geq 1$ to avoid the influence of each reinforcing element being diminished (Jewell 1980, Smith 1977).

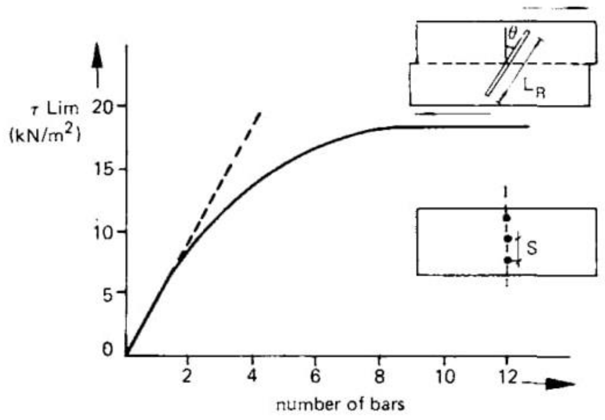

Figure 2-13: Influence of reinforcement spacing (Jewel 1980)

2.6 Reinforcement Mechanisms

Starting with the assumption that unreinforced soil is homogenous and isotropic, the inclusion of reinforcement may either make the soil anisotropic (systematic placement) or could maintain the isotropy (random distribution) (Lin 2005, Shukla, Sivakugan et al. 2009). The mechanism is best explained by the diagram in Figure 2-14. This is an illustration of a soil mass which is axially loaded (σ_a) with confining pressure (σ_b).

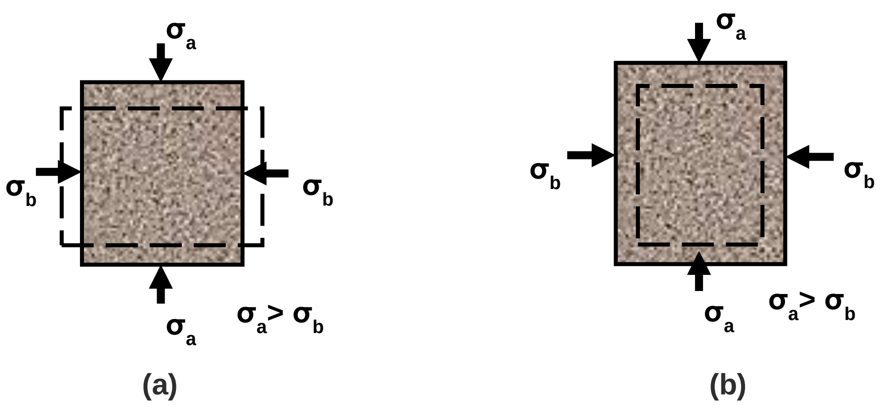

Figure 2-14: Reinforcing mechanism concept model for (a) unreinforced soil (b) reinforced soil

The conceptual deformations that would occur are illustrated in Figures 2-14 (a) for unreinforced soil, compared to the deformations (if any) that could be expected from soil reinforced with randomly distributed elements (b).

The inclusion of reinforcement in soil introduces surface friction and interlocking between the soil particles and the material. The friction increases resistance to the mechanical sliding and rolling over effects between soil particles, whereas the interlocking bonds mobilise the tensile strength of the reinforcing element and thereby absorb some of the stress transferred to the soil from loading. This reduces deformation in all directions. It can therefore be said that randomly distributed reinforcements serve as friction and tension resistance elements to the principal pressures in the Mohr-Coulomb envelope (Lin 2005, Shukla, Sivakugan et al. 2009). It was further observed by O-Rourke, Druschel and Netravali (1990) that hardness of the reinforcing element has an inverse relationship with frictional strength due to the mechanism of shear transfer. The smoother and harder the reinforcing element, the more it promoted sliding of the sand grains, whereas soft surfaces would promote particle rolling, as illustrated in Figure 2-15.

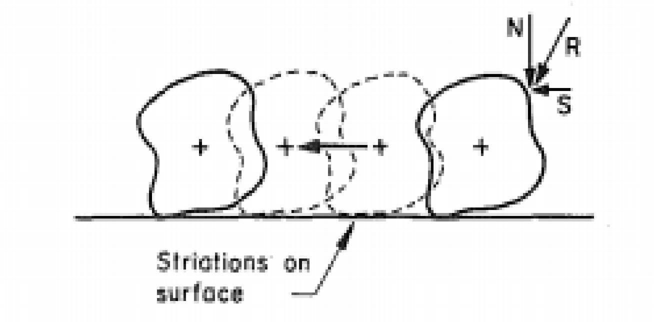

(a) Rigid reinforcement: skidding effect

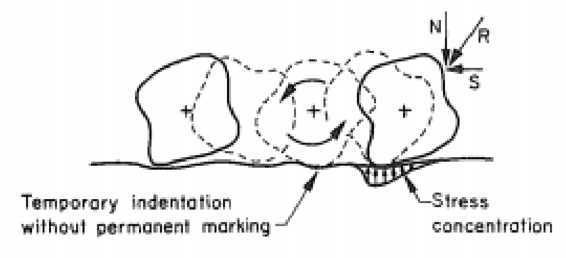

(b) Soft reinforcement: rolling effect

Figure 2-15: Comparison of shear transfer mechanism of rigid and soft reinforcement (O'Rourke, Druschel et al. 1990)

There was further indication from studies conducted that the shear strength of reinforced soil is linearly related to the percentage of reinforcement in the shear zone (Benson, Khire 1994, Gray, Ohashi 1983). This is because the increase in shear strength in the shear zone was attributed to the tension in the reinforcing element during shearing developing as a result of the element being anchored in the soil outside the shear zone as depicted in Figure 2-16. It was this tension that contributed to the increase in shear strength.

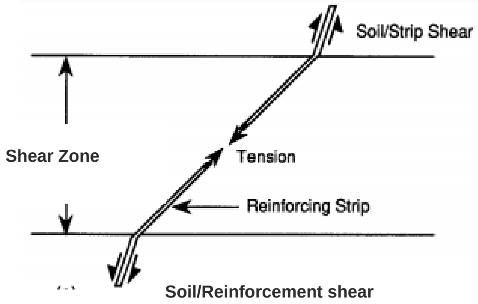

Figure 2-16: Anchoring in reinforcement mechanism (Benson, Khire 1994)

Other studies undertaken provided insight into the shear mechanism using the Mohr-Coulomb failure criterion. Triaxial compression tests conducted on sand by Maher and Gray (1990), Zornberg (2002) and Consoli et.al (2007), using various forms of extensible reinforcement in the form of fibre, resulted in an analysis which found a curved or bilinear principal stress envelope reflected by a threshold confining pressure as shown in Figure 2-17.

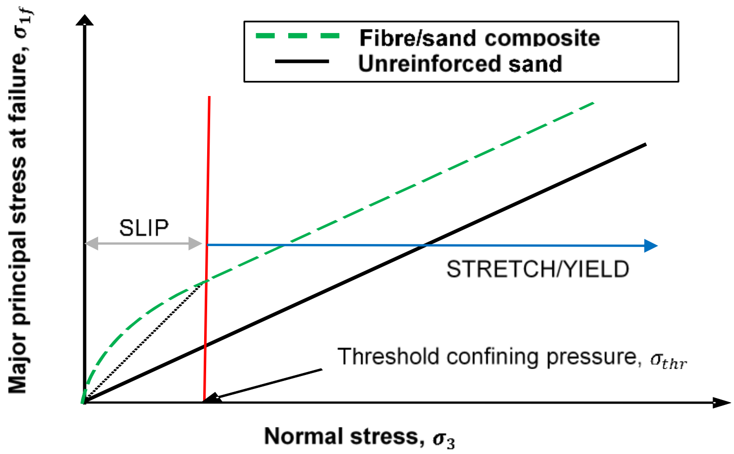

Figure 2-17: Fibre reinforced sand model failure envelope from triaxial tests (Maher, Gray 1990)

Before reaching the threshold confining pressure, the reinforced soil exhibited higher friction angles which are indicative of improved slip and pull. This is reflected by the curve in Figure 2-17. Beyond the threshold pressure, the shear strength envelope shows a linear relationship between major principal stress and normal stress, parallel to the unreinforced sand. At this point stretching and yielding of fibre occur. The curvilinear and linear failure envelopes were further demonstrated by direct shear tests conducted by Nataraj and McManis (1997) on clay, using randomly distributed fibrillated (network) fibres (polypropylene). At lower pressures, the graph was curved, but was linear at higher pressures as shown in Figure 2-18. The curvilinear envelope depicts the shear strength envelope of soil reinforced with extensible reinforcement.

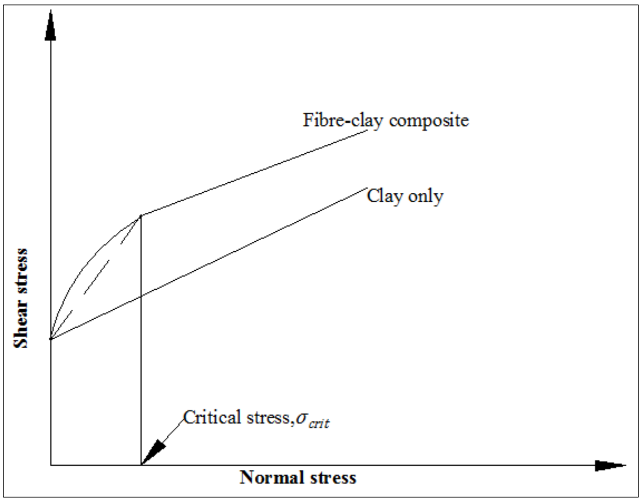

Figure 2-18: Fibre reinforced clay model failure envelope from direct shear tests (Nataraj, McManis 1997)

2.7 Determining the shear strength of reinforced soil composite

The equivalent shear strength of reinforced composites can be defined as a function of the reinforcement-induced distributed tension, t, (Maher & Gray 1990, Gregory & Chill 1998). An assumption is made that this tension is parallel to the shear plane, as shown in Figure 2-19.

Based on this assumption of parallelism, the normal stress acting on the shear plane is not affected by the reinforcement-induced tension. The shear stress (τ) of the reinforced soil is therefore a summation of the shear strength of the unreinforced soil (τ_s) and the reinforcement-induced tension (t).

$$\tau = \tau_s + t \qquad [2\text{-}4]$$

In the absence of parallelism, the direct contribution of this tension to shear strength would be reduced. However, the perpendicular component would increase normal strength which would result in an increase in the soil shear strength.

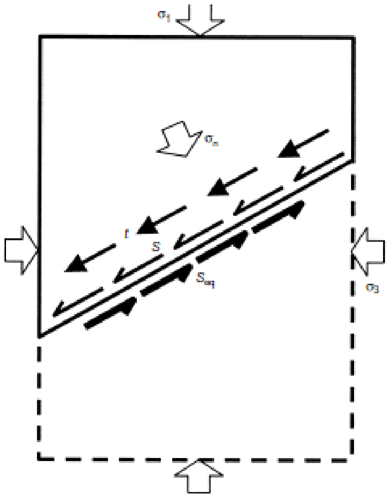

Figure 2-19: Schematic representation of the shear strength in a triaxial fibre-reinforced specimen (Zornberg 2002)

In the case where the average normal stress is lower than the threshold stress ($\sigma_{n,ave} < \sigma_{n,crit}$), the failure is governed by fibre pull-out. In this instance, the shear strength equation is:

$$\tau_p = \tau_{s,p} + t_p \quad [2\text{-}5]$$

The determination for reinforcement induced tension when failure is governed by fibre pull-out is given by Zornberg (2002), using a discrete approach, as:

$$t_p = \alpha \cdot \beta \cdot \omega \cdot (c_{i,c} \cdot c + c_{i,\varphi} \cdot tan\ \varphi \cdot \sigma_{n,ave}) \quad [2\text{-}6]$$

Where: φ is the soil friction angle,

α is the empirical coefficient accounting for accounting for the direction of the reinforcement-induced tension (assumed to be 1 for random distribution),

β is the reinforcement aspect ratio, and

ω is the volumetric reinforcement content

$c_{i,c}$ is the interaction coefficient of cohesive component of interface shear strength ($c_{i,c} = \frac{a}{c}$)

$c_{i,\varphi}$ is the interaction coefficient of frictional component of interface shear strength ($c_{i,\varphi} = \frac{\tan\delta}{\tan\varphi}$)

Combining equations [2-2] and [2-3] and assuming a linear failure envelope gives the equation for shear strength, when failure is governed by fibre pullout, as:

$$\tau_p = (c + \sigma_n \cdot \tan\varphi) + (\alpha \cdot \beta \cdot \omega \cdot c_{i,c} \cdot c + \alpha \cdot \beta \cdot \omega \cdot c_{i,\emptyset} \cdot \tan\varphi \cdot \sigma_{n,ave}) \qquad [2\text{-}7]$$

Because of the random orientation of the reinforcement, the average normal stress acting on the elements is not necessarily equal to the normal stress. Sensitivity evaluation conducted by Zornberg (2002), however, indicated that an assumption can be made that they are equal because equivalent shear is not very sensitive to the difference. The final equation when normal stress is below critical stress therefore becomes:

$$\tau_p = c_p + \sigma_n \cdot (\tan\varphi)_p \qquad [2\text{-}8]$$

Where $\quad c_p = \left(1 + \alpha \cdot \beta \cdot \omega \cdot c_{i,c}\right) \cdot c$

$$(\tan\varphi)_p = (1 + \alpha \cdot \beta \cdot \omega \cdot c_{i,c}) \cdot \tan\varphi$$

When normal stress is above critical stress ($\sigma_{n,ave} < \sigma_{n,crit}$), where failure is governed by tensile breakage, then the equivalent shear strength can be determined by

$$\tau_t = c_t + \sigma_n \cdot (\tan\varphi)_t \qquad [2\text{-}9]$$

Where: $\quad c_t = c + \alpha \cdot \omega \cdot \sigma_{f,ult}$

$$(\tan\varphi)_t = \tan\varphi$$

An approach different to the above statistical model defined by Zornberg (2002), was a mechanical model from Gray and Ohashi (1983) and Maher and Gray (1990) based on direct shear tests. An assumption was made that the shearing action causes reinforcement to distort at specific angles (θ , ψ), whether it is placed vertically or inclined (Figure 2-20 (a) and (b)).

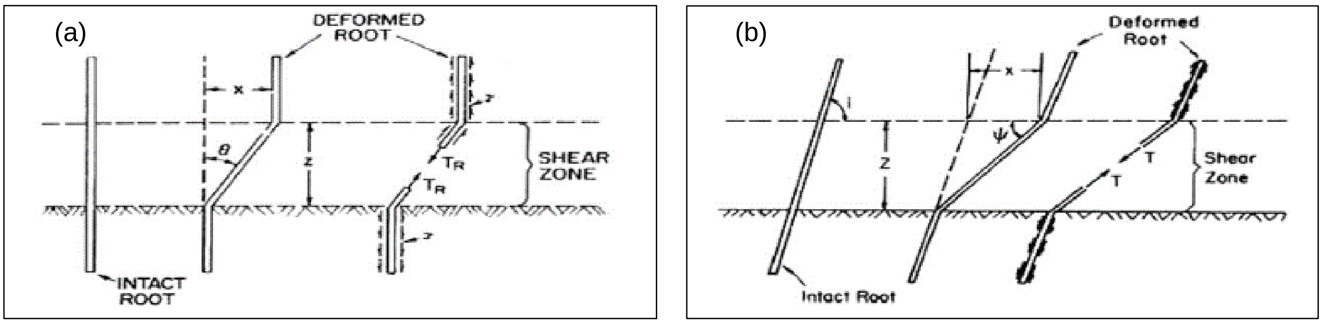

Figure 2-20: Mechanical Model (a) vertically placed fibre reinforcement (b) inclined fibre reinforcement (Gray & Ohashi, 1983)

Further assumptions made were relating to the length of the reinforcement and that it was long enough to extend to both sides of the failure plane, thus avoiding pull-out failure. The resultant tension was therefore due to reinforcement modulus (E_r), interface friction (φ_r), reinforcement diameter (d_r) and shear zone thickness (z). The relationship is such that:

$$\sigma_t = \left[\frac{4E_f\varphi_r}{d_r}\right]^{1/2}(z\{\sec\theta - 1\})^{1/2} \qquad [2\text{-}10]$$

In the case where fibres are perpendicular to the shear plane (Figure 2-20(a)), the increase in shear strength ($\Delta\tau$) is given by equation 2-11:

$$\Delta\tau = t_t(\sin\theta + \cos\theta\tan\varphi) \qquad [2\text{-}11]$$

Where the mobilised tensile strength per unit area is calculated as follows:

$$t_t = \left(\frac{A_r}{A}\right)t \qquad [2\text{-}12]$$

In the case where reinforcement is inclined (Figure 2-20(b)), the increase in shear strength ($\Delta\tau$) is determined as follows:

$$\Delta\tau = t_t\left[\sin\left(90 - \Psi\right) + \cos\left(90 - \Psi\right)\tan\varphi\right]$$

[2-13]

Where: $\Psi = \tan^{-1}\left[\frac{1}{k+(\tan^{-1} i)^{-1}}\right]$

with i as the initial orientation angle of the fibre and k as the shear distortion ratio given by:

$$k = \frac{x}{z} \qquad [2\text{-}14]$$

where x is the horizontal shear displacement as shown in Figure 2-20.

Both the mechanical and discrete models allow for the determination of the shear strength. In studying the soil properties, including shear strength, certain variables can affect the behaviour of soil reinforced with extensible reinforcement. Studies carried out by Gray and Ohashi (1983) found that the increase in shear strength of these reinforced soil composites was directly proportional to the reinforcement area ratio and concentration up to 1.7%, and the maximum increase is when reinforcement is at 60% orientation to the shear plane (determined with direct shear tests). Other studies using various testing methods have been conducted on reinforced soils to determine what the other factors influence the behaviour. These are discussed in detail in chapter 4.

3 SOIL REINFORCEMENT MATERIALS

3.1 Introduction

This chapter focuses on materials that can be used for reinforcement. It highlights the origin, manufacturing, structure and resultant properties which indicate the expected behaviour in a reinforcing model. The chapter ends with a discussion on the treatment processes of plastic recycling.

3.2 Materials classification

Reinforcement materials are broadly categorised into either natural or synthetic materials. The natural types are those that can be extracted from naturally existing sources, such as coir from coconut trees. Synthetics are man-made materials such as plastics.

3.2.1 Natural fibres

Natural fibres are readily available and environmentally friendly which makes them a viable option for use as reinforcement. More than this, the advantages of using natural fibres are stated by Merandi et al (2008) as:

1) Ease of placement: Materials do not require specialised equipment for placing. Conventional mixing equipment can be used.
2) Achieving homogeneity: Homogenous mix can be attained, maintaining isotropic properties.
3) Construction ability: Construction is not limited by weather conditions except in cases where care has to be taken due the ability of natural fibres to absorb moisture.

A few examples of fibres, brief description thereof, their use and reason for use is given in Table 3-1. These natural materials are plant dry matter referred to as lignocellulose, which is made up of lignin and cellulose, as indicated in the name. Lignin is a hydrocarbon polymer which provides rigidity in the plant, and although lignin itself is hydrophobic, the stiffening it provides assists cells to withstand changes in water pressure as the water moves through the plant (Myburg, Lev-Yadun et al. 2013). Cellulose is also a polymer composed of hydroxyl groups which result in hydrogen bonds that give resistance to hydrolysis, alkali and oxidising agents, but degradable in chemical solutions (Azwa, Yousif et al. 2013). It is these bonds and the resultant crystalline structure that give cellulose tensile strength.

Table 3-1:Examples of natural fibres used for reinforcement (Prabakar, Dendorkar et al. 2004, Sivakumar, Vasudevan 2008, Maliakal, Thiyyakkandi 2013)

FIBRE	DESCRIPTION	USE	EXPLANATION
Coir	Obtained from the seeds of coconut trees	Reinforcement	Improved stress-strain response
		Erosion control	Offers better moisture resistance than most fibres
Bamboo	An extraction from bamboo pulp	Reinforcement	High tensile strength
Sisal	Extracted from sisal leaves	Reinforcement	High tensile strength
Cane	From sugarcane	Reinforcement	Increased shear strength

The rigidity from the lignin and tensile strength from the cellulose make plant material viable for use as reinforcement, but the overall mechanical properties depend on the structure, cell dimensions, microfibrillar angle (the angle between the axis and microfibils as shown in Figure 3-1) and the chemical composition (Hearle 1963, Bledzki, Gassan 1999, John, Thomas 2008). According to Mohanty et al. (2000) and Azwa et al. (2013) the microfibrillar angle determines the stiffness of the material. Their research indicated that the smaller the angle the stiffer the material and consequently enhances the mechanical properties.

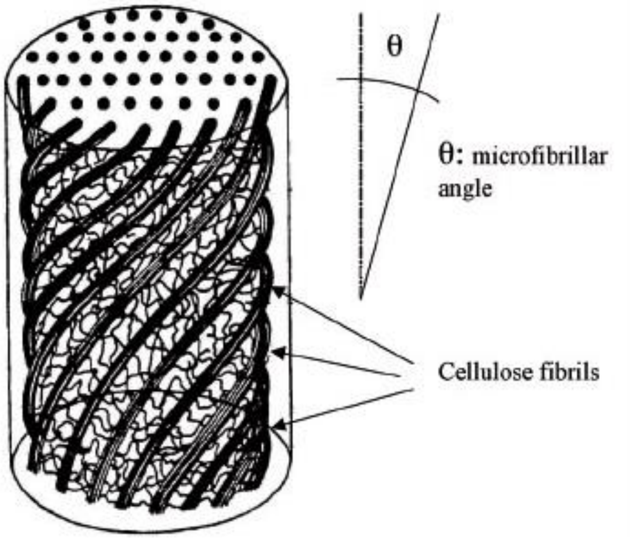

Figure 3-1: Microfibrillar angle for a single fibre of plant material (Baley 2007)

It cannot be ignored, however, that the performance of soil reinforced with natural materials can be compromised by moisture absorption and ultraviolet exposure (Li, Zornberg 2012). The water decreases interface friction in the reinforced composite between the reinforcement and the soil, whereas ultraviolet exposure leads to lignin degradation.

Studies have been conducted on natural materials which indicate viability of use as reinforcement. One example is coir fibre from coconut fruit. Coir is made up mainly of lignin, cellulose, pectin, tannin and other substances which are water soluble but because of its high lignin content it retains 80% of its tensile strength when wet for a period of 6 months (Sivakumar, Vasudevan 2008, Hejazi, Sheikhzadeh et al. 2012). This makes it suitable for temporary reinforcement only. It was also found that the compressive strength of coir reinforced soil increases with a coir percentage increase up to 1% content (Ravishankar, Raghavan 2004, Chauhan, Mittal et al. 2008). Another natural material strong in tension found to increase unconfined compressive strength is bamboo (Swamy 1984, Mustapha 2008, Kozlowski 2011).

Research conducted on Sisal by Prabakar and Sridiar (2002) using 0.25%, 0.5%, 0.75% and 1% concentration levels with different lengths ranging from 10mm to 25mm produced a non-linear relationship with shear stress up to the 20mm length, but decreases in shear strength were evident for concentrations beyond 0.75%.

3.2.2 Synthetic materials

Synthetic materials are those which are manmade from plastics (scientifically referred to as polymers) such as polyester, polypropylene, polyterephthalate, polyethylene etc. For purposes of this review these materials have been categorised under two broad categories: geosynthetics and plastics (which relates to polymers not falling under the geosynthetics category).

3.2.2.1 Geosynthetic family

Geosynthetics are defined by the ASTM committee D35 as planar products manufactured from polymeric material which are used to perform various functions such as improving drainage, erosion control and reinforcement of soil. The different types of geosynthetics and their functions are summarised in Table 3-2. According to Koerner (2012) and Nicholson (2014), the geosynthetics that can be used for reinforcement are geotextiles, geogrids and geomembranes. Although geosynthetics are not the focal point of this study it worth noting that studies conducted on these materials for reinforcement have shown increases in shear strength. This is a result of the tensile resistance from the reinforcing element and the shear resistance from increased friction because of the soil-reinforcement adhesion (Ingold, Miller 1983, Gray, Al-Refeai 1986, Lin 2005, Sarsby 2007, Shukla, Sivakugan et al. 2009, Nguyen, Yang et al. 2013).

1 **Table 3-2: Type and functions of geosynthetics (Koerner 2012)**

Type	Function	Image
Geotextiles	These are made from natural or polymeric fibre in to sheets which can be woven, nonwoven, stitched or knitted. They are primarily used for separation, containment, filtration, reinforcement. Image taken from Times Fibrefill (Times Fibrefill 2012)	
Geogrids	Manufactured from polymeric products, these geosynthetics are used mainly for reinforcement purposes. They are made of ribs which intersect to form openings and are thus categorised based on their geometry, namely uniaxial, biaxial and triaxial grids. Image taken from BS Specialist Products (2018).	
Geocomposite	This particular type is multifunctional as it is a combination of two or more geosynthetics to serve purposes of filtration, separation, barrier, drainage and/or reinforcement. Image taken from Agru America Inc. (2018).	
Geomembrane	This is a synthetic membrane which has very low permeability and used to control fluid movement. It is often used to contain waste in landfills and dams. Image obtained from Dacheng Building Material (2016).	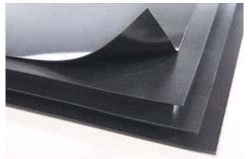

Geocells	These are cellular confinement systems manufactured from HDPE membranes and made up of single cells which are interconnected. They are mainly used for erosion control and reinforcement. Image from Tigergrid Geosynthetics (2015).	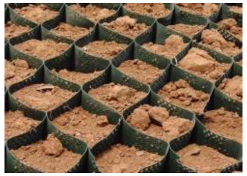
Geopipe	This is made from HDPE and mainly used as part of a subsoil drainage system. Image from Gundle Geosynthetics (2014).	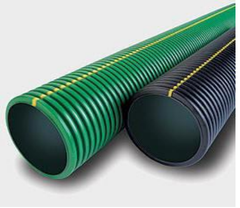
Geocontainer	This is a large geotextile bag that is filled in soil. These bags are placed to control erosion and in some cases, may also be used to create artificial barriers for flood control. Image from Tessilbrenta (2016).	
Geosynthetic Clay Liner (GCL)	A GCL is made up of two geotextile or geomembrane sheets with a thin layer of clay between them. This is mainly used for the containment of liquids. Image from Samridhi Petrochem (2015).	

1

3.2.2.2 Plastics

The second type of synthetic material is plastic, which includes polymers that do not fall within the geosynthetics family. Plastic is defined by the United States Environmental Protection Agency (1990) as “resins or polymers that have been synthesised from petroleum or natural gas derivatives. The term ‘plastics’ encompasses a wide variety of resins each offering unique properties and functions.”

The use of plastics such as polyethylene, polyvinyl chloride (PVC), polypropylene, etc. as reinforcement has been investigated by various researchers. Research, using different types of plastics and testing methods, undertaken by various researchers such as Consoli et al (2002), Falorca & Pinto (2011), Pradhan, Kar & Naik (2012), confirmed the improvement in certain engineering properties of the soils used. These studies informed the basis of this investigation.

3.3 Types and Structure of Plastics

The most basic definition of the structure of a polymer is that it is a chemical made of many repeating monomer units which are carbon based molecules (but can be oxygen, nitrogen, sulphur, chlorine, fluorine, phosphorous, and silicon) which are polymerized (Klein 2011). Monomers are molecules that can be bonded with identical molecules, through a process called polymerization which uses heat, pressure and a catalyst, to form polymers.

In 1988 the Society of Plastics Industry (SPI), which is the plastics industry trade association, developed a coding and resin identification system to assist recyclers in determining and classifying different types of plastics. In working with ASTM international (American Standard for Testing Materials) the existing RIC system was updated and documented in 2010 as ASTM D7611: Standard Practice for coding plastic manufactured articles for resin identification (Society for Plastics Industry 2015). This standard provided for seven different categories, as detailed in Table 3-3. These categories have different molecular structures resulting in different properties.

3.3.1 Polyethylene Terephthalate (PET)

PET is made up of repeated $C_{10}H_8O_4$ monomer units which is created through polycondensation of ethylene glycol and terephthalic acid. The molecular structure, shown in the chemical reaction below, is such that a large six-sided carbon ring is formed which is responsible for the stiffness and strength in the polymer.

$C_8H_6O_4 + C_2H_6O_2 \rightarrow C_{10}H_8O_4 + 2H_2O$

This polymer is most commonly used for soft drink and water bottles but can be used in the geotextile industry and its fibres used for clothing and carpet manufacturing.

Table 3-3:Resin Identification Codes

Resin number	**Plastic type**	**Plastic type code**	**Resin Identification Code (RIC)**
1	Polyethylene Terephthalate	PET	
2	High Density Polyethylene	HDPE	
3	Polyvinyl Chloride	PVC	
4	Low Density Polyethylene	LDPE	
5	Polypropylene	PP	
6	Polystyrene	PS	
7	Other resins	Other	

3.3.2 High Density Polyethylene (HDPE)

Repeating units of C_2H_4 (ethylene) in a linear chain result in the formation of HDPE, shown in the following chemical equation:

$Y[CH_2 + CH_2] \rightarrow Z[C_2H_4]$

Y is the repeating number of units used to form Z units in the HDPE chain. The formation, properties and uses are discussed in detail in section 3.4. This polymer is most widely used to make plastic corrosion resistant piping.

3.3.3 Polyvinyl Chloride (PVC)

Vinyl chloride (CH_2=CHCl) is formed when a catalyst is used in a reaction between ethylene, oxygen and hydrogen chloride. This is then subjected to reactive compounds which cause double bond to open, and one of the single bonds are used to link monomers, forming a chain which is the PVC polymer. The chemical reaction is shown below, where '=' signifies a double bond and *'n'* is the number of repeating units:

$$CH_2 = CHCl \rightarrow [C_2H_3]_n$$

The formula as it stands produces a rigid plastic, which is termed unplasticised PVC, and is commonly used in plumbing and electrical industries for pipe, fittings and conduits. Plasticised PVC is achieved through dehydrohalogenation process to form a more flexible form of the polymer which is used for manufacturing items such as waterproof clothing and garden hoses.

3.3.4 Low Density Polyethylene (LDPE)

This polymer is formed from repeating units of C_2H_4 (ethylene) as shown in the formula below.

$$Y[CH_2 + CH_2] \rightarrow Z[C_2H_4]$$

It differs from HDPE in that it is branched as opposed to linear. The details are discussed under polyethylene in section 3.4.

3.3.5 Polypropylene (PP)

Much like the PVC, PP is formed from the breaking of a double bond resulting in a single bond linking molecules to form a chain, which becomes the monomer. In this instance, the double bond in a propylene molecule (CH_2=$CHCH_3$) is broken to form a chain as shown in the following formula:

$$CH_2 = CHCH_3 \rightarrow [C_3H_6]_n$$

The semi-crystalline structure of PP results in a hard, yet flexible, water and chemical resistant plastic that can be used for toys, outdoor furniture and indoor or outdoor carpets.

3.3.6 Polystyrene (PS)

Polystyrene is made of repeating units of $CH_2CHC_6H_5$. The chemical reaction yields a six sided carbon ring. The presence of the ring prevents the chains from forming a crystalline structure, resulting in a rigid polymer which is used to make products such as coat hangers.

However, a different form called expanded polystyrene is formed by foaming, using pentane or carbon dioxide, resulting in a lightweight polymer that is commonly used as protective packaging.

3.3.7 Other

This category includes all types of plastics that do not fit into the above groups of polymers. These have been used in various industries and serve multiple purposes, but are mostly known to be engineering plastics (in the recycling industry) or multi-layer materials in specialised packaging.

Apart from HDPE and LDPE, the abovementioned categories of plastics exhibit hardness and rigidity as a consequence of their molecular structure. These properties are good in increasing the shear strength of soil due to their response to a compressive force. When looking at the shear strength parameters, more specifically the internal friction angle, a more flexible plastic is required to increase frictional resistance to a shearing force. These would fall under the polyethylene group.

3.4 Polyethylene

Polyethylene is primarily made up of methylene units (CH_2) bonded to form ethylene (CH_2=CH_2), which are in turn linked to form a polymer chain as shown in Figure 3-2.

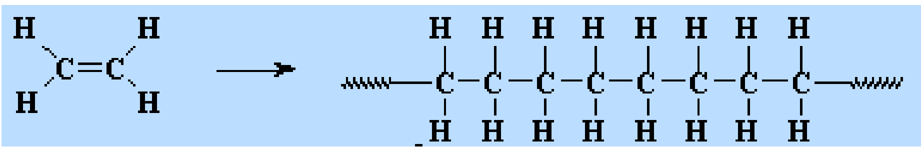

Figure 3-2: Polyethylene chain of linked monomers

The repetition of this molecule (C_2H_4) can be in linear form or it can be branched. By controlling the molecular structure of polyethylene, products with different densities can be produced with difference properties. The different classes are:

- Ultra-high-molecular-weight polyethylene (UHMWPE)
- Ultra-low-molecular-weight polyethylene (ULMWPE or PE-WAX)
- High-molecular-weight polyethylene (HMWPE)
- High-density polyethylene (HDPE)
- High-density cross-linked polyethylene (HDXLPE)
- Cross-linked polyethylene (PEX or XLPE)
- Medium-density polyethylene (MDPE)
- Linear low-density polyethylene (LLDPE)
- Low-density polyethylene (LDPE)

The most common classes are HDPE and LDPE. These differ in their molecular structure due to the polymerization method used in their manufacturing. Ziegler-Natta polymerization results in linear polymer chain formation, which is called HDPE. LLDPE is made through free radical vinyl polymerization which results in branching. Due to their different structures, these plastics have different properties. The more linear a chain is, the higher the tensile strength of the polyethylene. However, according to Gedde (2013) the properties are direction dependent (anisotropic). He illustrates this through a measurement of Young's modulus for polyethylene at room temperature. In the direction of the chain-axis, Young's modulus is 300GPa. In the transverse direction, it is only 3GPa. This is due to the different types of bonds which are formed in the different directions. A strong covalent bond is formed in the chain direction, but a weaker secondary bond acts in the transverse direction (Figure 3-3).

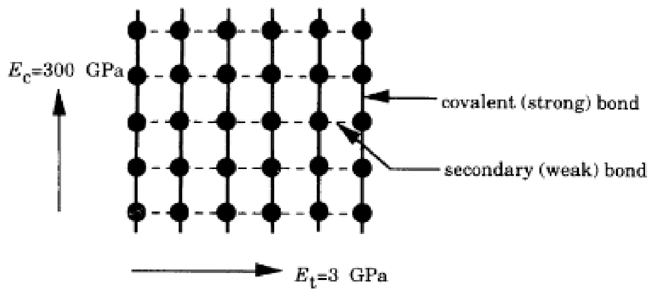

Figure 3-3: Polyethylene anisotropy of Young's Modulus (Gedde 2013)

Branching provides additional bonds in different directions leading to LDPE having a more consistency in properties in different directions. By limiting the number of branches and shortening them, a more linear LDPE can be formed simply called linear low-density polyethylene (LLDPE). As a result of the more linear structure, LLDPE has higher tensile strength than LDPE. Due to the branching, LLDPE still maintains the consistency in properties in all directions. Figure 3-4 is an illustration of the different polymer chains.

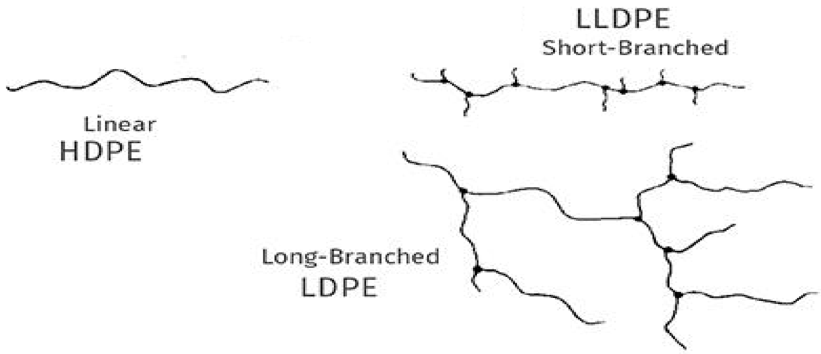

Figure 3-4: Schematic of HDPE, LDPE and LLDPE molecules (Sepe 2014)

Branching affects density as well. The more linear the chain, the more closely it can approach another chain, leading to a densely packed network. This means that the linear HDPE has a higher density than LDPE. Density, however, only affects the strength and stiffness of the material. Toughness and creep resistance are affected by the bonds in the molecular structure and length thereof.

With HDPE and LDPE being the most common plastics in the polyethylene group, they make up most of the plastics that reach recycling plants from waste.

3.5 Plastics recycling

Numerous avenues exist for the treatment of plastics. According to Al-Salem, Lettieri and Baeyens (2009) the four main routes are primary (re-extrusion), secondary (mechanical), tertiary (chemical) and quaternary (energy recovery) schemes and technologies. Primary recycling, involves re-introducing clean scrap of a single polymer to the extrusion cycle to produce products of the similar material. This method is not used by recyclers as they would not be able to meet the required quality. It is therefore applied in the manufacturing processing line itself. Secondary treatment is the route most taken by recyclers. This method makes use of plastic waste, which is generally reduced in size through mechanical means to a desired shape or form, such as flakes, pellets or powder. Advanced thermo-chemical treatment (a tertiary method) involves the use of a range of technologies to produce fuels and/or products to be used in the petrochemical industry. This method still requires research in terms of design and background knowledge to produce certain products or chemicals. Quaternary treatments are used mainly for municipal solid waste. The energy recovery has been researched up to the point that it is produced in kilns and reactors, with no integration with converting plants. Because of the shortcomings of the tertiary and energy recovery treatment methods, the primary and secondary recycling route are the most applied by recyclers. An illustration of the process is given in Figure 3-5 (A - E).

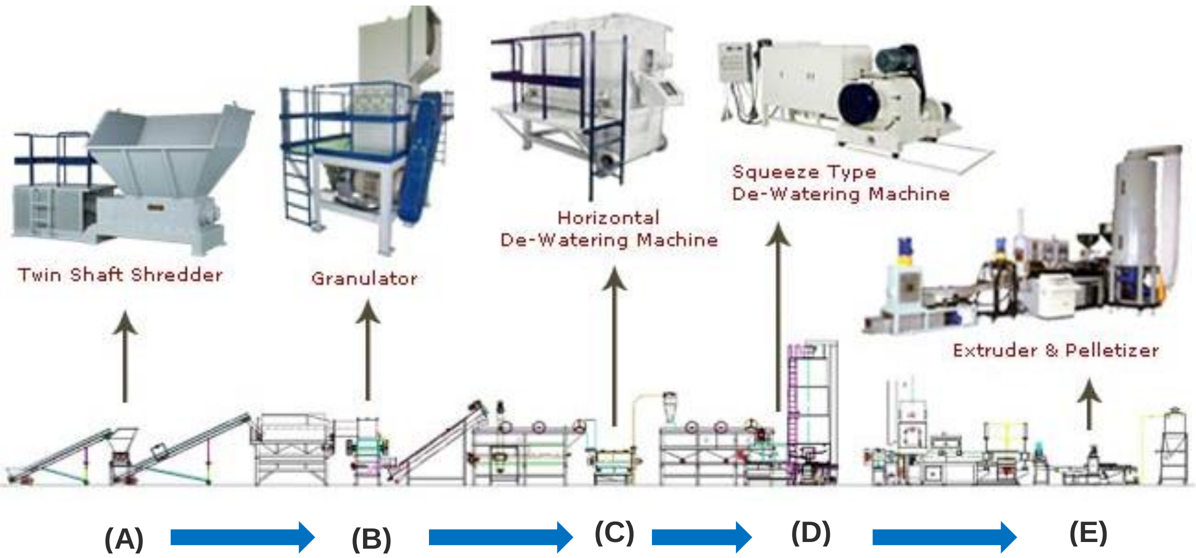

Figure 3-5: Plastic recycling process (Recycling Facts Guide 2016)

The Plastics Federation of South Africa (2015), as part of a plastics environmental initiative ('The Environmark'), provides details of the process in Figure 3-5. The recycling process begins with the collection of waste materials from various sources, which includes factories, homes, retail stores and garbage disposal sites. This waste is then sorted, often by type and colour, and then graded according to the different categories in table 3-1. The different types of plastics are then compressed and made into bales which are delivered to recyclers. The bales are opened, and the process depicted in Figure 3-5 starts with the loose material being fed into a shredder (A) and/or granulator (B) to be cut up into smaller pieces. The granules or shredded material are put through washing equipment (C) to remove any labels, residual contents and soil from garbage disposal site. This shredded material, more commonly referred to as flake, is the first form of reinforcement used in this research. The washed granules or flakes are then dried (D) and fed into an extruder and melted (E). The molten material is extruded through a multi-hole die in the form of continuous strings which are then cooled and chopped up into pellets using a revolving cutter (E). This is the final product which is sold to manufacture new plastic products from recycled plastics.

Based on this recycling process, it is important to note that the flakes are the original plastic material which has only been reduced in size. The pellets, on the other hand, are treated with heat and the impact and change in molecular structure is unknown. As a result, the behaviour and response in the reinforcement model can therefore not be compared to the mechanism discussed in the following chapter. However, previous studies could be used to ascertain the effect of certain procedures, parameters and variables during the experiment phase and consequently inform the testing procedure for this research.

Plastics are widely utilised for storage and containment of liquids, with most being disposed of after short, single use and resulting in overburdening of landfill sites. Recycling is one of the main strategies for waste reduction (King, Burgess et al. 2006). Practical re-employment of this plastic waste material would have environmental benefits when used in large quantities and having established the tensile resistance properties, frictional components and the reinforcement mechanisms in the previous chapter, could offer a sustainable alternative for soil reinforcement (Basu, Misra et al. 2013, Dikgang, Leiman et al. 2012). Further to this the costs of obtaining steel reinforcement or geosynthetics far outweigh the cost of recycled plastics, which makes it a more cost-effective solution. However, the behaviour of the two product outputs as reinforcing elements of the recycling process (flakes and pellets) is unknown. Research conducted has been mainly of fibres and strips with predetermined dimensions, as discussed in the following chapter. Determining how the flakes and pellets perform as reinforcement elements therefore forms the basis of this study.

4 REVIEW OF PREVIOUS STUDIES

4.1 Introduction

This chapter is a review of previous studies on the use of plastics in fibre and strip form, as reinforcement material. Research involving various types of polymers and fine- grained soils is discussed to understand the behaviour of polymers as reinforcement material. This is then followed by research which focuses on coarse grained soil and lastly, those related to the testing method used for this investigation. A summary of the literature review concludes the chapter.

4.2 Studies on fine grained soil (clay)

The interaction mechanism between cohesive soils and reinforcing elements is difficult to quantify, however, a few studies have been carried out to determine the effect of synthetic material inclusions on the shear strength of cohesive soils (Lin 2005). Tests conducted by Nataraj and McManis (1997), Mirzababaei (2012) and Estabragh et al. (2013) on soil reinforced with synthetic materials all showed an increase in shear strength which is dependent on the moisture absorption capacity of the material used. A comparison was thus drawn between studies using reinforcement elements which absorb moisture, such as palm fibres (Estabragh, Bordbar et al. 2013) and carpet waste (Mirzababaei, Miraftab et al. 2012), and those that do not, such as polypropylene fibres (Nataraj, McManis 1997).

Triaxial tests with confining pressures of 200kPa, 300kPa and 400kPa, were conducted by Estabragh (2013) on clay soil using palm fibres with length of 4mm and widths of 2mm, and varying content of 10%, 20% and 30%. This showed an increase in shear strength and friction angle to a maximum of approximately 18% and 33% from unreinforced soil, respectively, at a fibre content as high as 30%. The adverse effect of the palm-fibre inclusions, at the same concentration, were measured using the oedometer, which resulted in a 30% increase in compressibility and swelling indices. Mirzababaei et al. (2012) took this further by comparing material with different water absorption capacity. This study used two carpet fibres. The first was made of 100% nylon (type 1) with water absorption capacity of 4.1% to 4.5%. The second type (type 2) was made of 60% polypropylene (no water absorption capacity), 20% SBR latex (no water absorption capacity), 15% nylon (4.1 to 4.5 % absorption capacity) and 5% wool (13% to 15% water absorption capacity). The test results showed that fine grained soil compressive strength increased with the use reinforcement material with some water absorption capacity (type 2) at higher content (5%) compared to elements with higher water absorption capacity (type 1), at the same content percentage. These studies point to the effect of clay soils being dependent on moisture content and the difference between absorption potential of the fibres used. This is mainly applicable to cohesive soils due to low permeability. Sandy soils are free-draining and therefore do not hold water.

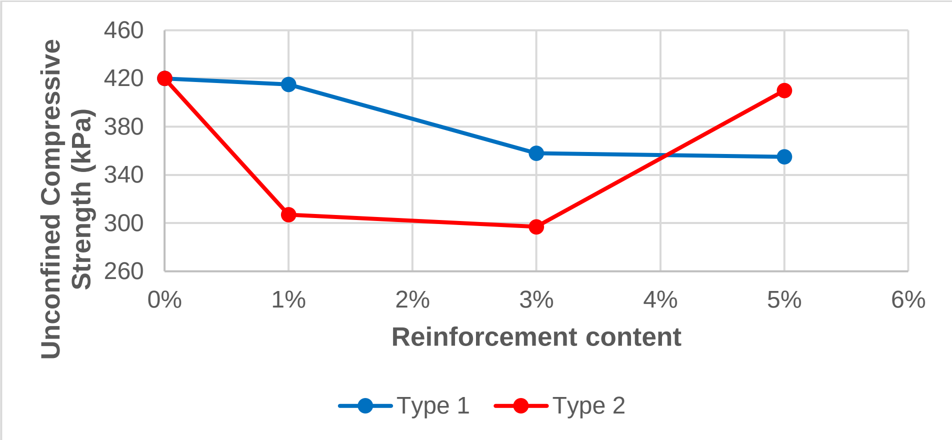

Figure 4-1: Peak compression strengths at optimum moisture content (Mirzababaei, Miraftab et al. 2012)

Comparing these studies to those using synthetic material with no water absorption capacity we draw on research conducted by Nataraj & McManis (1997) and Pradhan, Kar & Naik (2012). The research by Nataraj and McManis (1997) involved the use of polypropylene fibrillated fibres randomly distributed in clay at content of 0.1%, 0.2% and 0.3%. Using direct shear tests, it was found that an optimum value as low as 0.3% fibre-content resulted in maximum shear strength increase as shown in Figure 4.2.

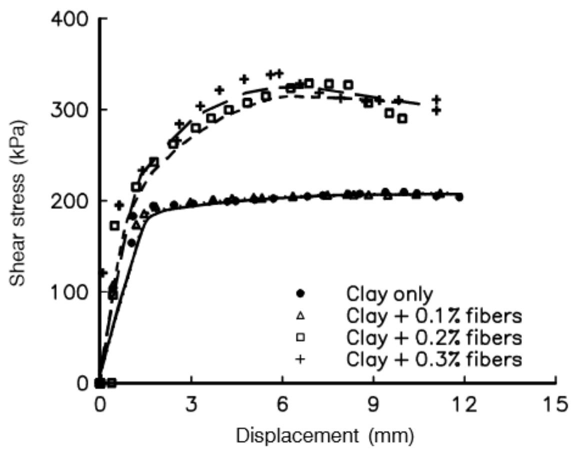

Figure 4-2:Stress-strain relationship of unreinforced and reinforced clay (Nataraj, McManis 1997)

The study by Pradhan, Kar & Naik (2012) was to determine that effect of the random inclusion of polypropylene fibres on the strength characteristics of cohesive soil. Direct shear tests, CBR tests and unconfined compression tests were conducted on low plasticity clay reinforced with polypropylene fibres. The length and amount of fibre was varied. The fibres were 0.2mm in diameter with varying average lengths of 15mm, 20mm and 25mm, giving aspect ratios of 75. 100 and 125. The content varied between 0.1% and 1.0% for the tests. Direct shear and CBR tests showed that an inclusion of polypropylene fibres results in an increase in strength characteristics as shown in Figure 4-3 (a and b). The shear tests revealed that there was an increase in cohesion and angle of internal friction for all fibre lengths. With shear resistance being a function of these two parameters, an increase in any one of them results in an overall increase in shear strength.

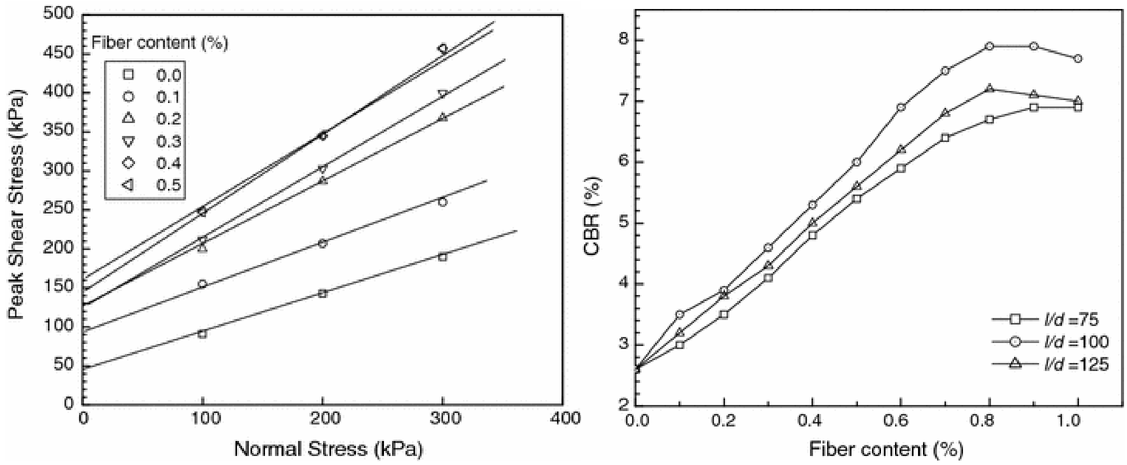

Figure 4-3: Changes in (a) peak shear stress and (b) CBR value with increases in fibre content (Pradhan, Kar et al. 2012)

With the unconfined compressive strength this optimum value for fibre content was found to be 0.5% and 0.8% for the CBR tests, resulting in the maximum increase in peak strength. All these optimum values for fibre content were for the aspect ratio of 100 (l/d) which was found to be where the increase in shear strength was at its maximum based on the shear tests. An observation of the stress-strain response in the unconfined compression tests revealed improved strain response at all aspect ratios, which confirms that the inclusion of fibres increases strain at failure up to an optimum fibre length and decrease thereafter. Figure 4-4 shows the stress-strain response of the different fibre lengths, with l/d = 100 as the optimum aspect ratio. The results from these studies on polypropylene imply that material with no water absorption capacity may improve shear strength properties of clay.

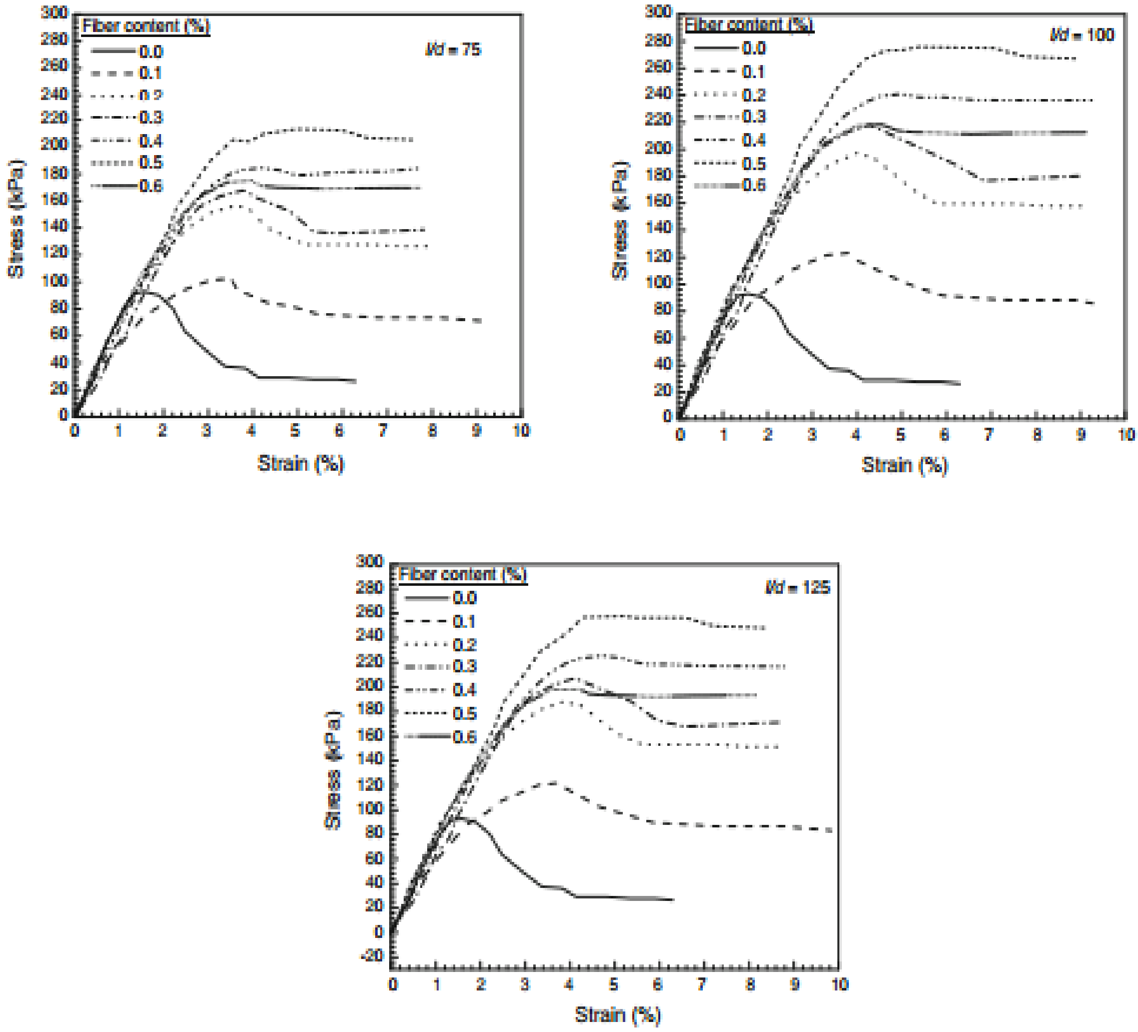

Figure 4-4: Stress-strain response for different fibre lengths(Pradhan, Kar et al. 2012)

4.3 Studies on coarse-grained soil (sand)

Various factors such as particle size and density influence the behaviour of fibre reinforced sands. Direct shear tests were used by Sadek et. al (2010), with nylon fishing wire fibres (a synthetic plastic), to study the effect of particle size. Ottawa and black green line (BGL) sands with a mean grain sizes of 0.39mm and 1.45mm, respectively, were compared. The finer Ottawa sand (D_{50}=0.39mm) showed a maximum increase in shear strength of 17% at 1.5% fibre concentration, with the coarser sand (D_{50}=1.45mm) resulting in shear strength improvement of 22% at the same concentration. Figure 4-5 confirms that the increase in shear strength of coarse sand is higher compared to fine sand, at higher fibre content. The effect of the reinforcement was more significant in fine sands at lower concentrations (Al-Refeai 1991).

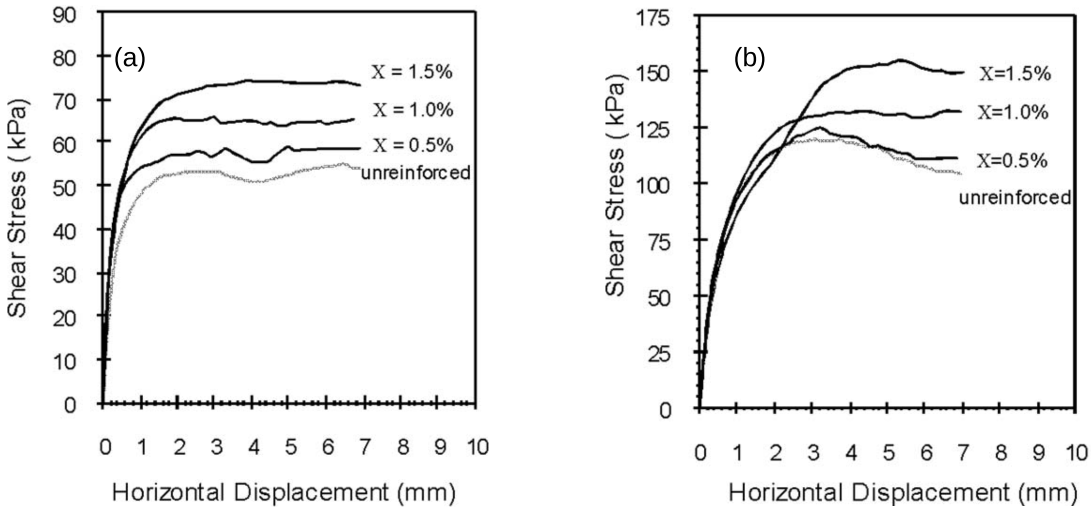

Figure 4-5: Shear strength improvement between (a) fine and (b) coarse sands (Sadek, Najjar et al. 2010)

This means, the increase on shear strength is dependent on the fibre content and coarse/fineness of the sand. These findings were confirmed by Anagnostopoulos et al. (2013) whose results showed significant improvements in the peak shear strength of fine sands (22.5%) with polypropylene fibre concentration of 0.5% compared to 2.4% for coarse grained soils. The results were relevant for medium soils, but the increase in shear strength for highly dense soils was found to be insignificant.

Further research by O'Rourke, Druschel & Netravali (1990) looked at tests using soils at different densities reinforced with HDPE (lining and pipe) and PVC (lining and pipe). Over 450 direct shear tests were conducted using the ASTM D3080 standard. The results of this study revealed that the interface frictional resistance is dependent on soil density. This is evident in the increase in maximum shear stress (Figure 4-6 (a)) and displacement (Figure 4-6 (b)) when the unit weight increases from 15 kN/m^3 to 17 kN/m^3 for both HDPE and PVC reinforced soil.

Benson & Khire (1994) investigated HDPE to determine the feasibility of reinforcing soil with polyethylene strips. CBR tests according to ASTM D1883 standards were conducted to determine the effect of the inclusion of HDPE strips in uniformly graded sand (SP according to Unified Soil Classification System). The length of the strips was varied at 24mm, 48mm and 72mm, yielding aspect ratios (length to width) of 4, 8 and 12, to determine how length of the strips affected the reinforcement of the sand. These strips were mixed in the sand at concentrations between 1% and 4%. The results of these tests showed an increase in shear strength and resistance to deformation, as shown in Figure 4-7, with increases in aspect ratio (a) and strip content (b). The largest increases were obtained with an aspect ratio of 8. The implication was that there is an optimum aspect ratio for achieving the highest possible shear strength and resistance to deformation when using polyethylene strips for soil reinforcement. This was confirmed by Pradhan, Kar & Naik (2012) and Wanyama (2017) when the results of their research also revealed an optimum aspect ratios, beyond which, the increase in the engineering properties was not as high.

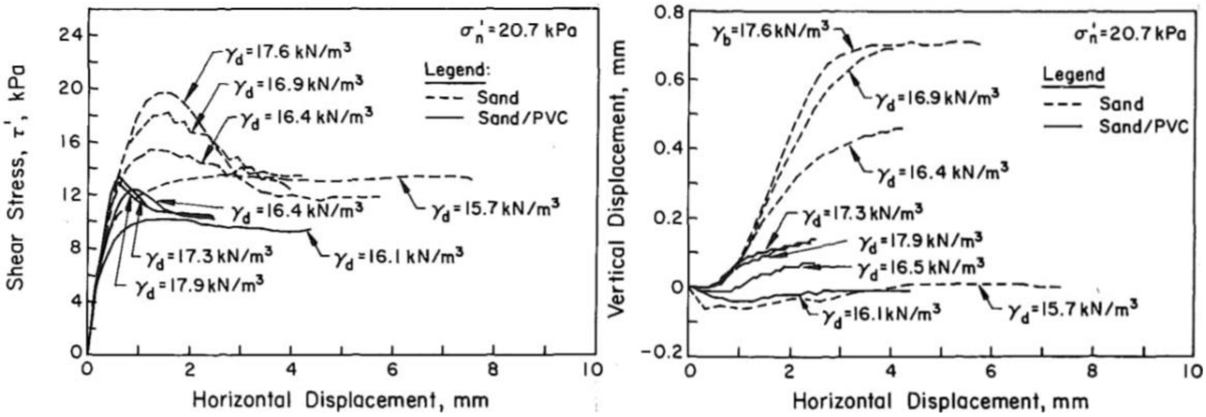

Figure 4-6: (a) Maximum shear stress and (b) Vertical displacement increase with incre(Benson, Khire 1994)ases in unit weight (O'Rourke, Druschel et al. 1990)

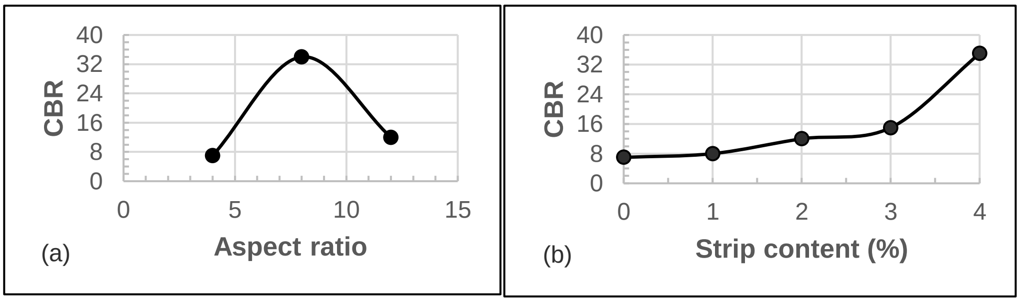

Figure 4-7: Changes in CBR value with (a) aspect ratio and (b) strip content (Benson, Khire 1994)

Having looked at studies on clay and sand using various types of polymers, it follows that the focus is shifted to research that was conducted using the same testing method that was employed in this investigation, the triaxial compression test.

4.4 Studies on triaxial compression tests

Research conducted by Consoli, Montardo et al. (2002) included triaxial tests, over and above unconfined compressive strength, to determine improvement in engineering behaviour of uniformly graded sand reinforced with PET fibre of 12, 24 and 36mm lengths with a diameter range of 0.18 to 0.20mm and varying concentration between 0 and 0.5%. The triaxial tests showed an increase in angle of internal friction, which meant that the shear strength of the soil increases. This confirmed the improvement in engineering behaviour noted in the increase in compressive strength when the unconfined compression tests were conducted. The effect of fibre length was, however, not evident in the unconfined compression tests. This was revealed in the triaxial tests where it was found that the greatest improvement was with the longer 36mm length strips. Later studies conducted by Consoli, Heineck et al. (2007) found that for a fibre-soil composite there exists a threshold confining pressure below which the shear strength increase is attributed to increased friction (slip/pull). This confirmed earlier findings by Maher & Gray (1990). This study involved conducting triaxial compression tests on sand with randomly distributed glass-reinforced plastic fibres mixed at concentrations to a maximum of 6%. The fibre diameter was 0.3mm with aspect ratios (length to diameter) of 60, 80 and 125. The improvement in shear strength above the threshold were mainly due to stretching of the fibre. This change in the failure mechanism was reflected by a bilinear envelope as shown in Figure 4.8 (b), whereas Figure 4.8 (a) is a linear envelope evident from unreinforced soil.

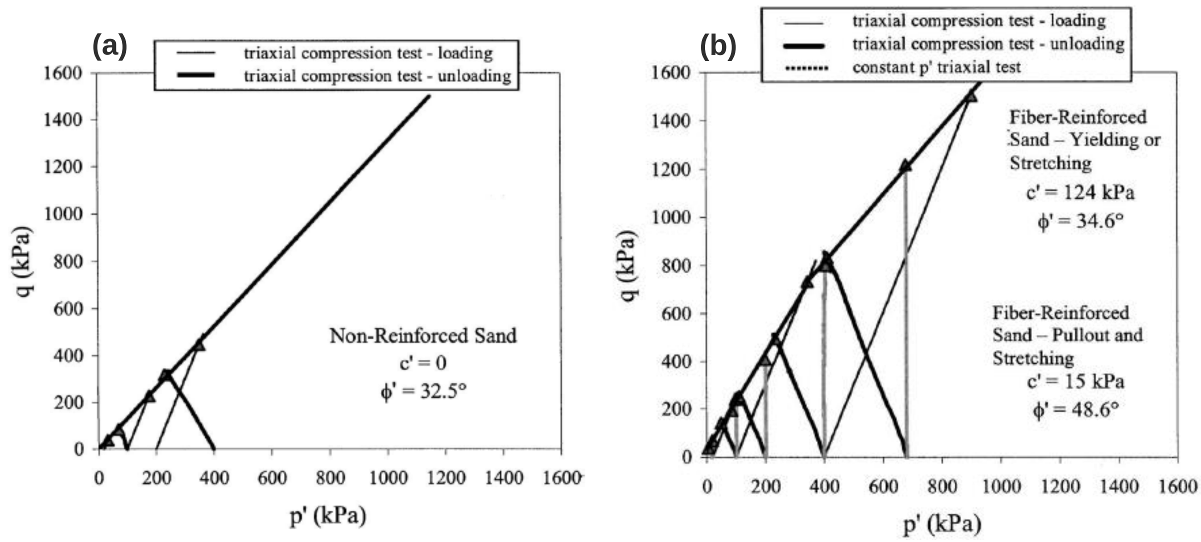

Figure 4-8: Shear strength envelopes for (a) unreinforced sand and (b) fiber-reinforced sand (Consoli, Heineck et al. 2007)

Further to this, Maher and Gray (1990) found that the threshold confining pressure is influenced by the grading of the soil. This was further investigated by A-Refeai (1991) conducting triaxial tests on sandy soils with various grades. These were fine sands with sub-rounded particles and medium-grained sand with sub-angular particles, with the former exhibiting more pronounced effects of reinforcement. As much as an increase in the particle size had no effect on the threshold confining stress, it was found that it lowered the contribution of the reinforcement to the increase in shear strength.

The same conclusion of a bilinear failure envelope defined by the threshold confining pressure was reached by Gray & Al-Refeai (1986) where it was also found that the increase in shear strength has a linear relationship with fibre content. This research was conducted using Glass reinforced plastic fibres at concentrations between 0% and 6%, randomly mixed with sand. The length of the fibres varied from 13mm to 38mm with a diameter of 0.3mm. The strength increased up to a maximum value corresponding to the concentration of 6% and aspect ratio (length to diameter) of 84.

A more recent study by Wanyama (2017) using HDPE plastic strips at varying lengths between 7.5mm and 30mm randomly mixed at concentrations from 0.1% and 0.3%. Triaxial tests were conducted at different confining pressures ranging from 50kPa to 400kPa, on samples compacted at different energy levels (280kN-m/m3 and 589 kN-m/m^3). These tests showed improvements in friction angle to an optimum content of 0.2% with strip width of 6mm and lengths up to 15mm, for both the low (LE) and high (HE) compaction efforts (Figure 4-9).

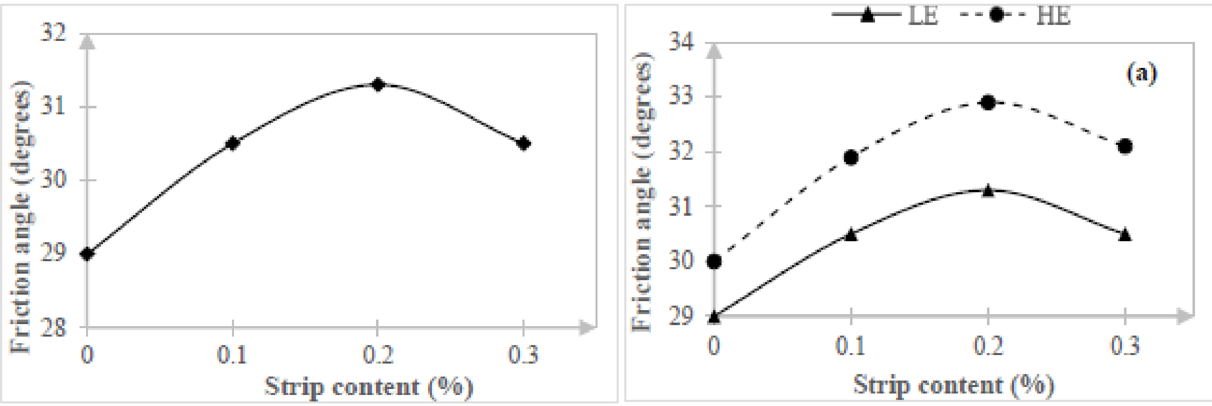

Figure 4-9: Effects of strip content and compaction effort of friction angle (Wanyama 2017)

Cohesion, however, showed negative impacts up to 0.2% content followed by an increase with overall decreases for strip lengths up to 30mm (Figure 10).

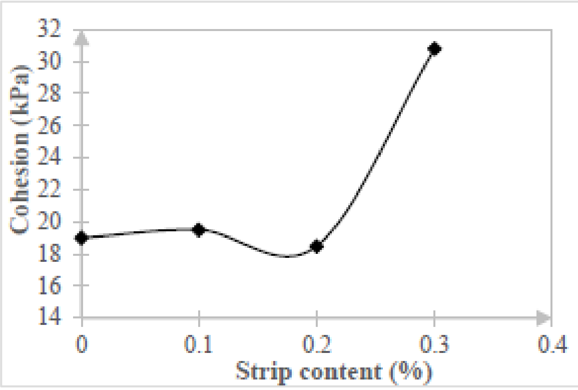

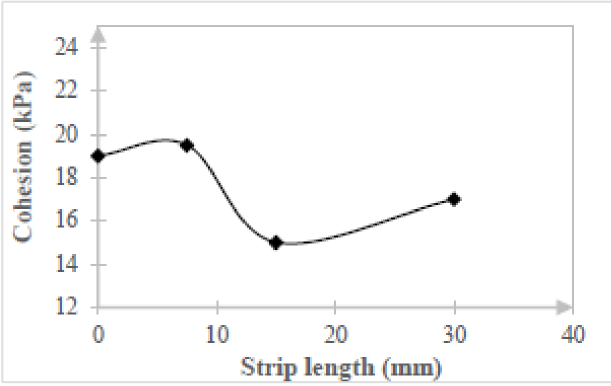

Figure 4-10: Effects of content and strip length on cohesion (Wanyama 2017)

The studies conducted indicate that the increase in the shear strength of soils reinforced with synthetic material, is significantly influenced by the concentration of the inclusions (Michalowski, Cermák 2003, Maher, Gray 1990).

4.5 Summary of literature reviewed

The literature reviewed in chapter 2 to 4, established that the shear strength of the soil is affected by the reinforcement used and its distribution. The choice in reinforcement could be broadly categorised into extensible and inextensible form. This was followed by a close examination into polymers, their properties and how these affect their performance as potential reinforcement elements. The review ended with a discussion on previous research undertaken for fine and coarse-grained soils using different tests, as well as focused on the triaxial tests, to determine the behaviour of soils using polymers as a reinforcing material.

In determining the shear strength increase in reinforced soil composites, it was established that the influencing factors are:

- Reinforcement behaviour
- Confining pressures
- Fibre concentration

Table 4.1 provides a summary of previous studies discussed in this chapter and the following conclusions can be drawn from the literature review in its entirety:

1. Research has been conducted on reinforcement on coarse-grained and fine-grained soils. Studies reveal that the influencing factors in granular soils are the grain size and density (O'rourke, Druschel et al. 1990, Sadek, Najjar et al. 2010)with the failure

mechanism explained by the interaction between soil and polymers. In cohesive (fine-grained) soils, it is mainly the moisture content effects which influence shear strength increases (Nataraj, McManis 1997, Mirzababaei, Miraftab et al. 2012, Estabragh, Bordbar et al. 2013).The interaction in cohesive soils is difficult to quantify.

2. The structure of polymers (plastics) determine mechanical properties. With the failure mechanism of a soil-fibre composite differing between hard and soft, such that the increase in shear strength in soft polymers is due primarily to the fibre induced tension during shearing (Maher, Gray 1990, Gregory, Chill 1998, Zornberg 2002), the tensile strength in LLDPE is desirable for triaxial testing where the shear plane is not predetermined (as in direct shear testing). The limited studies and properties of LLDPE provided the basis for this research.
3. There exists an optimum value of concentration for all fibres and strips which varies between 0.25% and 6%, depending on the polymer type and form used. Shear strength increases up to this optimal concentration, but a loss in shear strength occurs with concentrations beyond this value. Higher concentrations increase the ratio of polymer-to-polymer interfaces, thus reducing frictional resistance that exists with soil-polymer interfaces.
4. The properties, characteristics and behaviour of polymer-reinforced soils are influenced by the aspect ratio (length to width/diameter) of the reinforcement. Studies on polymer reinforcement is limited to elements of known dimensions.
5. Based on the theory of reinforcement, random distribution maintains the isotropy of the shear strength as it intercepts all possible shear planes and eliminates the possible development of planes of weakness which would run parallel to reinforcing elements (Lin 2005, Shukla, Sivakugan et al. 2009). This makes it a desirable method of placement, over and above its practicality and time and cost saving advantages.

With all the studies looked at on the use of polymers as reinforcement material throughout the literature review, limited research material exists on use of LLDPE. This research, therefore, was a study on the potential use of recycled LLDPE. The material was obtained from an already existing recycling process which produces the product in two forms: flakes and pellets. It was these two forms of the LLDPE that was used for this investigation.

Table 4-1: Summary of previous studies reviewed

Author(s)	Soil type	Reinforcement material	Test type(s)	Test variables/Parameter(s)	Findings
Gray & Ohashi (1983)	Sand	PVC fibre	Direct Shear	Length: 20 – 250mm Content: 0.25 – 0.5%	Shear strength increased to peak Bilinear strength envelops
Gray & Al-Refeai (1986)	Sand	Glass-reinforced plastic fibres	Triaxial	Length: 13 – 38mm Content: 0 - 6%	Shear strength increases to peak Bilinear envelope
O'Rourke, Drushel & Netravali (1990)	Sand	HDPE, PVC	Direct shear	Hardness: 35 – 85 Shore D value	Frictional strength increases with soil density, but decreases with hardness
Maher & Gray (1990)	Sand	Glass-reinforced plastic	Triaxial	Content: 0 – 6% Aspect ratio: 60,80,125	Increases in shear strength stiffness to peak
Benson & Khire (1994)	Sand		Direct shear, CBR	Length: 24, 48, 72mm Content: 1 – 4%	Shear strength and CBR values increased Bilinear envelope
Naharaj & McManis (1997)	Clay & Sand	Polypropylene fibrillated fibres	Direct shear, UCS, CBR	Content: 0.1 - 0.3%	Peak compressive strength and CBR value increased significantly for both soils

Authors	Soil type	Reinforcement material	Test type(s)	Test variables/Parameter(s)	Conclusions
Michalowski & Cermák (2003)	Sand (fine & coarse)	Polyamide monofilament, Polypropylene fibres	Triaxial	Confining pressure: 0 – 600kPa	Increases in fibre content increased shear strength more in coarse sand compared to the fine.
Consoli, Heineck et al. (2007)	Sand	Polypropylene fibre	Triaxial	Ave length: 24mm Ave diameter: 0.023mm Content: 0.5%	Linear failure envelope for unreinforced soil Non-linear envelope for fibre reinforced sand Lower confining pressures yielded lower cohesion, but higher friction angle
Sadek, Najjar & Freiha (2010)	Sand	Nylon fishing wire	Direct shear	Soil grain size: 0.39 – 1.45mm	Increase in coarse sand was higher compared to fine sand
Mirzababaei& Miraftab (2012)	Clay	Carpet waste	UCS		Increase in CBR value depended on the initial dry unit weight and moisture content of the soil

Authors	Soil type	Reinforcement material	Test type(s)	Test variables/Parameter(s)	Conclusions
Pradhan, Kar et al. (2012)	Clay	Polypropylene fibres	Direct shear, CBR, UCS	Content: 0 – 1% Aspect Ratio: 75, 100, 125	Increased shear strength, UCS and CBR value
Estabragh, Bordbar et al. (2013)	Clay	Palm fibres	Triaxial	Content: 10, 20, 30%	Increased compressibility and swelling indices
Wanyama (2017)	Sand	HDPE	Triaxial	Length: 7.5 – 30mm Content: 0.1 – 0.3% Compaction energy: 280 & 589 kN-m/m^3	Increased friction angle to optimum content and aspect ratio

5 RESEARCH MATERIALS AND METHODOLOGY

5.1 Introduction

In this chapter, details of the materials, apparatus used in the study, sample preparation as well as experimental procedures are presented. A summary of the classification and characterisation tests conducted on the Cape Flats sand and the properties of the reinforcement material are included in this section. All laboratory work for the preparation and testing of samples was conducted according to the American Standard Test Methods (ASTM).

5.2 Research Materials

5.2.1 Cape Flats sand

The soil that was used for the study was obtained from Afrimat quarry in the Phillippi area in the Western Cape. This sand was called the Cape Flats sand and was readily available within the province. It was a light grey, clean quartz sand shown in Figure 5-1. The Figure depicts photomicrographs obtained from an FEI Nova NanoSEM230 scanning electron microscope. Samples, from the Afrimat quarry, were taken from two different areas of the stockpile and the micrographs are shown in Figure 5-1 (a) and (b) with Figure (b) having a higher magnification These micrographs revealed the smaller grains to be angular and the larger grains slightly elongated and sub-angular, both with medium sphericity.

Classification and characterisation tests were conducted on the soil. A summary of the tests conducted, including the standard used, is given in Table 5-1.

Table 5-1: Soil classification tests conducted

Property	Method	Test Standard
Sieve Analysis	Particle size distribution	ASTM D6913-04
Specific gravity	Small Pycnometer method	ASTM D854-10
Minimum dry density	Method A: funnel	ASTM D4254-00
Maximum dry density	Vibratory table	ASTM D4253-00

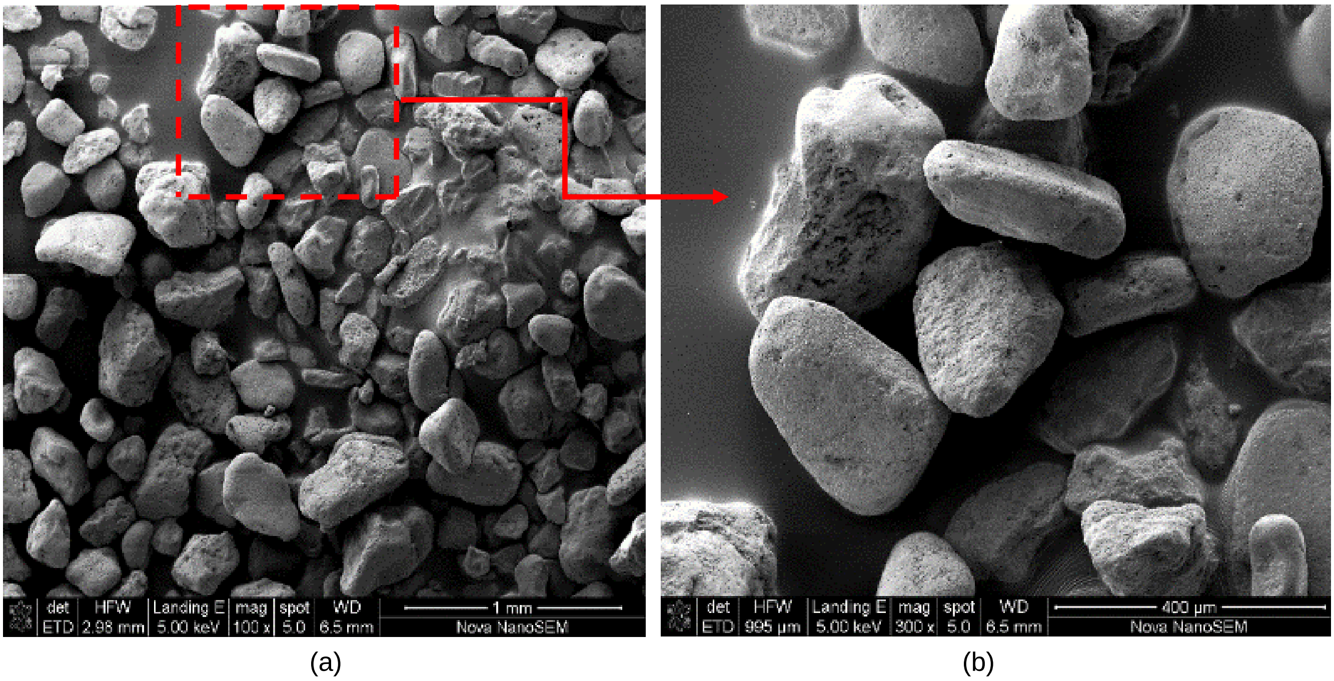

Figure 5-1: Soil particle images

The results of these test and mechanical properties were summarized in Table 5-2 and the grading curve shown in Figure 5-2. The soil is classified as a poorly graded sand (SP) with a narrow particle range of 0.075 – 1.15mm.

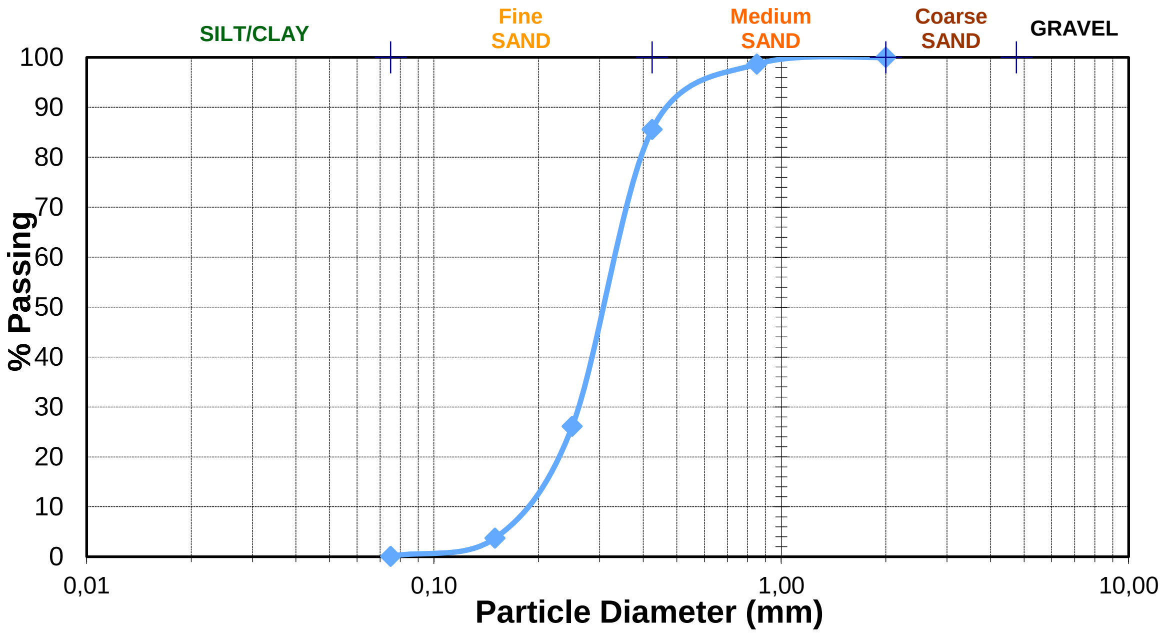

Figure 5-2: Particle size distribution curve

Table 5-2: Characteristics of Cape Flats sand

Characteristics	Unit	Value
Specific Gravity, G_s	-	2.64
Average minimum Dry Density	Mg/m^3	1.554
Average maximum Dry Density	Mg/m^3	1.657
Mean grain size, D_{50}	mm	0.32
Maximum grain size, D_{100}	mm	1.15
Particle size range	mm	0.075 – 1.15
Coefficient of uniformity, C_u	-	1.8
Coefficient of curvature, C_c	-	1.176
USCS	-	SP

5.2.2 Reinforcement material

The reinforcement material selected for this study was recycled plastic obtained from Atlantic Plastic Recycling at the Beaconvale plant in Cape Town. It was a high strength linear low-density polyethylene (LLDPE), a clear film that was manufactured through blown film extrusion and is commonly used as packaging material as films produced with this resin are extremely tough and have good impact strength and good tear resistance. The typical physical properties of the material are summarized in Table 5-3 obtained from an international manufacturer and supplier of polymers. The MD and TD are the machine direction and transverse direction, respectively, which relate to the direction relative to the polymer orientation during testing for property. MD means parallel to the direction of the polymer and TD is perpendicular.

Table 5-3: Typical physical properties of LLDPE use in study (Westlake Chemical Corporation (n.d.))

Property		Unit	Value
Melt Index		g/10 min	0.5
Density		kg/m^3	917
Haze		%	18.0
Dart Impact		g/mil	750
Tensile strength at Break	MD	MPa	59
	TD	MPa	45
Elongation at Break	MD	%	600
	TD	%	900

The recycling plant received bundles of used plastic from different sources and sorted it into bales, as shown in Figure 5-3 (a). The bales went through the recycling process where they were shredded into flakes, washed and dried, fed into an extruder where they were melted and then water cooled in a bath before they were cut into pellets (as detailed in section 3.5). The reinforcement material used for this study was extracted at two points in the recycling process. The first were the LLDPE flakes as shown in Figure 5-3 (b), which were taken after the washing process. The second material was the end product of the recycling process, which were the pellets in Figure 5-3 (c), a hardened form of the flakes.

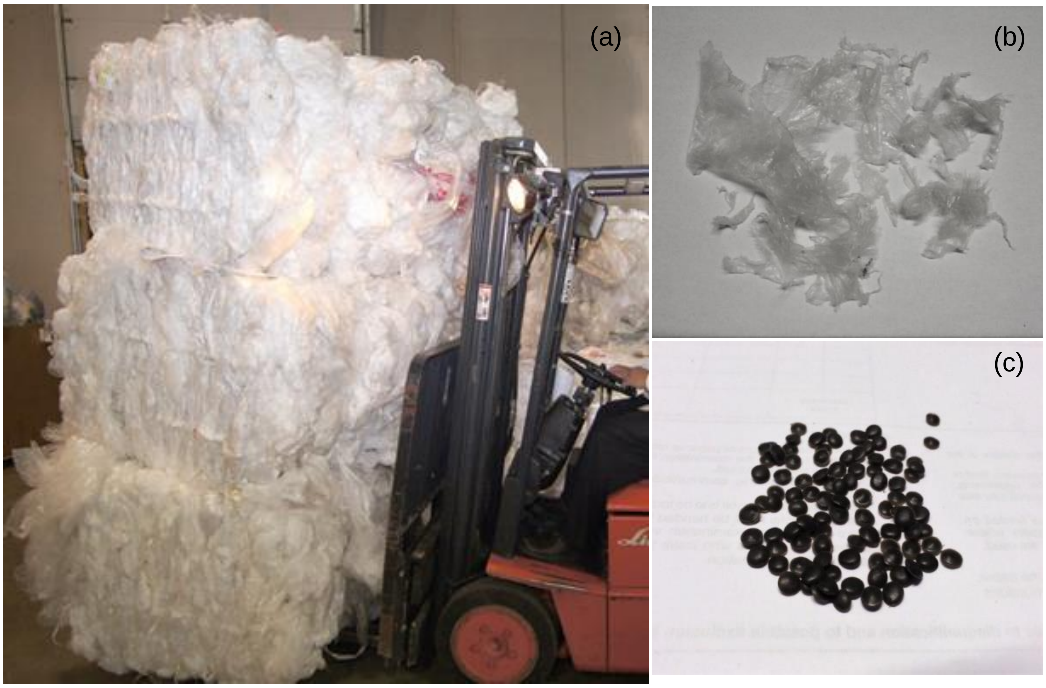

Figure 5-3: Recycling plant (a) bales (ProAct 2013), (b) LLDPE flakes and (c) LLDPE pellets

Incorporating the flakes and pellets as reinforcing elements in the sand and investigating the effect on the shear strength parameters formed the basis of this study.

5.3 Laboratory tests

The tests conducted were triaxial compression tests according to ASTM D7181-11 standards. This is a standard test method for soils under consolidated and drained conditions.

5.3.1 Test apparatus

The equipment used for the tests was the LoadTrac-II/FlowTrac-II/Cyclic-RM Triaxial system manufactured by Geocomp Corporation, which consisted of hardware components with supporting software. The hardware components were the LoadTrac-II load frame, two FlowTrac-II chambers and the triaxial test cell, which were connected to a computer with a monitor, as shown in Figure 5-4.

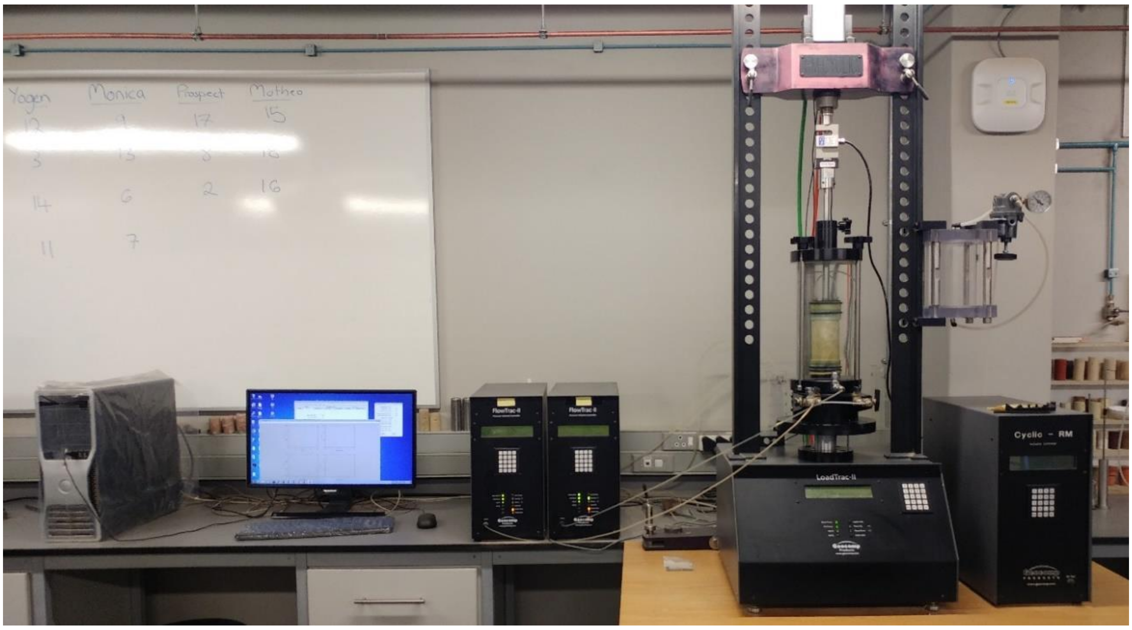

Figure 5-4: LoadTrac II/Flow Trac II Triaxial apparatus

The LoadTrac-II load frame consisted of components that generated the force on a test specimen using an embedded control system. This force and the resultant displacement were measured using linear variable differential transducers (LVDT). The main functions of the FlowTrac-II chambers were to generate and control pressures on a specimen, as well as measure volume changes. The first unit was for pressures within a specimen and the second unit was for control of confining pressures around the specimen. These units were connected to triaxial test cell which was placed on the platform of the load frame. The test cell was a chamber made of perspex glass which held the water used to confine the test specimen.

The pressures and volume changes for the test specimen situated in the test cell were measured using LVDT's. Although the triaxial apparatus was fully automated and capable of running tests under static loading, the LoadTrac frame and FlowTrac units had front panels with an LCD and keypad which allowed for the manual control of the units and monitoring thereof. All these units were connected to a desktop computer fitted with a network card, which was used to run the tests and store the results data.

The triaxial software had capabilities to run various tests using the hardware and therefore divided the test into separate phases. The first phase was initialisation during which small amounts of pressure were applied and maintained vertically and horizontally to check for leaks. A pressure differential provided an indication of a leak. The next phase is consolidation, which was achieved by applying specified stresses to consolidate the specimen. This was followed by the saturation phase, during which incremental increases in cell and pore pressures resulted in saturation of the specimen to a specified ratio. After this, consolidation was allowed for. The testing finished with the shear phase, which sheared specimen in the drained or undrained condition, using stress or strain control.

5.3.2 Methodology

All preparations, excluding the reinforcement, were done according to ASTM D7181-11 (2011), the Standard Test Method for Consolidated Drained Triaxial Compression Test for Soils.

5.3.2.1 Soil preparation

Approximately 10 kg of Cape Flats sand was set aside from the stockpile from which 1kg at a time was placed in an oven set to 105°C and dried overnight for 16-24 hours to achieve a near dry state, as stipulated by ASTM D2216-10 "Standard test methods for laboratory determination of water content of soil and rock by mass". The sample was allowed to cool for an hour before being placed in an air tight container ready for test specimen preparation.

Tests conducted according to ASTM D4254-00 (2000) and ASTM D4253-00 (2000) gave a minimum density of 1.554 Mg/m^3 and a maximum density of 1.796 Mg/m^3.

5.3.2.2 Reinforcement preparation

The initial step was to remove any foreign matter, which were a few HDPE flakes, as the testing was to be conducted only using LLDPE flakes. Thereafter the LLDPE flakes were sorted using a sieve 13,2mm sieve (Figure 5.5 a) to remove those which had a cross-sectional dimension exceeding 18.8mm. This was based on the diameter of the funnel (Figure 5-5 b) to be used in the preparation of the test specimen. The allowable cross-sectional dimension of the flakes was 95% of the diameter of the funnel, to allow for free flow during placing.

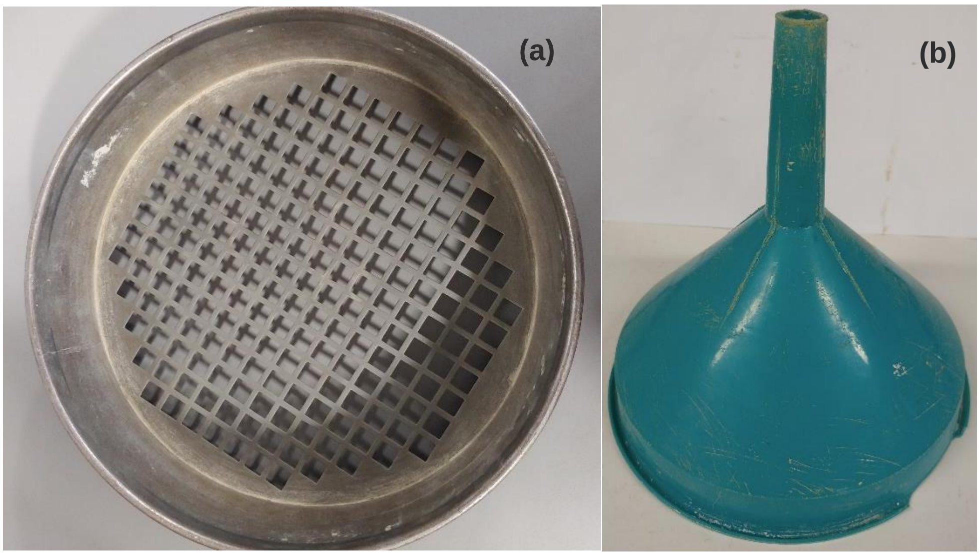

Figure 5-5: (a) Sieve and (b) funnel used in reinforcement preparation

The preparation of the pellets involved measurement of their diameter and thickness to obtain the average dimensions and mass of the material to be used. The complete sample of pellets obtained from the recycling plant weighed 850g. Using statistical methods for sample selection, Equation 5-1 was applied to determine how many grams of pellets had to be measured for the average dimensions to be considered as representative sample.

$$\boldsymbol{n} = \frac{\boldsymbol{Z^2 \times \sigma^2}}{\boldsymbol{ME^2}}\left[\frac{\boldsymbol{N}}{\boldsymbol{N-1}}\right] \quad [5\text{-}1]$$

Where n = the required sample size

Z = Z-score of 1.96 based on 95% confidence interval

σ = standard deviation of 0.4

ME = Margin of error of 5%

N = Population size of 850g of pellets

Based on this calculation, a total of 265g of pellets were measured to arrive at the average diameter of 5.31mm and thickness of 2.10mm per pellet. Once these dimensions were determined the pellets were ready for use in preparing test specimen.

5.3.2.3 Test specimen preparation

The selection of the size of the specimen was dependent on the maximum grain size of the sand and the available mould sizes. With the requirement of the standard (ASTM D7181-11 2011) being that the largest grain size being smaller than one sixth of the specimen diameter, the minimum size of mould required was 7mm. The second requirement was an average-height-to-average-diameter ratio between 2 and 2.5. The best mould to use was a 50mm (which exceeds the required 7mm) diameter split mould with an average-height-to-average-diameter ratio of 2.4. Several trials were run in the lab to determine the volume and density that would be required for the test specimen using this mould. The calculations resulted in 360g of sand used for each test specimen. The prepared sand was dry, clean and uncemented, which allowed for free flow through the funnel during handling and placing.

Previous studies conducted at the University of Cape Town provided the basis for determining the concentration values for the flakes (Petersen 2009, Sobhee 2010, Williamson 2012, Wanyama 2017). The concentrations were 0.1 %, 0.25 %, 0.5 %, 0.75 % and 1%, based on the dry mass of the soil.

In determining the pellet content, an equation obtained from known mathematical relationships was used:

$$\rho = \frac{w_f}{w_s} \qquad [5\text{-}2]$$

Where ρ was the desired percentage, w_f the weight of fibres, and w_s was the dry weight of the soil.

These percentages were suitable for the flakes. The mass of a single pellet (0.033g) amounted to 0.046% concentration, which resulted in the concentrations being increased to 1 %, 2 %, 3 %, 5 % and 7.5 %. For each sample, the total mass of 360g was divided into 5 portions of 72g, then mixed with the desired concentration of flakes or pellets as depicted in Figure 5-6 (a-e). Each portion was then poured into a split mould fitted with a latex membrane, shown in Figure 5-7 (b), using a funnel. A partial vacuum was applied to remove air between the mould and membrane to prepare for compaction. Each layer was compacted using the dry tamping method as per section 6.4.4 of ASTM D7181-11. The tamper used (Figure 5-7 (a)) had a drop height of 150 mm, drop mass of 800 g with a 35.5 mm diameter base plate.

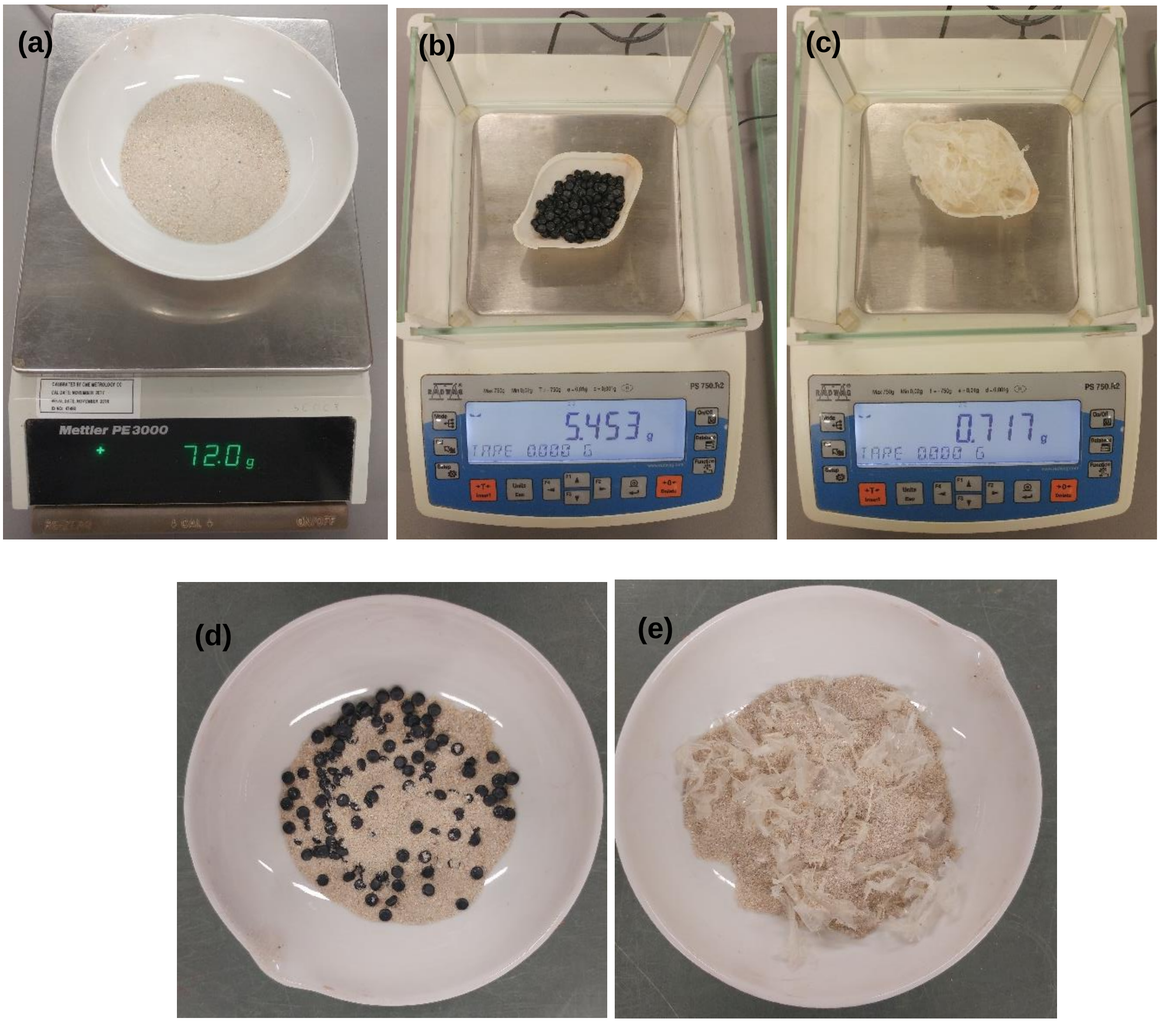

Figure 5-6: Specimen layer preparation prior to compaction

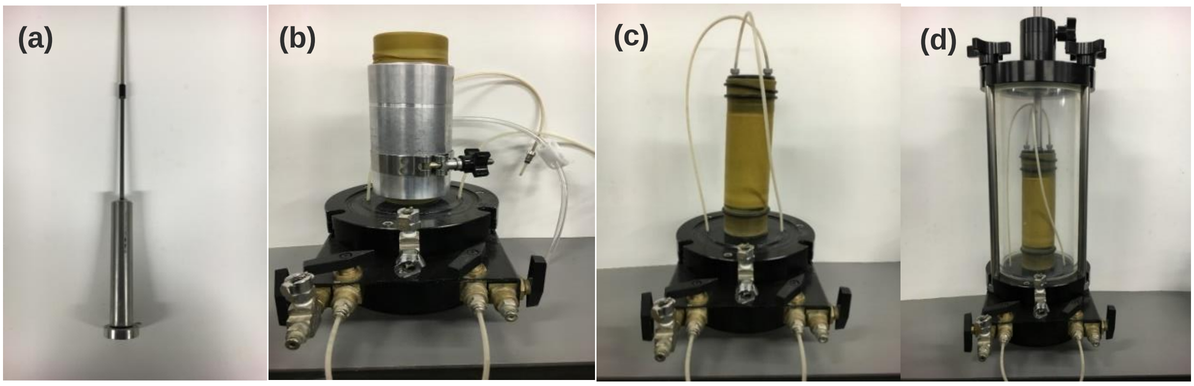

Figure 5-7: Test specimen preparation

From trial tests conducted it was discovered that the procedure used for compaction resulted in membrane damage as well as crushing of the soil material, leading to a change in grading. The repetitive action of compaction was therefore limited to achieve the medium dense state for sand considering the upper and lower limits within that range. Compaction was therefore done by applying fifteen and thirty blows per layer, to required average dry densities of 1.669 Mg/m^3 and 1.686 Mg/m^3, respectively, which were in the medium dense state (with relative densities of 51% and 58%). The compaction energy and relative densities for each test was calculated using the equations below, taken from Das & Sobhan (2013).

$$E = \frac{Number\ of\ blows\ per\ layer \times Number\ of\ layers \times Weight\ of\ hammer \times Hammer\ drop\ height}{Volume\ of\ mould}$$

[5-3]

$$D_r = \frac{\rho_{d(max)}}{\rho_d}\left[\frac{\rho_d - \rho_{d(min)}}{\rho_{d(max)} - \rho_{d(min)}}\right]$$ [5-4]

Where: D_r = Relative density

$\rho_{d(max)}$= Maximum dry density

ρ_d = Required dry density

$\rho_{d(min)}$ =Minimum dry density

Compaction energy used were 420kN-m/m3 (low compaction effort) and 841kN-m/m3 (high compaction energy). This meant that each concentration of fibre or pellets had 2 tests to be performed. One test was the specimen using the low compaction effort (LCE) and the second test was the specimen which employed high compaction effort (HCE), both with the same concentration of pellets/flakes. The specimen cap was placed after the compaction was completed, with o-rings secured around the cap and the base to seal the specimen as shown in Figure 5-7 (c). The split mould was removed and the diameter and height of the assembled specimen, as per Figure 5-7 (c), were measured to ensure that the height-to-diameter ratio is between 2 and 2.5 as per ASTM D7181-11. Further to this, the mass and volume of the sample was calculated to determine the density and relative density. The triaxial cell was placed over the prepared specimen ready for testing (Figure 5-7 (d)). The tests were conducted on an unsaturated sample, with a strain rate of 0.075%/min, by using a single and separate specimen for each of the confining pressures. The confining pressures used were different stresses that soil may be subjected to in the field equal to 75kPa, 150kPa and 300kPa.

5.3.3 Testing schedule

A schedule was prepared for the tests to be conducted in the lab. The tests were divided into two groups. The first group were tests that were conducted on soil that was compacted with low energy. The second group was on tests where the compaction energy was increased. Each group was divided into three segments. The initial tests conducted were the control tests to form the basis for comparison of the reinforced samples. Second to this were the samples where the LLDPE flakes were used as reinforcement. The third and final segment consisted of soil samples mixed with the pellets.

A total of 66 tests were carried out, excluding repeatability tests. The first 6 tests were the control tests, conducted on plain sand with no flakes/pellets to establish a benchmark to which changes in behaviour with the addition of the flakes/pellets can be compared. 30 tests were conducted for the specimens reinforced with the flakes. The remaining 30 tests were the samples containing pellets. The reinforcement material was mixed at varying concentrations and the test specimen subjected to different compaction energy and pressures. Table 5-4 describes the symbols used in the test schedule that is detailed in Table 5-5.

Table 5-4: Description for symbols used in test schedule

SYMBOL	DESCRIPTION
LCE	Low compaction energy (15 weight drops)
HCE	High compaction energy (30 weight drops)
PS	Pure sand
SF	Sand-flakes mix
SP	Sand-pellets mix
C75	75kPa confining pressure
C150	150kPa confining pressure
C300	300kPa confining pressure
R75	75kPa confining pressure for repeatability tests
X (a)	Reinforcement amount, where (a) is the actual concentration percentage

Table 5-5: Laboratory testing schedule

Test	Material	Reference number – LCE	Reference number - HCE
Repeatability	Cape Flats sand	LCE / PS / R75	-
		LCE / PS / R75	-
		LCE / PS / R75	-
Control	Cape Flats sand	LCE / PS / C75	HCE / PS / C75
		LCE / PS / C150	HCE / PS / C150
		LCE / PS / C300	HCE / PS / C300
Specimen testing	Cape Flats sand and flakes	LCE / SF / C75/ X0.1	HCE / SF/ C75 / X1
		LCE / SF / C75 / X0.25	HCE / SF / C75 / X2
		LCE / SF / C75 / X0.5	HCE / SF / C75 / X3
		LCE / SF / C75 / X0.75	HCE / SF / C75 / X5
		LCE / SF / C75 / X1.0	HCE / SF / C75 / X7.5
		LCE / SF / C150/ X0.1	HCE / SF / C150 / X1
		LCE / SF / C150 / X0.25	HCE / SF / C150 / X2
		LCE / SF / C150 / X0.5	HCE / SF / C150 / X3
		LCE / SF / C150 / X0.75	HCE / SF / C150 / X5
		LCE / SF / C150 / X1.0	HCE / SF / C150 / X7.5
		LCE / SF / C300 / X0.1	HCE / SF / C300 / X1
		LCE / SF / C300 / X0.25	HCE / SF / C300 / X2
		LCE / SF / C300 / X0.5	HCE / SF / C300 / X3
		LCE / SF / C300 / X0.75	HCE / SF / C300 / X5
		LCE / SF / C300 / X1.0	HCE / SF / C150 / X7.5
	Cape Flats sand and pellets	LCE / SP / C75/ X1	HCE / SP/ C75 / X1
		LCE / SP / C75 / X2	HCE / SP / C75 / X2
		LCE / SP / C75 / X3	HCE / SP / C75 / X3
		LCE / SP / C75 / X5	HCE / SP / C75 / X5
		LCE / SP / C75 / X7.5	HCE / SP / C75 / X7.5
		LCE / SP / C150/ X1	HCE / SP / C150 / X1
		LCE / SP / C150 / X2	HCE / SP / C150 / X2
		LCE / SP / C150 / X3	HCE / SP / C150 / X3
		LCE / SP / C150 / X5	HCE / SP / C150 / X5
		LCE / SP / C150 / X7.5	HCE / SP / C150 / X7.5
		LCE / SP / C300 / X1	HCE / SP / C300 / X1
		LCE / SP / C300 / X2	HCE / SP / C300 / X2
		LCE / SP / C300 / X3	HCE / SP / C300 / X3
		LCE / SP / C300 / X5	HCE / SP / C300 / X5
		LCE / SP / C300 / X7.5	HCE / SP / C150 / X7.5

5.4 Test Data processing and analysis

Triaxial tests were conducted according to ASTM D7181-11 with confining pressures of 75 kPa, 150kPa and 300kPa for each concentration of the flakes and pellets. These were conducted on an unsaturated soil, with a strain rate of 0.075%/min to maximum strain of 10%.

The output data consisted of axial displacement, vertical deviator force, confining stress and pore pressure. The axial displacement was converted to strain by dividing by the height after consolidation and the deviator force converted to stress by diving by the cross-sectional area of the test sample. The confining stress is equal to the major principal total stress and to obtain the effective minor principal stress (σ_3). the difference between the confining stress and pore pressure was calculated. Adding this to the deviator stress gave the major principal stress (σ_1). These values were used to plot Mohr's circle as illustrated in Figure 5-8.

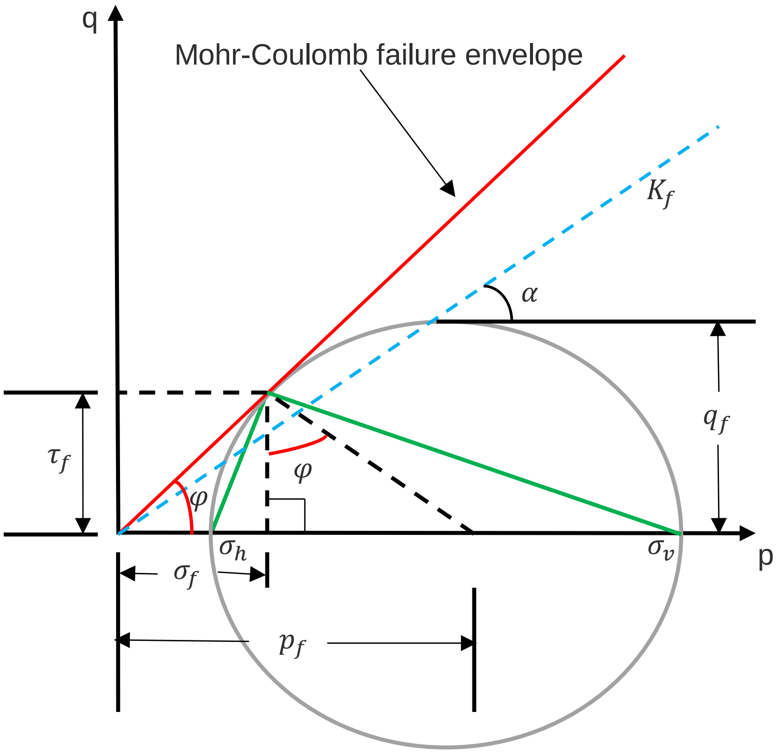

Figure 5-8: Mohr circle at failure (Geocomp Corporation (n.d.))

The data extracted from a typical Mohr circle that was used in the calculation of the parameters and analysis are detailed in Table 5-7:

Table 5-6: Mohr circle data

Symbol (s)	Description
σ_1 or σ_v	Major principal stress
σ_3 or σ_h	Minor principal stress
σ_d	Deviator stress
σ_f	Normal stress at failure
τ_f	Shear stress at failure

The equations used for the calculations of the parameters are as follows

$$\sigma_d = \sigma_1 - \sigma_3 \qquad [5\text{-}5]$$

$$p_f = \frac{\sigma_v + \sigma_h}{2} \qquad [5\text{-}6]$$

$$q_f = \frac{\sigma_v - \sigma_h}{2} \qquad [5\text{-}7]$$

$$\tau_f = \frac{q}{cos\emptyset} = \frac{\sigma_v - \sigma_h}{2cos\emptyset} \qquad [5\text{-}8]$$

$$\sigma_f = p - q \sin\emptyset = \frac{\sigma_v + \sigma_h}{2} - \frac{\sigma_v - \sigma_h}{2} \sin\emptyset \qquad (where\ \sin\emptyset = \tan\alpha) \qquad [5\text{-}9]$$

Mohr's circles were plotted for a set of tests under the three confining pressures (75 kPa, 150 kPa and 300 kPa) to obtain a failure envelope which was used in the analysis of the results.

This was further reduced by using the t-s coordinate (Craig 2004) system which was a plot of shear stress and normal stresses, where shear stresses were calculated with the equation:

$$t = \frac{\sigma_1 - \sigma_3}{2} \qquad [5\text{-}10]$$

and normal stress is given by:

$$s = \frac{\sigma_1 + \sigma_3}{2}, \qquad [5\text{-}11]$$

which yielded a linear relationship of $t = f(s)$, shown as the K_f-line in Figure 5-7. This relationship was used to calculate the internal friction angle where:

$$\tan\alpha = \frac{t}{s} = \frac{\frac{\sigma_1-\sigma_3}{2}}{\frac{\sigma_1+\sigma_3}{2}} \qquad \text{and} \qquad [5\text{-}12]$$

cohesion: $c_\alpha = t - s \times \tan\alpha$ [5-13]

The Kf line, however, cut Mohr's circle at point X (Figure 5-7) with slope α and was not tangent as the failure envelope. The values of α and c_α can be converted to φ and c with the following equations:

$$\varphi = \sin^{-1}(\tan\alpha) \qquad [5\text{-}14]$$

$$c = \frac{c_\alpha}{\cos\varphi} \qquad [5\text{-}15]$$

5.5 Quality Assurance

5.5.1 Repeatability tests

Tests were conducted to verify the repeatability of the experimental procedure. A total of three tests were carried out on pure sand with no inclusions. They were conducted at a confining pressure of 75kPa, following the sample preparation and testing procedure as described in this chapter. The results, presented in the following chapter, indicated that the procedure was repeatable irrespective of the pressure and material.

5.5.2 Quality control

The following measures were taken to ensure uniformity in the experimental process and procedures in order to achieve the highest quality and integrity for the output data obtained:

1) The calibration of the instrument was confirmed with the laboratory manager who maintains all equipment in the facility.
2) All equipment used was cleaned and checked for physical deformations at the beginning and periodically during the testing program. This included confirming the drop height of the tamper used, checking the triaxial tubes for any leaks, ensuring scales are on level surfaces, etc.
3) All the sand used was taken from a single batch obtained from a Cape Town based quarry to ensure consistency in the soil characteristics for all the test samples.
4) Sand which had been dried was placed in an airtight container and used within 48hours to avoid moisture absorption as a result of hygroscopy. Any unused soil which had been dried was discarded.

5) Soil fabric may have changed during testing and as a result any sand that was used for testing was discarded after a single test. No sand was reused to avoid any fabric change influences on the results.
6) Each test used new flakes or pellets to avoid influences of deformation of the inclusions on the test outcome.
7) Mixing of the flakes and pellets with soil was done in small enough quantities (per layer) and long enough to ensure random inclusion.
8) A process called 'bleeding' was conducted on the triaxial tubes linking the chambers to the cell before each test, to remove all trapped air. This was to avoid pumping air into the triaxial cell when the confining pressures were being adjusted. This adjustment process was achieved using only water from the chamber.
9) The test specimen was prepared and tested immediately. No prepared specimen was left standing or unattended.

6 RESULTS AND DISCUSSION

6.1 Introduction

The results from the triaxial tests conducted using the recycled plastic, in the form of flakes and pellets, are presented in this chapter. A study is conducted on the effects of the different forms of LLDPE on the shear strength parameters as well as the influence of varying concentration and compaction effort on shear strength behaviour.

6.2 Repeatability results

Repeatability is the precision determined from multiple tests conducted under the same conditions and methods. The precision of the experiments conducted is defined as "the closeness of agreement between independent test results under stipulated test conditions" (ASTM E177 1992). This is determined using a repeatability limit denoted by r. The limit regulates systematic errors, which are caused by consistent errors in a particular direction, and random errors, which are caused by variations in the experiment which are unpredictable. It is the value below which the absolute difference between individual test results may be expected to occur with a probability of approximately 95% (ASTM E177, 1992). The closer to zero the value of r is, the higher the repeatability of the test. Any value higher than 1.00 is therefore considered to be unacceptable as this means that the probability of occurrence (i.e. repeatability) is lower than the required 95%.

Three tests were conducted on unreinforced sand samples at 75kPa confining pressure, with the results shown in Figure 6-1.

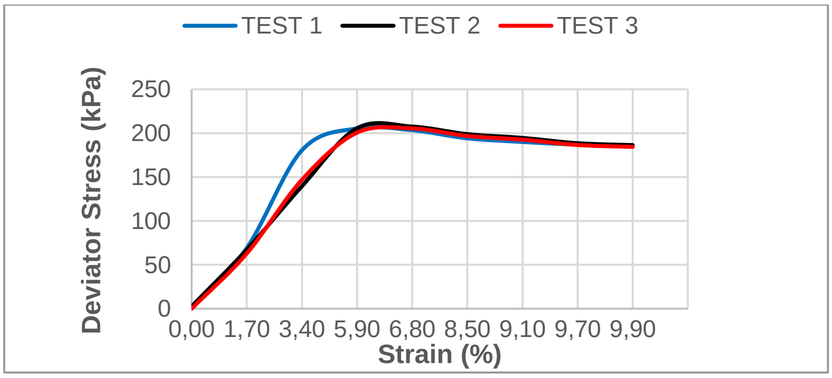

Figure 6-1: Repeatability tests on unreinforced soil

The strain and deviator stress at failure were determined, as per table 6-1 below, and the standard deviation (SD) calculated using equation 6-1. The repeatability limit was calculated using equation 6-2 taken from ASTM E177.

Table 6-1: Standard deviation and repeatability limits for triaxial tests

					Deviation from mean $(x-\mu)$			Error calculations	
Test #	**1**	**2**	**3**	**Mean**	**1**	**2**	**3**	**SD**	r
Strain at failure (%)	5.90	6.00	6.20	6.03	-0.13	-0.03	-0.17	0.152	0.421
Deviator stress at failure (kPa)	205.51	205.80	205.65	205.65	-0.14	0.16	0.00	0.145	0.061

$$SD = \sqrt{\frac{1}{N}\sum_{i=1}^{N}(x_i - \mu)^2} \quad [6\text{-}1]$$

$$r = 1.96\sqrt{2} \times SD \quad [6\text{-}2]$$

The r value for strain measurements was calculated to be 0.421%. This means that a change of at least 0.421% in strain was required for the triaxial apparatus to detect a change in shear stress at the 95% confidence interval. The deviator stress has a repeatability limit of 0.061kPa. A change of 0.061kPa is therefore the minimum change in deviator stress for which changes in shear stress can occur with a probability of approximately 95%. Both limits being below 1.00 gave the indication that the testing procedure was repeatable irrespective of the pressures and material.

6.3 Control tests

In determining the effect of the plastic inclusions on the soil shear strength and behaviour, control tests were conducted to form a comparative base from which an analysis could be conducted. These are tests that were done on unreinforced sand to establish the benchmark with which the reinforced soil behaviour could be compared. Figure 6-2 shows the stress-strain relationship of unreinforced sand at a low compaction effort. The peak deviator stresses were 218.8kPa at a confining pressure of 75kPa; 424.0kPa at 150kPa and 726.1 at 300kPa.

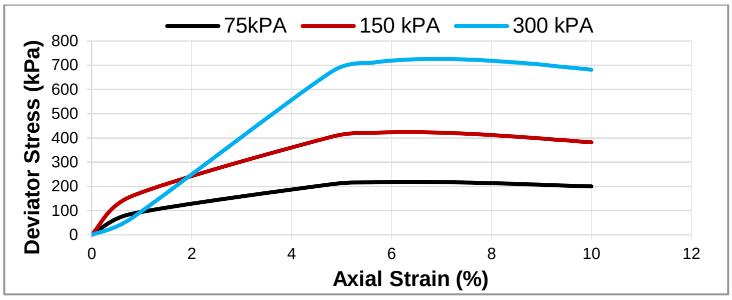

Figure 6-2: Stress-strain behaviour of unreinforced soil at LCE

The peak deviator stresses for high compaction effort were 231.6kPa, 448.8kPa and 772.6kPa at confining pressures of 75kPa, 150kPa and 300kPa as depicted in Figure 6-3.

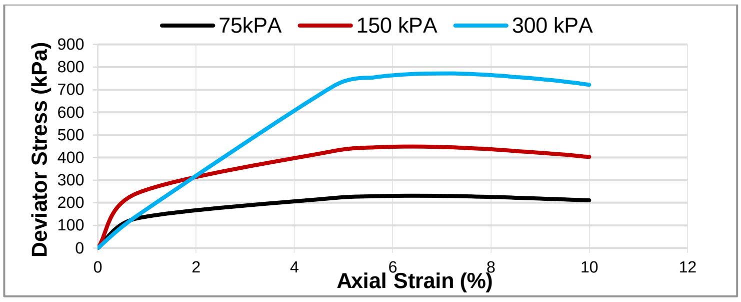

Figure 6-3: Stress-strain behaviour of unreinforced soil at HCE

A summary of the peak deviator stresses and strain at failure in table 6-2 shows the ratio of deviator stress to strain, which gives an indication of stiffness for the soil. There was a significant improvement in stiffness with an increase in confining pressures from stiffness ratio of 34.7 at 75kPa to 105 at 300kPa, for the low compaction effort tests. Higher ratios were recorded for the high compaction effort tests, across all confining stresses, starting from a ratio of 36.8 at 75kPa to 110.4 at 300kPa. This meant that increases in pressures and compaction effort resulted in improved stiffness.

Table 6-2: Deviator stress: Vertical strain ratio for unreinforced soil

Compaction effort	LOW			HIGH		
Confining pressure (kPa)	75	150	300	75	150	300
Deviator stress (kPa)	218.8	424.0	726.1	231.6	448.8	772.6
Strain (%)	6.3	6.3	6.9	6.3	6.3	7.0
Ratio	34.7	67.3	105.2	36.8	71.2	110.4

Figure 6-4 depicts the triaxial test results of unreinforced sand for the (a) low compaction effort and (b) high compaction effort at confining pressures of 75kPa, 150kPa and 300kPa.

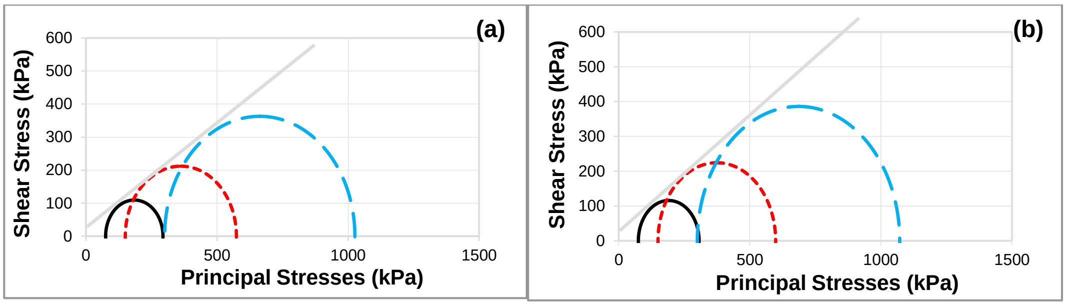

Figure 6-4: Shear strength envelope of unreinforced soil at (a) low compaction effort and (b) high compaction effort

From these results the angle of internal friction was determined from the slope of the line, as given in Appendix (9.1), to be 31.22° at low compaction effort (LCE) and 32.17° at high compaction effort (HCE), with apparent cohesions of 19.90kPa and 20.53kPa respectively.

6.4 Tests on reinforced sand

Triaxial compression tests were conducted on soil-plastic composite samples using randomly distributed plastic flake and plastic pellet inclusions at various concentration levels. The concentrations were determined as a percentage of the dry mass of the Cape Flats sand that was used. The flakes were mixed at 0.1%, 0.25%, 0.5%, 0.75% and 1.0% and the pellets mixed at 1%, 2%, 3%, 5%, 7.5% and 10%. The differences in the range are because of the higher mass of individual pellets. The tests were conducted on samples compacted with a low compaction effort (LCE) of 420kN-m/m^3 and a second set tested at a higher compaction effort (HCE) of 841kN-m/m^3. The confining pressures of 75kPa, 150kPa and 300kPa were used for the tests. The results of these tests are discussed separately for the flakes and pellets in the following sections.

6.5 Flake inclusions

The effect of the inclusions at concentrations of 0.1%, 0.25%, 0.5%, 0.75%, 1% on deviator stress at confining pressures of 75kPa, 150kPa and 300kPa was examined. This was followed by a detailed discussion on the various relationships which included the stress-strain behaviour of the soil-flake composite as well as the relationship between shear stress and normal stress.

6.5.1 Stress-strain behaviour

To analyse the stress-strain behaviour of soil-flake composite samples, the deviator stress was plotted against the vertical strain for specific concentrations between 0.1% and 1% tested at confining pressures of 75kPa, 150kPa and 300kPa. Figure 6-5 illustrates this behaviour for low compaction effort in (a), (b) and (c), as well as high compaction effort in (d), (e) and (f).

In these graphs, comparisons are drawn between the unreinforced sample and the samples with flake inclusions at specific concentration levels. There is an evident improvement in peak deviator stresses only at the low confining pressure of 75kPa with the higher confining pressures only reflecting improvements at 0.5%. The maximum peak deviator stress is recorded at the 300kPa confining pressure for the same level of concentration, for the sample subjected to the higher compaction effort.

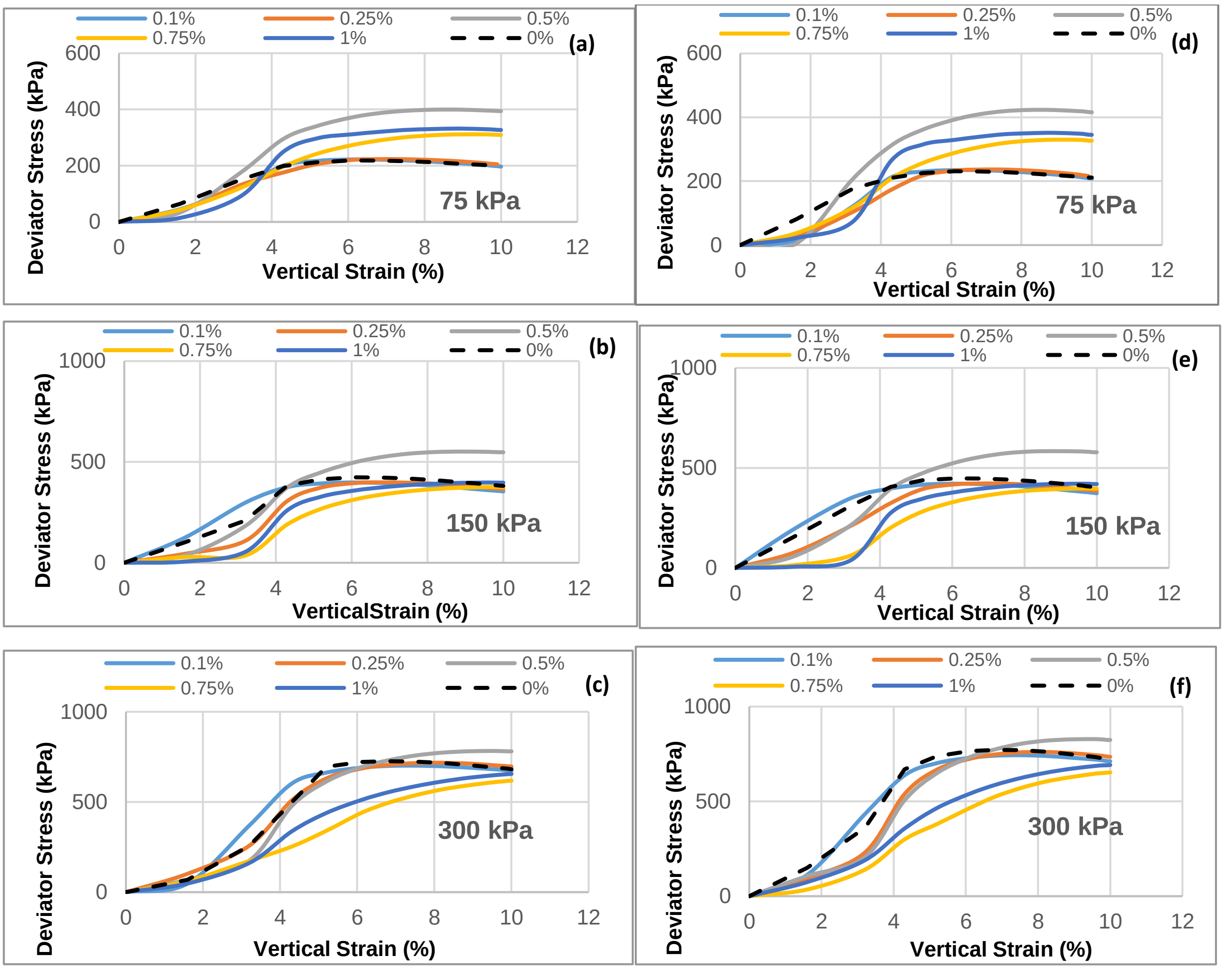

Figure 6-5: Stress-strain behaviour of reinforced soil for LCE and HCE

Figure 6-6 is a representation of the stress and strain relationship using a ratio of deviator to vertical strain at peak. This gives an indication of stiffness of the sample. The ratio is given for samples compacted with low effort in Figure 6-6 (a) and for those compacted with high effort in Figure 6-6 (b). At lower confining pressures both graphs show an increase in the ratio to a maximum at the 0.5% concentration. However, higher confining pressures reveal decreases in the stiffness ratio for both low and high compaction effort, to a minimum at the 0.75% concentration.

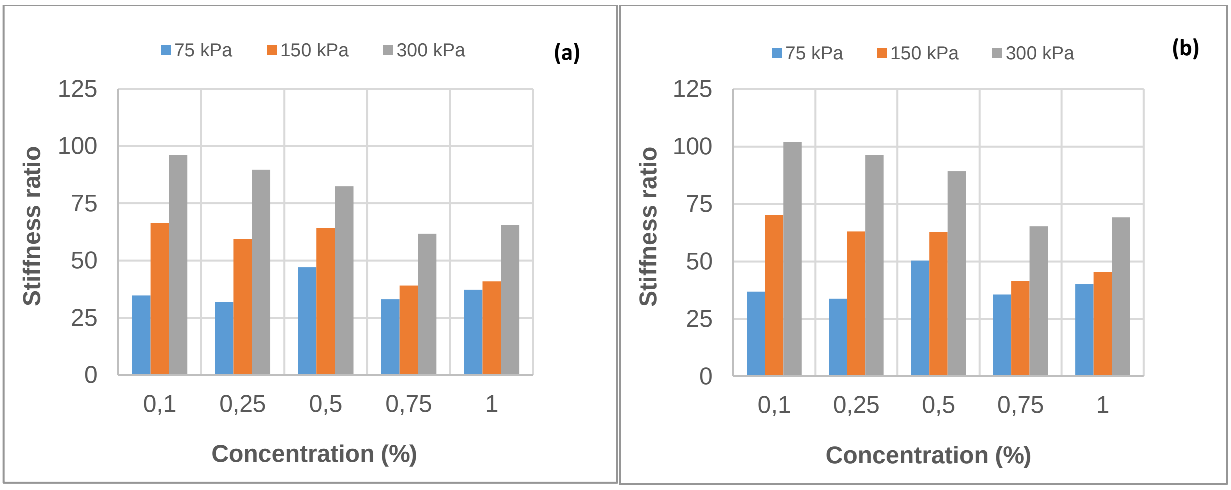

Figure 6-6:Concentration effects on stiffness for (a) LCE (b) HCE

6.5.2 Effects of concentration on deviator stress

A summary of the test results is provided in Table 6-3, which details the peak deviator stress, vertical strain at failure and the residual stress. Figure 6-6 is a plot of deviator stress against concentration for low compaction effort in (a) and a higher compaction effort in (c). A graphical representation of the relationship between residual stress and flake concentration levels is given in (b) for LCE and (d) for HCE. Both deviator and residual stresses show an increase to an optimum concentration level of 0.5%. This was applicable for both LCE and HCE.

The differences in peak and residual stresses were most notable at lower concentrations, with the largest being an 11% decrease at a concentration of 0.1% with a confining pressure of 150kPa for both LCE and HCE. Minimal or no decreases in peak stresses was experienced beyond the 0.5% concentration levels. This may be attributed to the tensile strength introduced by the flake inclusions, which increases with concentration resulting in minimal loss of soil strength after shearing.

Table 6-3: Summary of peak deviator stress, vertical strain at failure and residual deviator stress

		Peak deviator stress (kPa)		Vertical strain at failure (%)		Residual deviator stress (kPa)	
Concentration (%)	**Confining pressure (kPa)**	**LCE**	**HCE**	**LCE**	**HCE**	**LCE**	**HCE**
0	**75**	218.8	231.6	6.3	6.3	199.9	211.1
0.1		222.5	235.5	6.4	6.4	196.7	207.6
0.25		223.6	236.9	7.0	7.0	204.9	216.3
0.5		400.0	423.5	8.5	8.4	393.9	415.9
0.75		311.7	330.6	9.4	9.3	309.3	326.5
1		332.4	352.3	8.9	8.8	327.0	345.2
0	**150**	424.0	448.8	6.3	6.5	381.8	403.1
0.1		398.3	421.8	6.0	6.0	353.6	373.3
0.25		399.1	422.5	6.7	6.7	365.0	385.4
0.5		551.5	584.5	8.6	9.3	548.0	578.5
0.75		375.7	397.7	9.6	9.6	375.6	396.5
1		397.6	421.7	9.7	9.3	397.1	419.2
0	**300**	726.1	772.6	6.9	7.0	681.5	721.8
0.1		701.8	744.3	7.3	7.3	673.9	711.4
0.25		717.4	760.8	8.0	7.9	696.3	735.1
0.5		782.8	830.0	9.5	9.3	780.6	824.1
0.75		618.0	652.4	10.0	10.0	618.0	652.4
1		655.5	692.0	10.0	10.0	655.5	692.0

These results were compared to the unreinforced soil at the various confining pressures using a ratio to determine the effect of the inclusions on peak deviator stresses. The ratio compares the peak deviator stress of the unreinforced sample with the peak deviator stresses of the soil-flake composite samples. Table 6.4 provides the relationship between the unreinforced soil and reinforced soil.

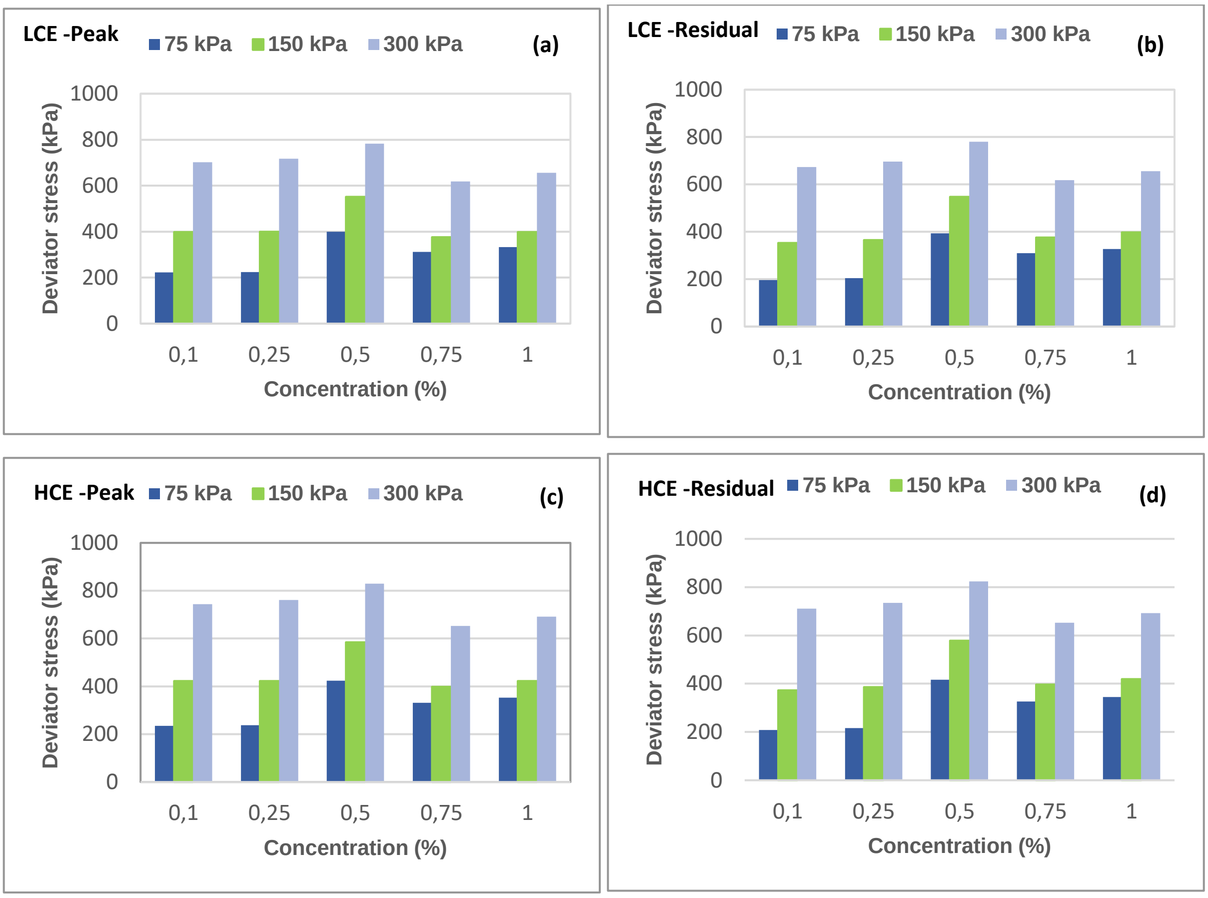

Figure 6-7: Peak deviator stresses (a) low compaction effort (c) high compaction effort and residual stresses (b) low compaction effort and (d) high compaction effort

Table 6-4: Concentration effects on peak deviator stress

PEAK DEVIATOR STRESS RATIO										
Confining Pressure (kPa)	**Concentration**									
	0.1%		**0.25%**		**0.5%**		**0.75%**		**1%**	
	LCE	**HCE**	**LCE**	**HCE**	**LCE**	**HCE**	**LCE**	**HCE**	**LCE**	**HCE**
75	1.0	1.0	1.0	1.0	1.8	1.9	1.4	1.6	1.5	1.6
150	0.9	0.9	0.9	0.9	1.3	1.4	0.9	0.9	0.9	0.9
300	1.0	1.0	1.0	1.0	1.1	1.2	0.9	0.8	0.9	0.9

Improvements in the peak deviator stresses were seen from concentrations of 0.5% and above, across all confining pressures. However, maximum influence occurred at the low confining pressure of 75kPa at the optimum 0.5% concentration.

6.5.3 Shear stress-normal stress behaviour

In analysing the relationship between shear stress and normal stresses, a plot of peak deviator stresses against normal principal stresses was obtained using the methodology in section 5.4. The major and minor principal stresses were used to draw Mohr's circles with the tangent defining the failure envelope for confining pressures 75kPa, 150kPa and 300kPa at flake concentrations varying from 0.1% to 1%. The apparent cohesion was given by the intercept on the vertical axis and the slope of the line giving the internal friction angle of the soil sample. Figure 6-8 depicts the failure envelopes for tests conducted on samples subjected to low compaction effort and Figure 6-9 for high compaction effort. In both cases, there is an evident departure from the linear failure envelope given by the results from the unreinforced samples tests in section 6.3, Figure 6.4.

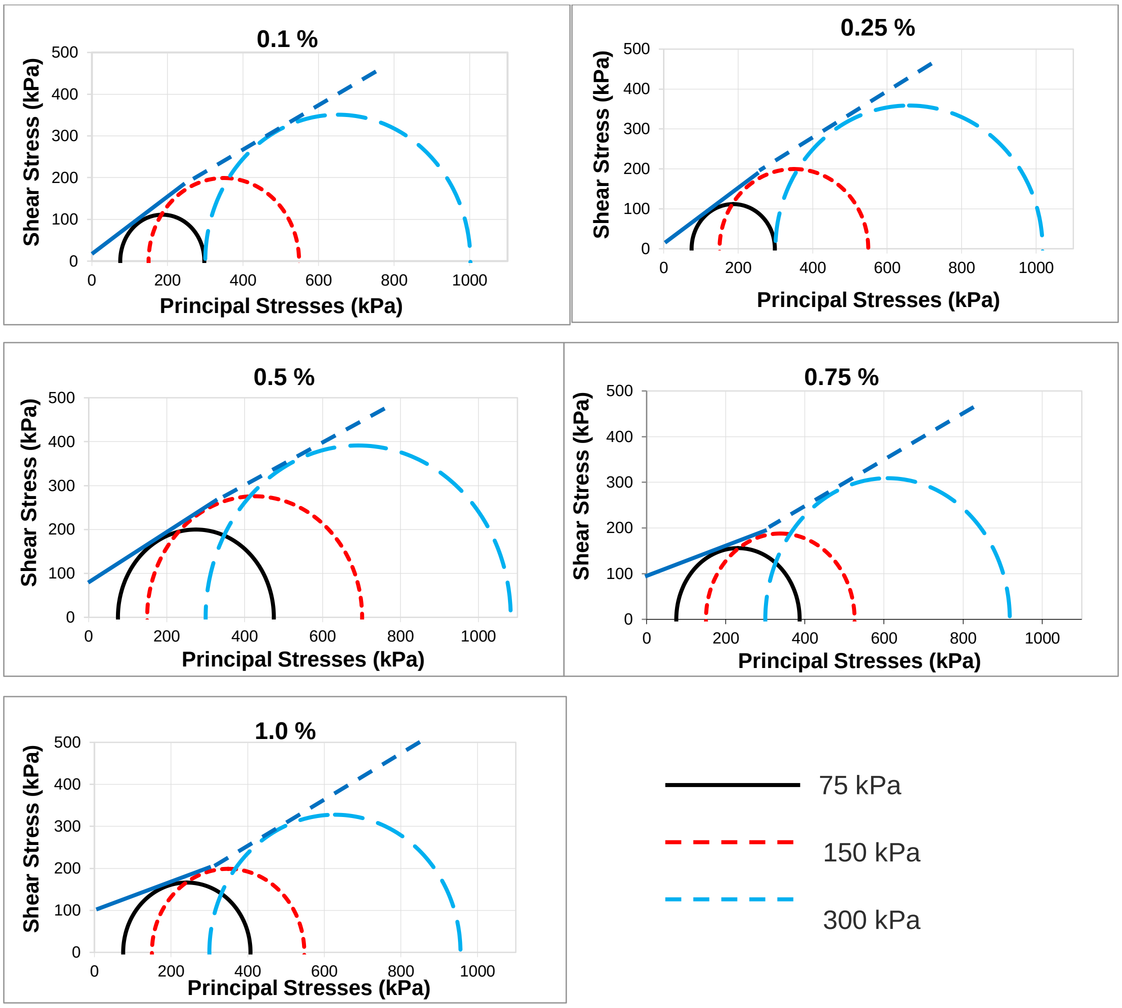

Figure 6-8:Failure envelopes for low compaction effort at various flake concentrations

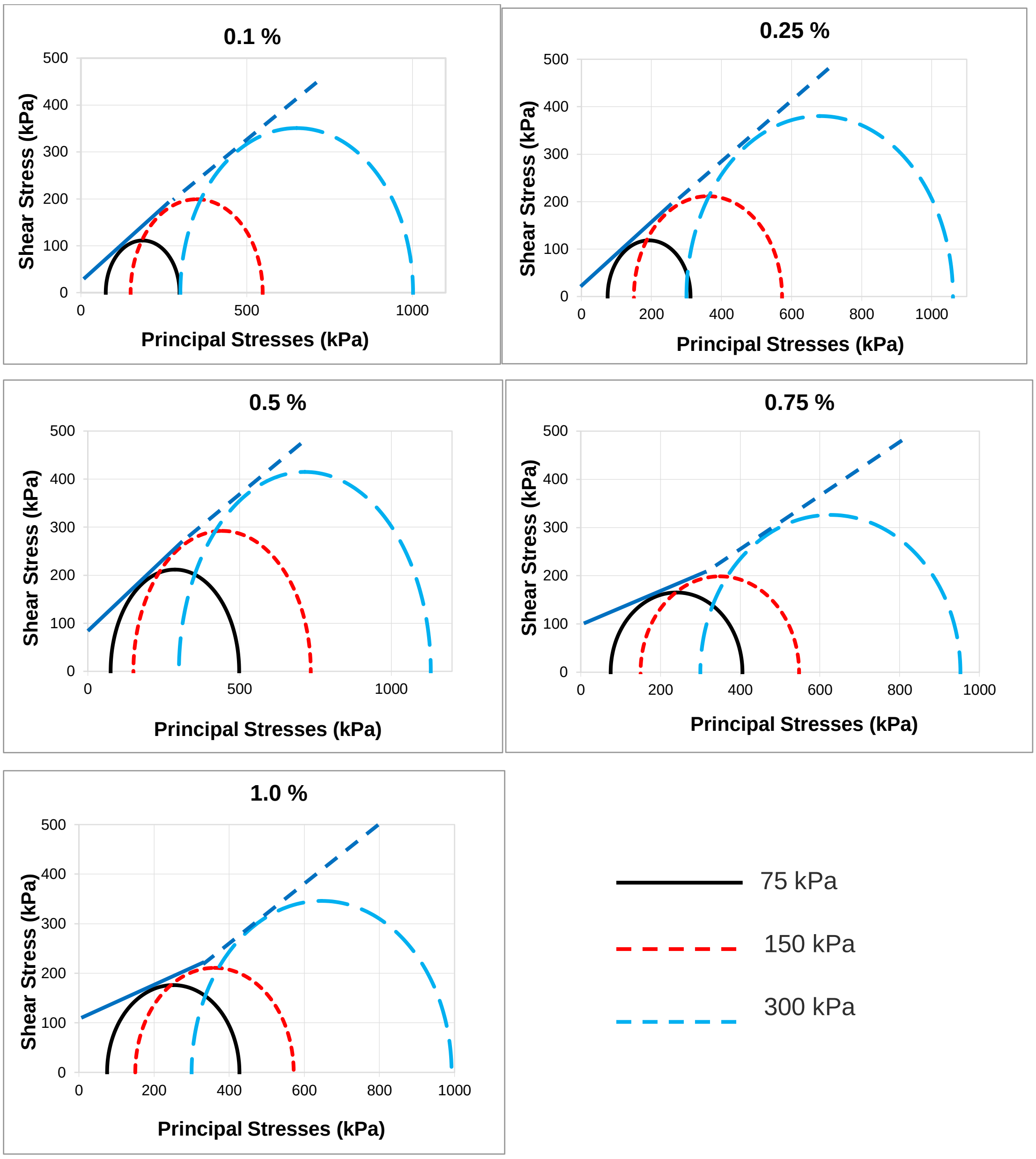

Figure 6-9:Failure envelopes for high compaction effort at various flake concentrations

Plots from the soil-flake triaxial tests showed bilinear failure envelopes with confining pressure increases, which became more pronounced with higher concentrations of the inclusions. At a certain confining pressure, the slope of the failure envelope changes, depicted by the change from a solid to a dashed line in Figures 6-8 and 6-9. Table 6-5 details these thresholds for the corresponding flake concentrations for the low and high compaction efforts.

Table 6-5: Threshold confining pressures for flake inclusions

Concentration (%)	LCE Threshold pressure (kPa)	HCE Threshold pressure (kPa)
0.1	238	275
0.25	250	300
0.5	283	304
0.75	268	285
1	285	272

The critical confining pressures were between 238kPa to 285kPa for LCE and ranged from 272kPa to 304kPa for HCE for the given concentration levels. The bilinear relationship is evidence of a change in behaviour before and after the threshold pressures. This may be governed by a change in the shearing mechanisms of the soil-flake composite. These results are consistent with the studies conducted by (Maher, Gray 1990, Zornberg 2002, Consoli, Heineck et al. 2007)

The tangent for the Mohr's circle formed the failure envelope from which the cohesion and friction angle could be obtained. The cohesion was given by the y-intercept and the slope of the tangent provided the internal angle of friction. Table 6-6 shows the values taken from the failure envelope.

Table 6-6: Shear parameters for flake inclusions

	Cohesion (kPa)		Friction angle (°)	
Concentration (%)	**LCE**	**HCE**	**LCE**	**HCE**
0.1	20.88	21.86	30.49	31.37
0.25	19.09	20.02	30.98	31.85
0.5	86.05	89.79	27.01	27.90
0.75	59.12	62.37	24.45	25.19
1.0	62.33	65.80	25.28	26.02

Concentration was plotted against these shear strength parameters for low and high compaction efforts. Figure 6-10 is graphical representation of the Figures obtained. In both cases it is evident that the behaviour between low and high compaction efforts does not change, with the exception that higher values were recorded for both parameters under HCE. An increase in cohesion to a maximum of 86kPa and 89kPa for LCE and HCE, respectively, at a concentration level of 0.5%. Internal friction angle in Figure 6-10 (b) reflected a constant decrease with the addition of the plastic flakes.

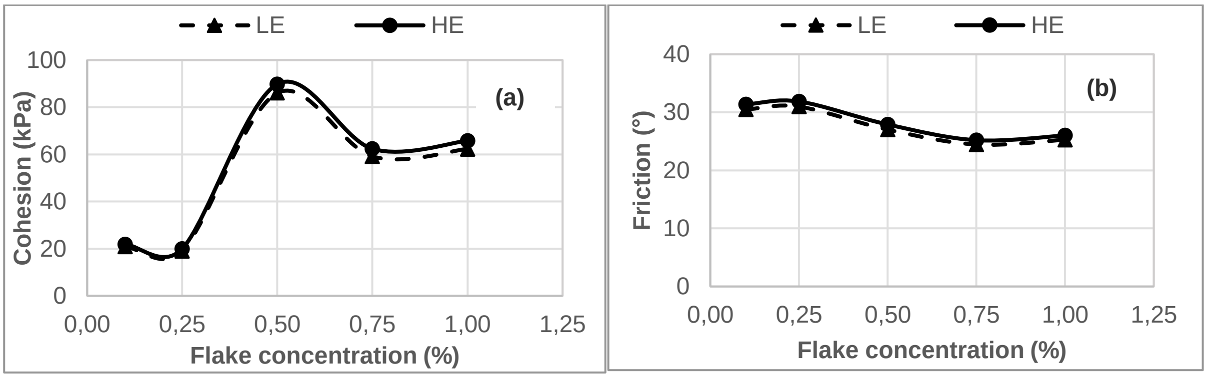

Figure 6-10: Changes in shear strength parameters with flake concentration

6.6 Pellet inclusions

The examination of results was conducted initially on the effect of the inclusions at concentrations of 1%, 2%, 3%, 5%, 7.5% and 10% on deviator stress at confining pressures of 75kPa, 150kPa and 300kPa, followed by a detailed discussion on the various relationships. These include the stress-strain behaviour of the soil with inclusions as well as the relationship between shear stress and normal stress.

6.6.1 Stress - strain behaviour

In the analysis of the stress-strain behaviour of soil samples the deviator stress was plotted against the vertical strain for specific concentrations between 1% and 10% tested at confining pressures of 75kPa, 150kPa and 300kPa. Figure 6-11 illustrates this behaviour for low compaction effort in (a), (b) and (c), as well as high compaction effort in (d), (e) and (f).

A study of these graphs, which are a comparison of the reinforced soil to the unreinforced specimen, indicates an improvement in peak stresses for confining pressures of 75kPa as well as 300kPa. This occurs at concentration percentages of 5 and 7.5 for the lower confining pressure and at 5% and 10% for 300kPa. The highest peak deviator stress was recorded at a concentration of 5% for 300kPa confining pressure on the soil that was subjected to high compaction effort. At 150kPa, (b) and (e), there is a notable decrease in deviator stresses for both low and high compaction efforts.

Figure 6-11 reflects an increase in confining pressures which results in higher deviator stress and strains at failure due to improvements in stiffness. The stiffness is a ratio of peak deviator stress to the vertical strain at failure.

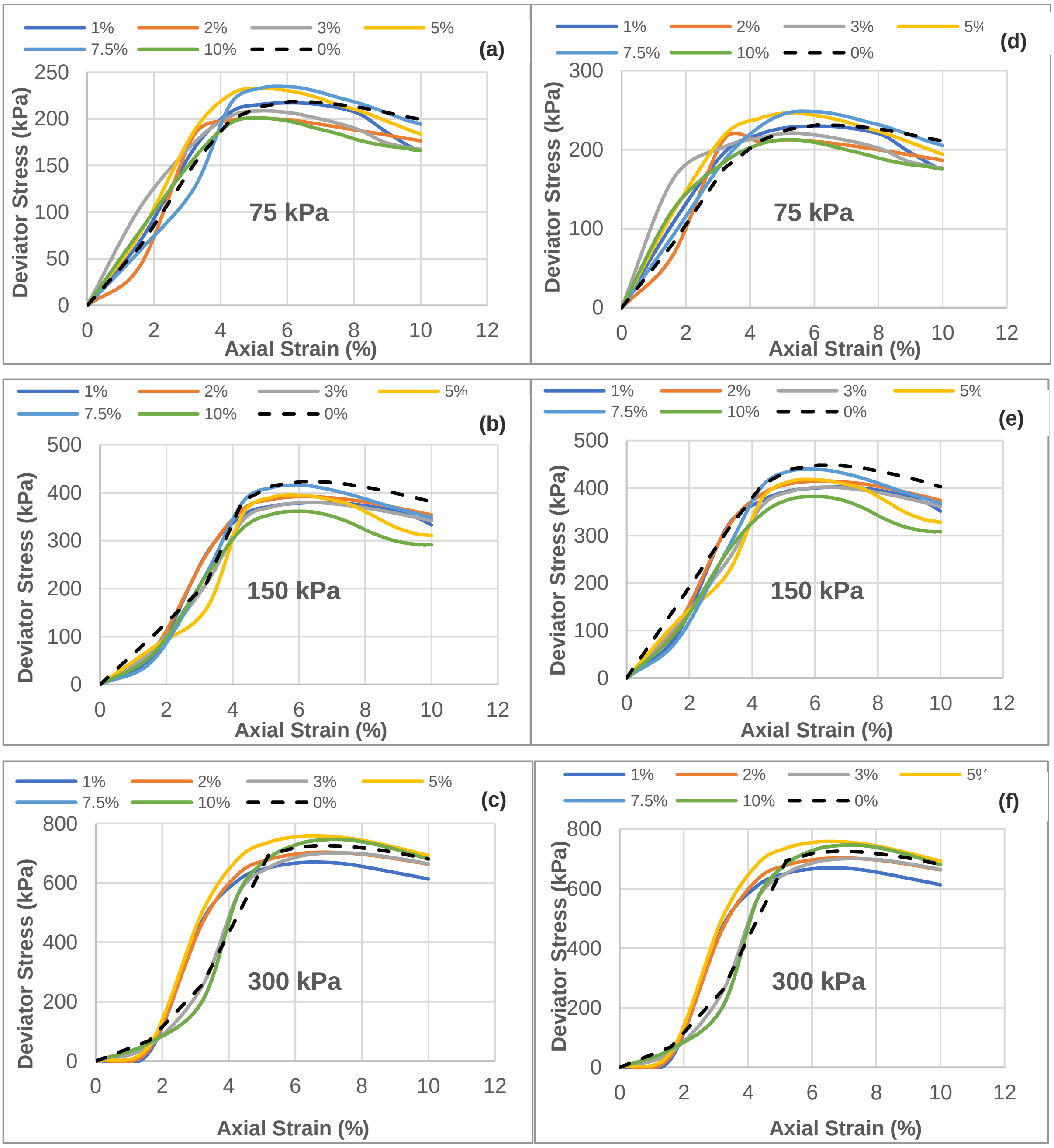

Figure 6-11: Stress-strain behaviour of reinforced soil for LCE and HCE

Figure 6-12 shows the effect of pellet concentration on the stiffness for confining pressures of 75kPa, 150kPa and 300kPa for (a) low compaction effort and (b) high compaction effort.

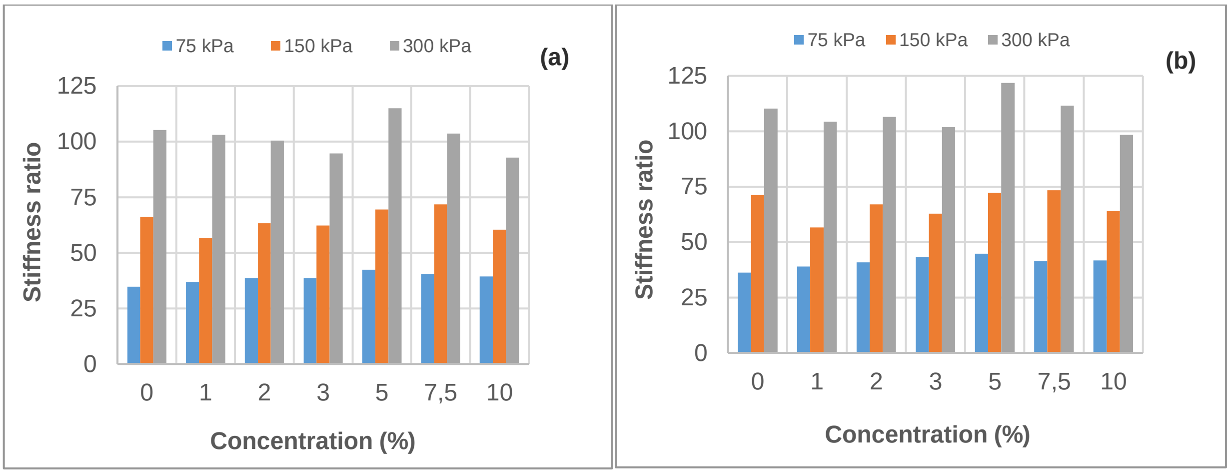

Figure 6-12: Concentration effects on stiffness for (a) LCE and (b) HCE

The stiffness ratio increased with an increase in confining pressure for both low and high compaction effort samples. At the low confining pressure, small improvements in stiffness are seen with an increase in pellet concentration to a maximum ratio of 42.4 (a) and 44.8 (b) at 5%, followed by a decrease for higher concentrations. The behaviour changes at higher confining pressures where there is an initial decrease in stiffness followed by an increase at 5% and a decline at higher concentrations.

6.6.2 Effects of concentration on deviator stress

A summary of the peak deviator stresses, vertical strains at failure and the residual stresses for the various concentrations and confining pressures is provided in table 6-7. A graphical representation of this table is provided in Figure 6-13 that plots deviator stress against concentration. These graphs reflected increases in (a) deviator and (b) residual stresses for low compaction efforts with peak deviator stresses reached at optimum concentrations of 5% for confining pressure of 75kPa and 7,5% for both confining pressures of 150kPa and 300kPa. This applies to the high compaction efforts results (c) and (d) where the concentrations for the peak deviator stresses were reached at the same optimum concentrations but reflected higher deviator stresses as per table 6-7.

Table 6-7: Summary of peak deviator stress, vertical strain at failure and residual deviator stress

		Peak deviator stress (kPa)		Vertical strain at failure (%)		Residual deviator stress (kPa)	
Concentration (%)	**Confining pressure (kPa)**	**LCE**	**HCE**	**LCE**	**HCE**	**LCE**	**HCE**
0	**75**	218.8	231.4	6.3	6.4	199.9	211.1
1		217.5	230.1	5.9	5.9	166.2	175.5
2		200.6	212.4	5.2	5.2	176.1	186.3
3		208.9	221.0	5.4	5.1	167.4	176.8
5		233.0	246.5	5.5	5.5	183.9	194.1
7.5		235.2	248.7	5.8	6	194.3	205.1
10		201.1	212.9	5.1	5.1	166.2	175.4
0	**150**	423.9	448.8	6.4	6.3	381.8	403.1
1		380.0	402.3	6.7	7.1	332.7	351.2
2		392.5	415.4	6.2	6.2	353.7	373.5
3		379.6	401.8	6.1	6.4	342.4	361.5
5		396.3	418.9	5.7	5.8	310.7	328.0
7.5		416.5	440.6	5.8	6	347.9	367.3
10		362.3	383.6	6	6	291.3	307.6
0	**300**	726.1	772.1	6.9	7.0	681.5	721.8
1		669.9	709.4	6.5	6.8	613.0	647.2
2		703.6	745.6	7	7	663.2	700.1
3		701.4	743.7	7.4	7.3	664.1	701.1
5		759.7	804.0	6.6	6.6	692.5	731.1
7.5		746.8	791.8	7.2	7.1	679.9	717.8
10		631.6	668.9	6.8	6.8	548.1	578.6

The maximum peak deviator stress was reached at the higher compaction effort with a confining pressure of 300kPa and an optimum pellet concentration of 5%. The highest residual stress depicts results which are consistent with maximum peak deviator stress findings for low compaction effort. A comparison of these results to the unreinforced soil was conducted for a closer examination at the various confining pressures using a ratio to determine the effect of the inclusions on peak deviator stresses.

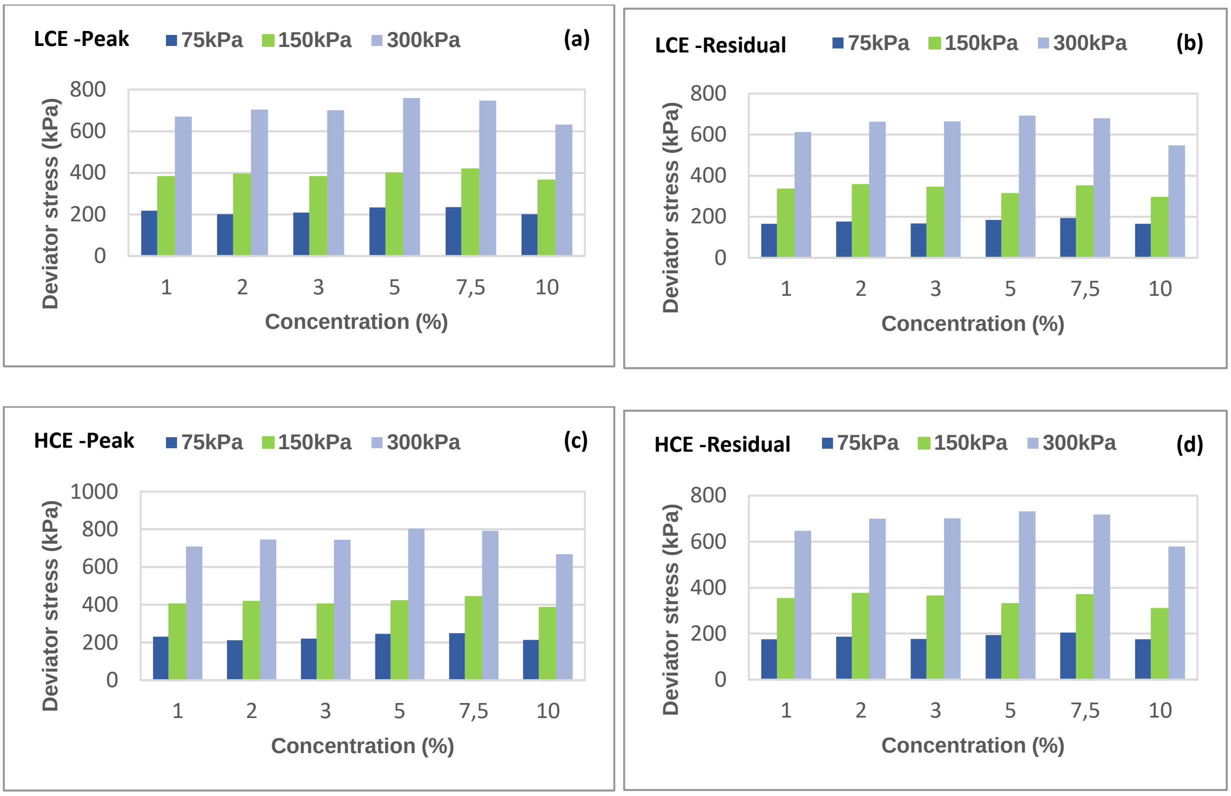

Figure 6-13: Peak deviator stresses (a) low compaction effort (c) high compaction effort and residual stresses (b) low compaction effort and (d) high compaction effort

Table 6-8: Concentration effects on peak deviator stress

PEAK DEVIATOR STRESS RATIO												
Confining Pressure (kPa)	**Concentration**											
	1%		**2%**		**3%**		**5%**		**7.5%**		**10%**	
	LCE	**HCE**	**LCE**	**HCE**	**LCE**	**HCE**	**LCE**	**HCE**	**LCE**	**HCE**	**LCE**	**HCE**
75	1.0	1.0	0.9	0.9	1.0	1.0	1.1	1.1	1.1	1.1	0.9	0.9
150	0.9	0.9	0.9	0.9	0.9	0.9	0.9	0.9	1.0	1.0	0.9	0.9
300	0.9	0.9	1.0	1.0	1.0	1.0	1.0	1.0	1.0	1.0	0.9	0.9

Table 6.8 provides the relationship between the unreinforced soil and reinforced soil. From the table, it can be seen that improvements in peak deviator stresses were experienced only at the low confining pressure of 75kPa for both the low and high compaction effort samples. At 150kPa and 300kPa the inclusions had no either impact or had resulted in decreases in peak stresses. Evident increases for these inclusions were at concentrations of 5% and 7.5% at 75kPa confining pressure.

6.6.3 Shear stress - normal stress behaviour

Plotting the shear stresses against principal stresses presented the failure envelopes in Figure 6-14 for low compaction effort and Figure 6-15 for high compaction effort. The pellet concentration was varied between 1% and 10% for the test conducted at confining pressures of 75kPa, 150kPa and 300kPa. An examination of the plots showed bilinear failure envelopes for the soils with inclusions compared to the linear envelope obtained from tests on the unreinforced sample in section 6.3, Figure 6-4.

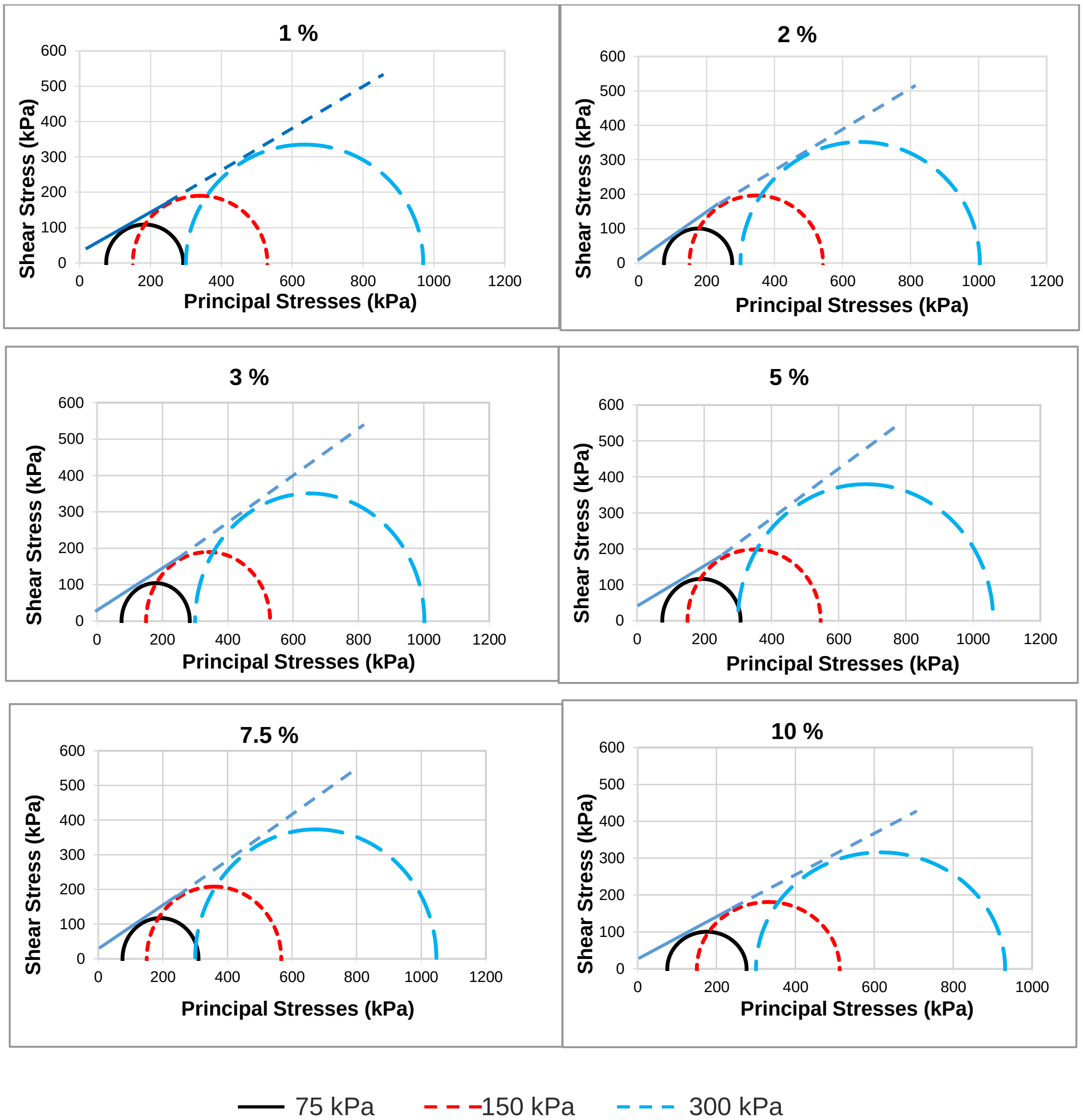

Figure 6-14: Failure envelopes for low compaction effort at various pellet concentrations

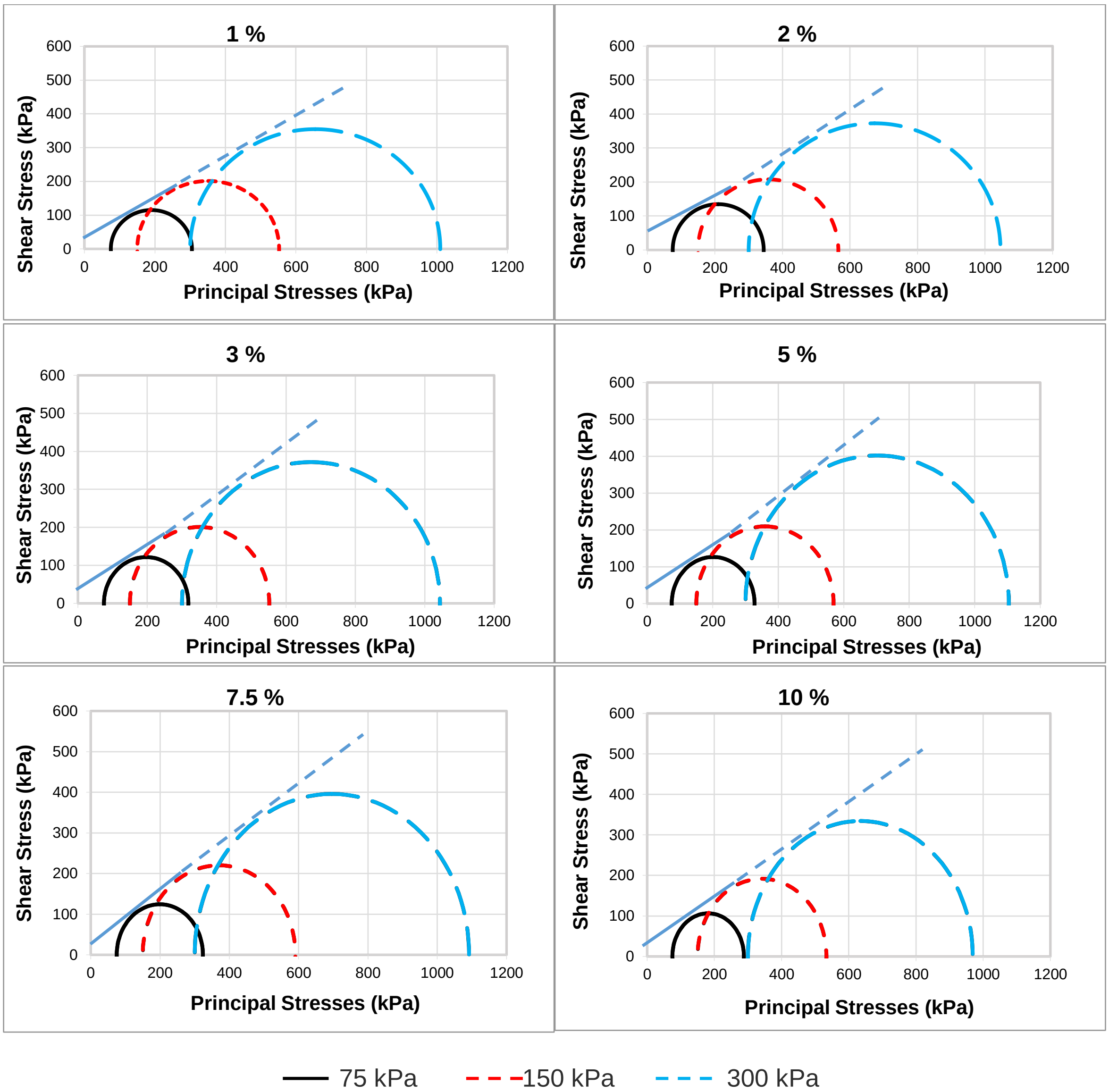

Figure 6-15: Failure envelopes for high compaction effort at various pellet concentrations

An analysis of the Mohr-Coulomb failure criterion presented in Figures 6.14 and 6.15 provided insight on the effects of confining pressure The tangents to the Mohr circle plots showed bilinear failure envelopes with confining pressure increases, which became more pronounced with higher concentrations of the inclusions. At a certain confining pressure, the slope of the failure envelope changes, depicted by the change from a solid to a dashed line in Figures 6-14 and 6-15. Table 6-9 details these confining pressures for the corresponding pellet concentrations for the low and high compaction efforts. There was an overall decrease in the threshold confining pressures with an increase in pellet concentration from 312.5 kPa at 1% concentration to 200kPa at 5% for LCE. The decrease for HCE was from 350kPa to 250kPa.

Table 6-9: Threshold confining pressures for pellet inclusions

Concentration (%)	LCE Threshold pressure (kPa)	HCE Threshold pressure (kPa)
1	312.5	350
2	250	270
3	275	250
5	200	275
7.5	230	250
10	262.5	225

The tangent for the Mohr's circle formed the failure envelope from which the cohesion and friction angle could be obtained. The cohesion was given by the y-intercept and the slope of the tangent provided the internal angle of friction. Table 6-10 shows the values taken from the failure envelope.

Table 6-10: Shear parameters for pellet inclusions

	Cohesion (kPa)		Friction angle (°)	
Concentration (%)	**LCE**	**HCE**	**LCE**	**HCE**
1	21.4	22.5	29.7	30.3
2	13.6	30.3	31.2	30.6
3	14.4	21.3	31.0	31.3
5	15.4	17.9	32.1	32.8
7.5	20.7	21.6	31.5	32.4
10	19.7	20.8	28.9	29.7

A graphical representation of these parameters is given in Figure 6-16 by plotting concentration against the cohesion (a) and friction angle (b) for both LCE and HCE. There was an initial decrease to 13.6 kPa in apparent cohesion for LCE followed by an increase to 20.7 kPa. The HCE curve showed an initial increase in cohesion to 30.3 kPa with a subsequent decrease to 20.8kPa.

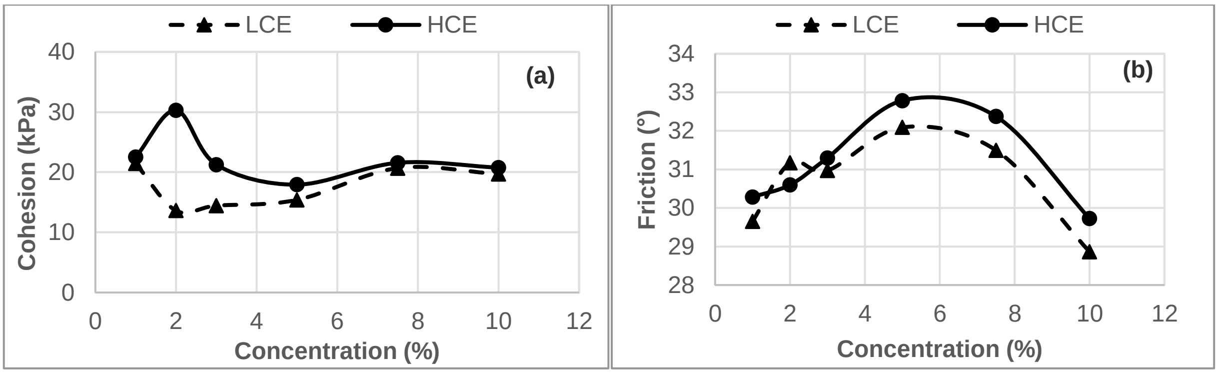

Figure 6-16: Changes in shear strength parameters with pellet concentration

Changes in the friction angle with increases in pellet concentration were as reflected in Figure 6-16 (b). This parameter increased from 29.7° at 1% to a maximum internal friction angle of 32.1° at 5% concentration for LCE. The values recorded for HCE were an increase to a maximum of 30.4° at concentration of 7.5%.

6.7 Results summary

When comparing the results between the unreinforced sand, flake reinforced sand and pellet reinforced sand the results are as depicted in Figures 6-17 to 6-18.

Figure 6-17 (a) and (b) below shows that flake inclusions increase the cohesion parameter, as opposed to the pellets which only show an increase at the higher compaction effort.

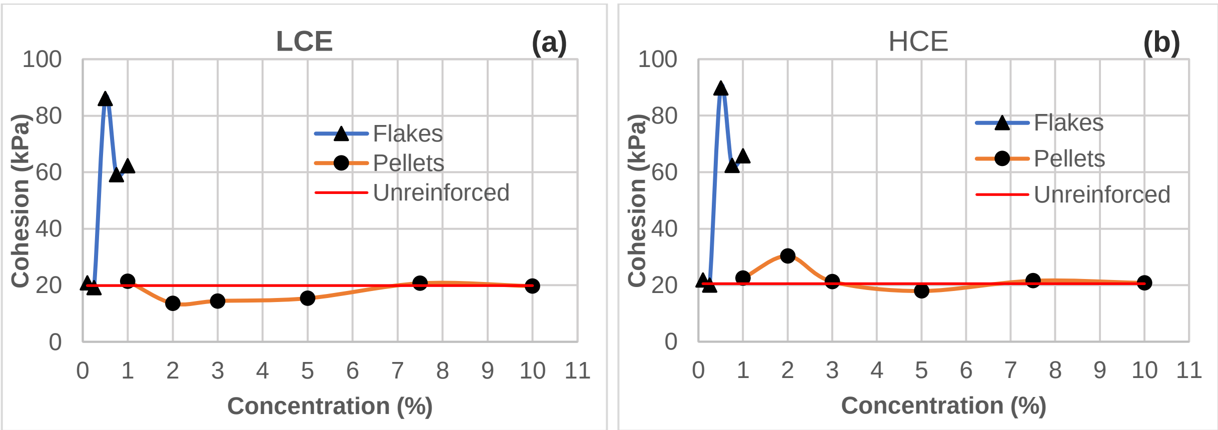

Figure 6-17: Comparison of cohesion between flake and pellet inclusions under (a) low compaction effort and (b) high compaction effort

The effects of the inclusions on internal friction angle parameter are different in that the flake inclusions cause a decrease and the pellets show an improvement to an optimum concentration (Figure 6-18 (a) and (b)).

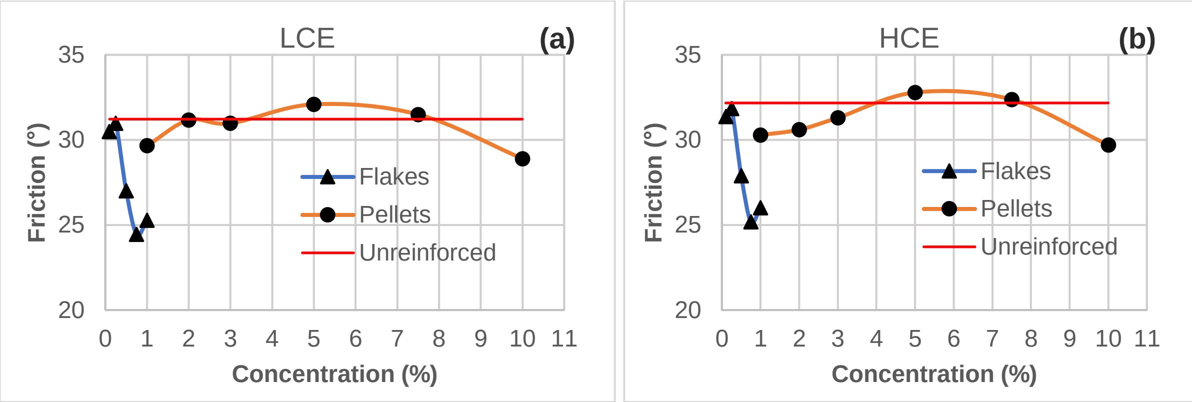

Figure 6-18: Comparison of internal friction angle between flake and pellet inclusions under (a) low compaction effort and (b) high compaction effort

In comparing the stress-strain relationships between the flakes and pellet inclusions, the stiffness ratio was used. The results are summarised in Figure 6-19 (a) to (c) for low compaction effort and Figure 6-20 (a) to (c) for high compaction effort. In both cases the pellet inclusions show improved stiffness at optimum concentration levels between 5% and 7.5% depending on the confining pressure.

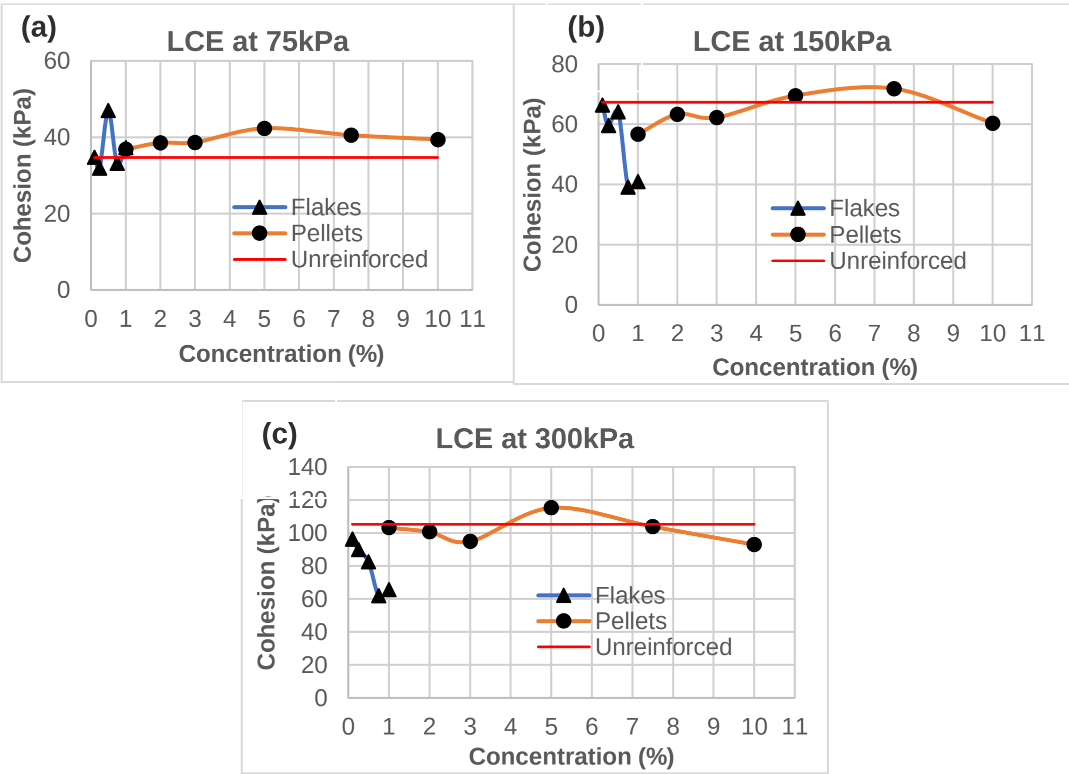

Figure 6-19: Comparison of stiffness ratio between flake and pellet inclusions at (a) 75 KPa (b) 150 kPa (c) 300 kPa confining pressures for low compaction effort

The flake inclusions show an initial improvement in the stiffness ratio at an optimum concentration of 0.5% at lower confining pressures. However, this ratio decreases at higher confining pressures, as shown in Figure 6-20 (b) and (c).

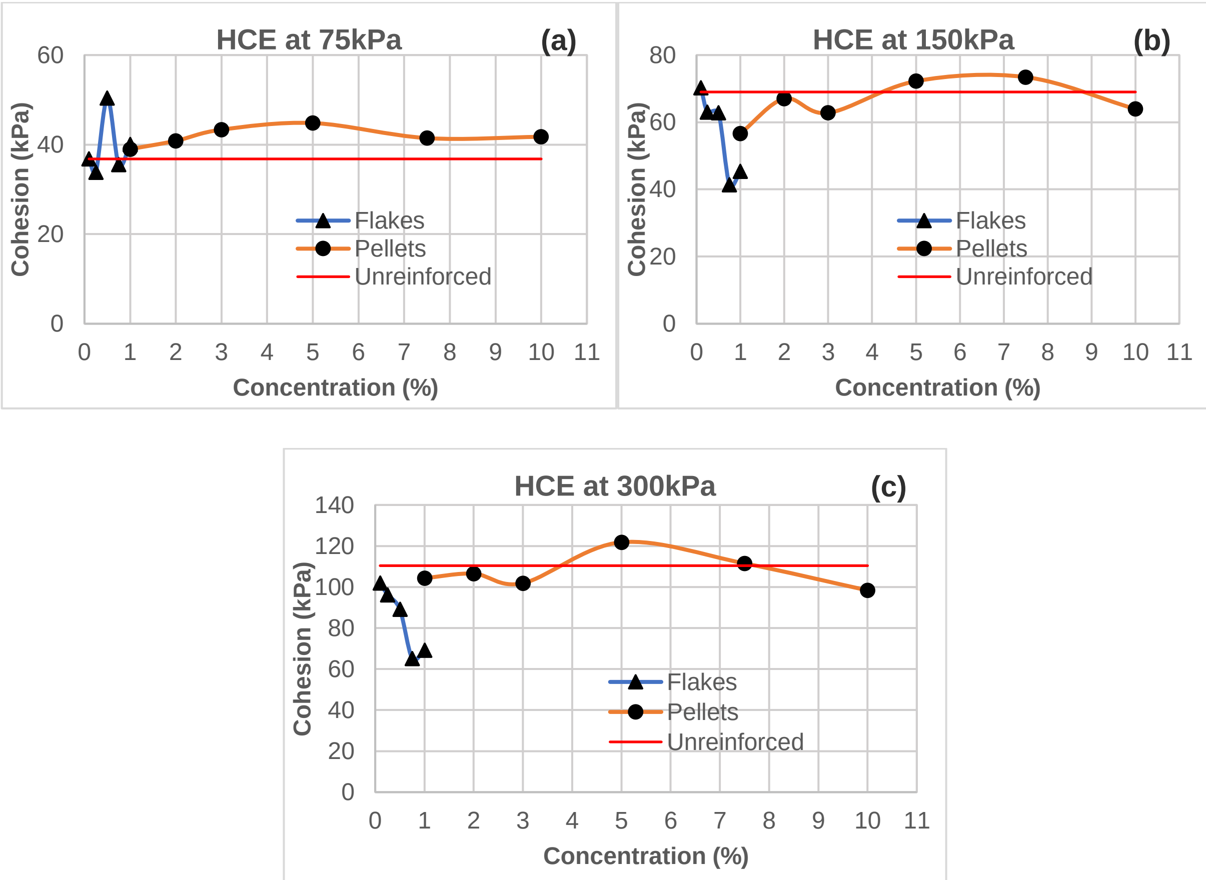

Figure 6-20: Comparison of stiffness ratio between flake and pellet inclusions at (a) 75 KPa (b) 150 kPa (c) 300 kPa confining pressures for high compaction effort

6.8 Application

Ground improvement techniques are often used in geotechnical engineering projects where poor soil conditions are encountered. Environmental and economic challenges have necessitated the use of alternative materials to serve this purpose and meet design specifications. The use of recycled plastic to improve the properties of geotechnical materials offers a multi-faceted engineering solution in that it addresses the environmental challenges by reducing waste and is economical as it uses existing processes and equipment as well as creating a new market. Utilisation of this material for soil reinforcement can be used in various geotechnical applications such as:

- Slope stabilisation
- Highway embankments
- Foundation material reinforcement for low cost housing
- Repairing landslides

In the evaluation of stability for embankments and foundations composed of granular materials such as Cape Flats sand used in this study, one of the critical properties is ultimate or peak shear strength (Reis Ferreira, Correia et al. 2016). In determining the effect of the inclusions used in this study on the peak shear strength, design examples are presented in the following sections. Rocscience Slide 7.0 software was used in the analysis, which has the capabilities of conducting 2D limit equilibrium analysis required for the design examples. Various methods exist for conducting the analysis, such as Spencer, Morgenstern-Price, Bishop simplified method, etc.

For the following design example, the Bishop method was selected because it is the most widely used method because of its simplicity. It is a method that divides the slope into slices to determine the factor of safety using vertical force and overall moment equilibriums about the centre of a trial surface. This is an iterative process for all the slices until the lowest factor of safety is determined. The equation used to calculate the factor of safety is:

$$F = \frac{1}{\sum(W \sin\alpha)} \sum \left[\left(c'b + \{W - ub\}\, tan\varphi' \frac{sec\alpha}{1 + (tan\alpha tan\varphi')/F} \right) \right]$$

Where F = Factor of safety

W = Slice self-weight (kN/m)

α = Angle from normal force to centre of individual slice (degrees)

c' = effective cohesion (kN/m^2)

b = Slice width (m)

μ = Pore water pressure (kN/m^2)

φ' = Effective internal friction angle (degrees)

6.8.1 Design example

This example is based on a roadway where the grading is raised 5m above the existing ground level. This is a low speed roadway with a single carriageway made of 3m lanes, as shown in Figure 6-21.

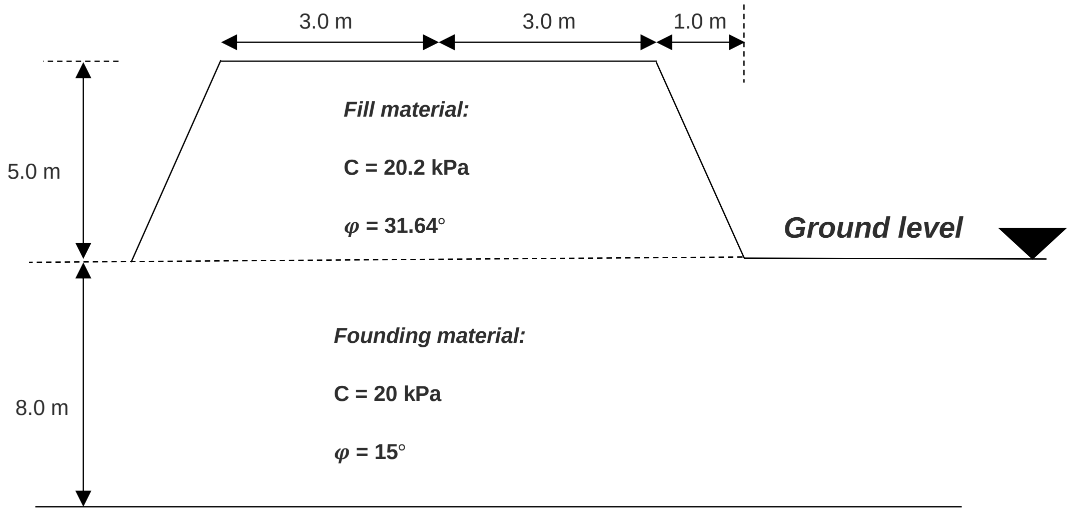

Figure 6-21: Schematic drawing of embankment

The embankment has a slope of 5V:1H, with unreinforced Cape Flats sand as the fill material and a silty clay soil as the founding material. With a water table well below the founding material and the soil being a free-draining granular material, pore water pressures effects can be disregarded for this analysis. The soil properties for the fill (taken from the control test results) and founding materials are summarised in Table 6-12.

Table 6-11: Design example material properties

Material	Dry unit weight ((kN/m			Cohesion (kPa)			Internal friction angle (°)		
				LCE	HCE	Average	LCE	HCE	Average
Fill	18.3	17.7	18.0	19.9	20.53	20.2	31.22	32.17	31.64
Founding	19.4			20.0			15.0		

The dry unit weight and the internal friction angle for the unreinforced Cape Flats sand (fill material) was determined during the testing stage. Although cohesion was shown to be 19.9kPa, this will be assumed to be zero for the design example as it is apparent cohesion. A soil model in Figure 6-22 shows the slope stability analysis for unreinforced fill material and no loading, which yielded a global factor of safety of 0.355.

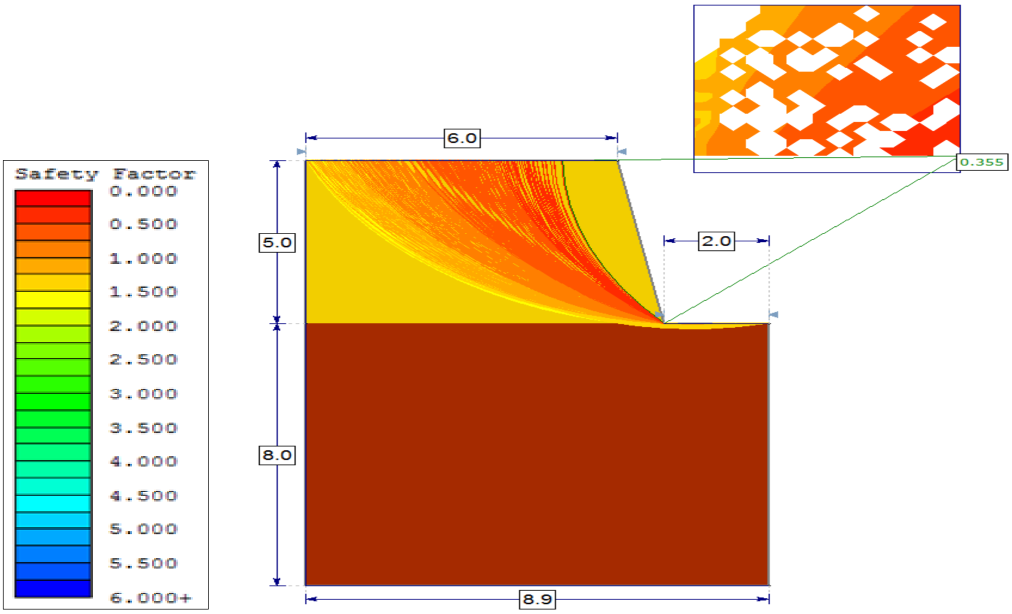

Figure 6-22: Design example model for unreinforced fill

Loading is then introduced in the form of two passenger vehicles with combined pressure of 29.44kPa in Figure 6-23. This is determined using the total mass of average car (1500kg) and average dimensions (length of 4.83m and width of 1.9m). The factor of safety is reduced to 0.332.

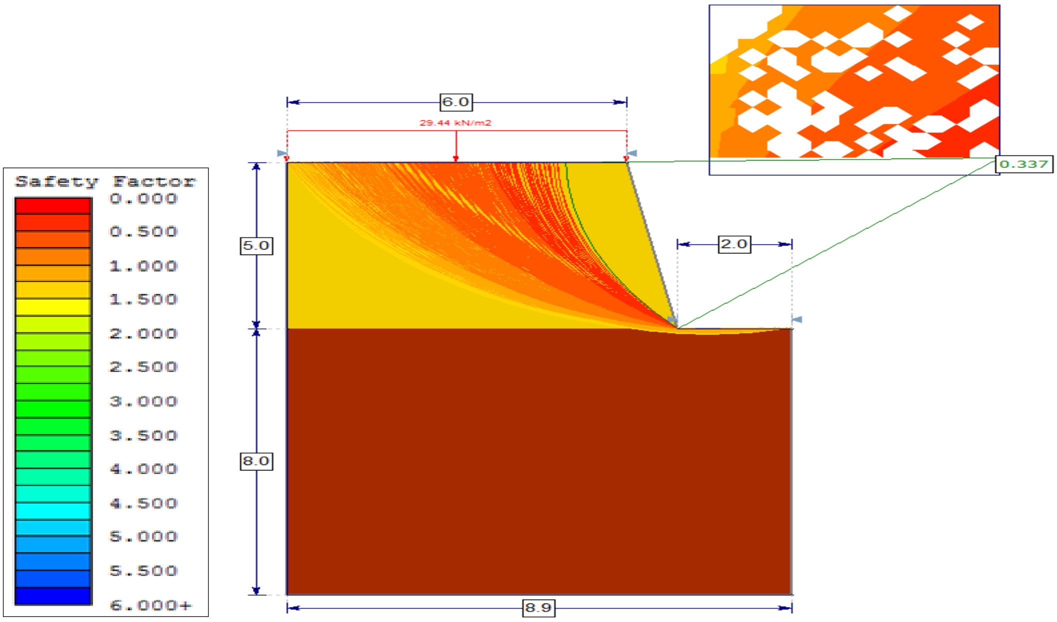

Figure 6-23: Design model for unreinforced fill with loading

For the reinforcement used we used the peak shear strength parameters for the optimum concentration for the flakes and pellets, separately as detailed in Table 6-13, for both low and high compaction efforts.

Table 6-12: Peak shear strength parameters used in model

Parameter	**Pellets**		**Flakes**	
	LCE	**HCE**	**LCE**	**HCE**
Cohesion (kPa)	27.5	38	75	75
Friction angle (degrees)	32.8	34.3	31.0	31.6
Unit weight (kN/m^3)	17.6	17.9	17.4	17.8

The results of the analysis showed in Figures 6-24 for pellet reinforced fill and Figure 6-25 for flake reinforced fill both reflect an improvement in the factor of safety from 0.332 to 1.452 and

2.940, respectively. These values are above the required minimum factor of safety of 1.25 (South African Institution of Civil Engineers,Geotechnical Division 1993)

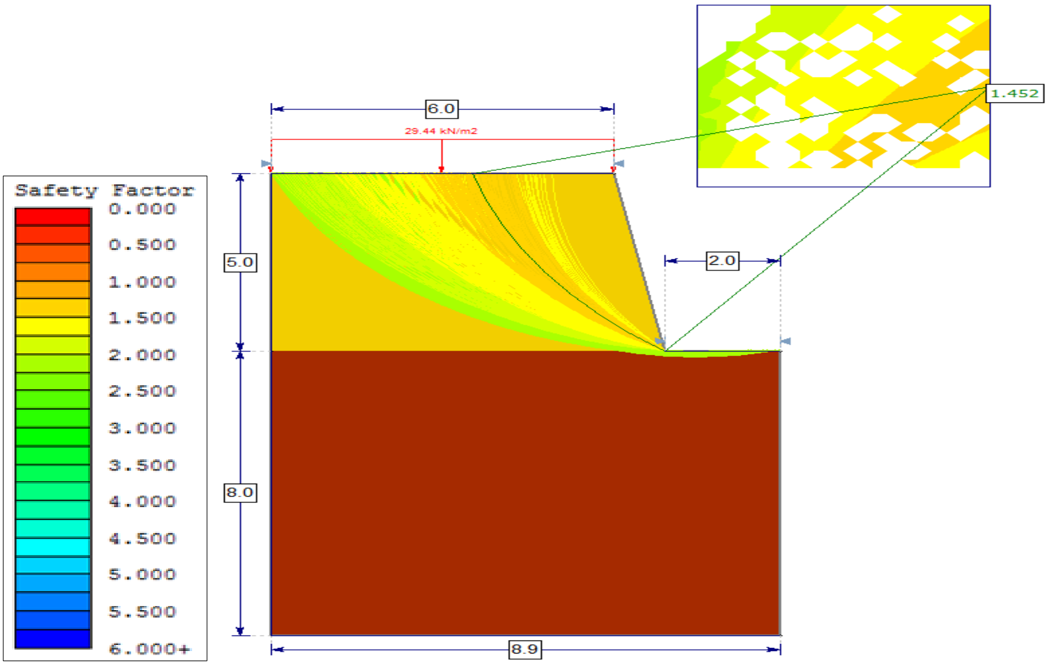

Figure 6-24: Minimum slip plane for pellet reinforced fill

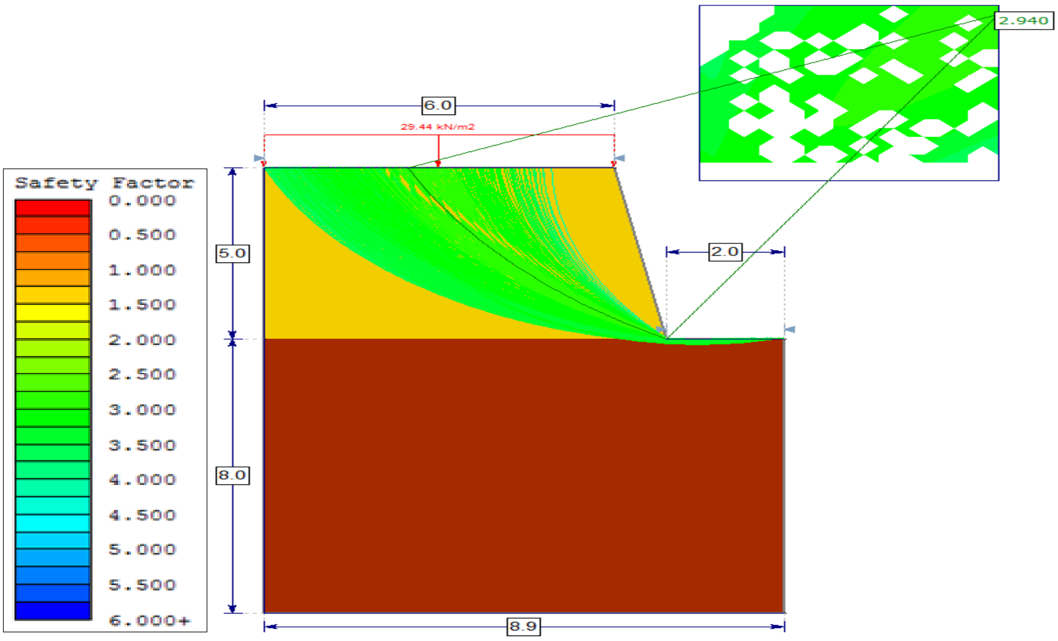

Figure 6-25: Minimum slip plane for flake reinforced fill

7 CONCLUSIONS AND RECOMMENDATIONS

7.1 Introduction

The necessity for this investigation stems from the need to find multi-faceted engineering solutions for soil reinforcement that are economical and address environmental challenges whilst meeting design specifications. It was a study into the effects of incorporating recycled plastic waste into Cape Flats sand. Two products from the recycling process were used. These were plastic flakes extracted at mid-stage and the other was the final product of the process in the form of pellets. Triaxial compression tests were conducted at confining pressures of 75kPa, 150kPa and 300kPa. The following conclusions can be made for the results presented in chapter 6.

7.2 Summary of conclusions

1. The study demonstrated increases in peak deviator stresses for both the pellets and flakes to optimum levels of concentration of 5% and 0.5%, respectively. Maximum stiffness for the soil-pellet composite was recorded at 5%, whereas there was an evident decrease for the soil-flake composite with higher levels of concentration.
2. The failure envelope of the unreinforced soil was linear, whereas the soil-plastic composites reflected bilinear envelopes. A threshold confining pressure was identified that defines the bilinear relationships. The soil-flake composite failure mechanism was characterised by slip and pull below this critical confining pressure. Above this pressure, failure is characterised by stretch and pull.
3. Increases in concentration of the pellets and flakes had different effects on the shear strength parameters, cohesion and internal friction angle. The soil-flake composite showed increases in cohesion with increased concentration up to optimum level of 0.5%, accompanied by a decrease in friction angle. However, increases in friction angle with concentration were reflected for the soil-pellet composite to at an optimum of 5%, with decreases in cohesion beyond this level. Therefore, increases in shear strength for the soil-flake composite are mainly due to improvements in cohesion, whereas friction is the main contributing factor for the soil-pellet composite. Randomly distributed pellets, therefore, serve mainly as frictional elements to the principal stresses in the Mohr-Coulomb envelope. This is supported by previous research conducted by Lin (2005) and Shukla, Sivajugan & Das (2009).

4. Increases in compaction effort showed improvements in both cohesion and internal friction angle for both soil composites.
5. In slope stability problems, there is an overall improvement in the factor of safety when soil is reinforced with flakes and pellets (as shown in the analysis in Figures 6-24 and 6-25) . The difference exists in that the soil-pellet composite reflects a higher global factor of safety at lower confining pressures, whereas the soil-flake composite shows a higher factor with pressures above the critical confining pressure.

It can therefore be said from these conclusions that the use of recycled plastic could be viable for use for soil reinforcement applications. With further investigations, this could offer a sustainable engineering solution that addresses economic and environmental challenges.

7.3 Recommendations

The following recommendations for further research are based on the results obtained from this study and will deepen insight with the aim of informing the feasibility of using recycled plastic in soil reinforcement applications.

1. The effects of the presence of water on the soil composites should investigated.
2. The use of 3D finite element analysis is an alternative that provides in-depth knowledge of deformations, which is specifically relevant for the soil-plastic composite. A focus towards this end will be an enhancement to the knowledge gained from the investigation that was conducted with this study.
3. This thesis focused on static loading. This can be further developed with an exploration on dynamic loading.
4. The effects of the reinforcement inclusions (flakes and pellets) on other soil properties such as drainage or permeability should be investigated.
5. Although plastic is not biodegradable, further studies in durability and potential damage due to prolonged exposure to UV light should be investigated.

8 REFERENCES

AGRU AMERICA INC., 2018-last update, AGRU Geocomposite. Available: https://agruamerica.com/products/geocomposite/.

AKBULUT, S., ARASAN, S. and KALKAN, E., 2007. Modification of clayey soils using scrap tire rubber and synthetic fibers. *Applied Clay Science,* **38**(1), pp. 23-32.

AL-REFEAI, T.O., 1991. Behavior of granular soils reinforced with discrete randomly oriented inclusions. *Geotextiles and Geomembranes,* **10**(4), pp. 319-333.

AL-REFEAI, T.O., 1991. Behavior of granular soils reinforced with discrete randomly oriented inclusions. *Geotextiles and Geomembranes,* **10**(4), pp. 319-333.

AL-SALEM, S., LETTIERI, P. and BAEYENS, J., 2009. Recycling and recovery routes of plastic solid waste (PSW): A review. *Waste Management,* **29**(10), pp. 2625-2643.

ANAGNOSTOPOULOS, C.A., PAPALIANGAS, T.T., KONSTANTINIDIS, D. and PATRONIS, C., 2013. Shear strength of sands reinforced with polypropylene fibers. *Geotechnical and Geological Engineering,* **31**(2), pp. 401-423.

ANDRADY, A.L. and NEAL, M.A., 2009. Applications and Societal Benefits of Plastics. *Philosophical Transactions: Biological Sciences,* **364**(1526), pp. 1977-1984.

ANKERTECHNIEK, 2016-last update, Punching shear reinforcement. Available: https://ankertechniek.com/product/punching-shear-reinforcement/.

ASTM D4253-00, 2000. *Standard Test Methods for Maximum Index Density and Unit Weight of Soils Using a Vibratory Table.* West Conshohocken, Philadelphia: American Society of Testing and Mate.

ASTM D4254-00, 2000. *Standard Test Method for Minimum Index Density and Unit Weight of Soil and Calculation of Relative Density.* West Conshohocken, Philadelphia: American Society of Testing and Materials.

ASTM D7181-11, 2011. *Standard Test Method for Consolidated Drained Triaxial Compression Test for Soils.* West Conshohocken, Philadephia: American Society of Testing and Materials.

ASTM E177, 1992. *Practice for Use of the Terms Precision and Bias in ASTM Test Method.* Philadelphia: American Society for Testing and Material.

AZWA, Z., YOUSIF, B., MANALO, A. and KARUNASENA, W., 2013. A review on the degradability of polymeric composites based on natural fibres. *Materials & Design,* **47**, pp. 424-442.

BABU, G.L.S. and CHOUKSEY, S.K., 2011. Stress–strain response of plastic waste mixed soil. *Waste Management,* **31**(3), pp. 481-488.

BACOT, J., ILTIS, M., LAREAL, P., PAUMIER, T. and SANGLERAT, G., 1978. Study of the soil reinforcement friction coefficient, *Symposium on Earth Reinforcement* 1978, ASCE, pp. 157-185.

BALEY, C., 2007-last update, High performance natural fibres. Available: http://www.jeccomposites.com/knowledge/international-composites-news/high-performance-natural-fibres.

BARNES, D.K.A., 2002. Biodiversity: invasions by marine life on plastic debris. *Nature,* **416**(6883), pp. 808-809.

BASU, D., MISRA, A., PUPPALA, A. and CHITTOORI, C., 2013. Sustainability in Geotechnical Engineering, *Proceedings of the 18th International Conference on Soil Mechanics and Geotechnical Engineering* 2013, pp. 2-6.

BENSON, C.H. and KHIRE, M.V., 1994. Reinforcing sand with strips of reclaimed high-density polyethylene. *Journal of Geotechnical Engineering,* **120**(5), pp. 838-855.

BLEDZKI, A.K. and GASSAN, J., 1999. Composites reinforced with cellulose based fibres. *Progress in polymer science,* **24**(2), pp. 221-274.

BOLT, H.M., 2005. Vinyl chloride—a classical industrial toxicant of new interest. *Critical reviews in toxicology,* **35**(4), pp. 307-323.

BONAPARTE, R., HOLTZ, R.D. and GIROUD, J., 1987. Soil reinforcement design using geotextiles and geogrids. *Geotextile testing and the design engineer.* ASTM International, .

BS SPECIALIST PRODUCTS, 2018-last update, EPS Geogrids. Available: http://www.corden-bssp.co.uk/product/eps-geogrids.

CHAUHAN, S., MITTAL, S. and MOHANTY, B., 2008. Performance evaluation of silty sand subgrade reinforced with fly ash and fibre. *Geotextiles and Geomembranes,* **26**(5), pp. 429-435.

CONSOLI, N.C., HEINECK, K.S., CASAGRANDE, M.D.T. and COOP, M.R., 2007. Shear strength behavior of fiber-reinforced sand considering triaxial tests under distinct stress paths. *Journal of Geotechnical and Geoenvironmental Engineering,* **133**(11), pp. 1466-1469.

CONSOLI, N.C., MONTARDO, J.P., PRIETTO, P.D.M. and PASA, G.S., 2002. Engineering behavior of a sand reinforced with plastic waste. *Journal of Geotechnical and Geoenvironmental Engineering,* **128**(6), pp. 462-472.

CRAIG, R.F., 2004. *Craig's soil mechanics.* CRC press.

DACHENG BUILDING MATERIAL, 2016-last update, PVC Geomembrane. Available: http://www.geotextile-fabrics.com/products/geomembrane/pvc-geomembrane.html.

DERRAIK, J.G., 2002. The pollution of the marine environment by plastic debris: a review. *Marine pollution bulletin,* **44**(9), pp. 842-852.

DIKGANG, J., LEIMAN, A. and VISSER, M., 2012. Analysis of the plastic-bag levy in South Africa. *Resources, Conservation and Recycling,* **66**, pp. 59-65.

EPA, 1990. *Report to Congress: Methods to manage and control plastic wastes.* EPA/530-SW-89-051. Washington D.C.: US Government Printing Office.

ESTABRAGH, A.R., BORDBAR, A.T. and JAVADI, A.A., 2013. A study on the mechanical behavior of a fiber-clay composite with natural fiber. *Geotechnical and Geological Engineering,* **31**(2), pp. 501-510.

FALORCA, I.M.C.F.G. and PINTO, M.I.M., 2011. Effect of short, randomly distributed polypropylene microfibres on shear strength behaviour of soils. *Geosynthetics International,* **18**(1), pp. 2-11.

FARRAG, K., ACAR, Y.B. and JURAN, I., 1993. *Pull-out resistance of geogrid reinforcements.*

GEDDE, U., 2013. *Polymer physics.* Springer Science & Business Media.

GENNARO, V., CEPPI, M., CROSIGNANI, P. and MONTANARO, F., 2008. Reanalysis of updated mortality among vinyl and polyvinyl chloride workers: Confirmation of historical evidence and new findings. *BMC public health,* **8**(1), pp. 21.

GEOCOMP CORPORATION, (n.d.). *Triaxial Software: User's Manual.* Acton, USA: .

GRAY, D.H. and AL-REFEAI, T., 1986. Behavior of fabric-versus fiber-reinforced sand. *Journal of Geotechnical Engineering,* **112**(8), pp. 804-820.

GRAY, D.H. and OHASHI, H., 1983. Mechanics of fiber reinforcement in sand. *Journal of Geotechnical Engineering,* **109**(3), pp. 335-353.

GRAY, D.H. and OHASHI, H., 1983. Mechanics of fiber reinforcement in sand. *Journal of Geotechnical Engineering,* **109**(3), pp. 335-353.

GREGORY, G. and CHILL, D., 1998. Stabilization of earth slopes with fiber reinforcement, *Proc., 6th Int. Conf. on Geosynthetics* 1998, International Geosynthetics Society, pp. 1073-1078.

GREGORY, M.R., 1978. Accumulation and distribution of virgin plastic granules on New Zealand beaches. *New Zealand Journal of Marine and Freshwater Research,* **12**(4), pp. 399-414.

GREGORY, M.R., 2009. Environmental implications of plastic debris in marine settings--entanglement, ingestion, smothering, hangers-on, hitch-hiking and alien invasions. *Philosophical transactions of the Royal Society of London.Series B, Biological sciences,* **364**(1526), pp. 2013-2025.

GUNDLE GEOSYNTHETICS, 2014-last update, HDPE geopipes. Available: http://www.gundlegeo.co.za/hdpe-geopipes/.

HAYASHI, S., YAMANOUCHI, T., OCHIAI, H. and SON, S., 1985. Mechanism of pullout resistance of polymer grids in soils. *Tsuchi-to-kiso, JSSMFE,* **33**, pp. 21-26.

HEARLE, J.W.S., 1963. The fine structure of fibers and crystalline polymers. III. Interpretation of the mechanical properties of fibers. *Journal of Applied Polymer Science,* **7**(4), pp. 1207-1223.

HEJAZI, S.M., SHEIKHZADEH, M., ABTAHI, S.M. and ZADHOUSH, A., 2012. A simple review of soil reinforcement by using natural and synthetic fibers. *Construction and Building Materials,* **30**, pp. 100-116.

INGOLD, T.S. and MILLER, K.S., 1983. Drained axisymmetric loading of reinforced clay. *Journal of Geotechnical Engineering,* **109**(7), pp. 883-898.

INGOLD, T.S., 1983. Laboratory pull-out testing of grid reinforcements in sand.

JEWELL, R., 1980. *Some effects of reinforcement on the mechanical behaviour of soils.* University of Cambridge.

JEWELL, R. and PEDLEY, M., 1990. A large scale experimental study of soil-reinforced interaction, Part 2. *Ground Engineering,* , pp. 44-50.

JOHN, M.J. and THOMAS, S., 2008. Biofibres and biocomposites. *Carbohydrate Polymers,* **71**(3), pp. 343-364.

JOHNSTON, R.S., 1985. *Pull-out testing of tensar geogrids.*

JONES, C.J.F.P., 1996. *Earth Reinforcement and Soil Structures.* 3rd edn. London: Thomas Telford.

JONES, C.J.F.P. and ZAKARIA, N.A., 1994. The use of geosynthetic reinforcement as a construction aid over super soft soils and voids, *Proc. 2nd Geotechnical. Eng. Conf.* 1994.

KALUMBA, D. and CHEBET, F., 2013. Utilisation of polyethylene (plastic) shopping bags waste for soil improvement in sandy soils. *Proc.18th ICSMGE,* .

KEDEL, 2014-last update, Paddock ground reinforcement grid, recycled plastic. Available: http://www.kedel.co.uk/drainage-and-ground-reinforcement/recycled-mixed-plastic-paddock-reinforcement-grid-400-x-500-x-40.html.

KING, A.M., BURGESS, S.C., IJOMAH, W. and MCMAHON, C.A., 2006. Reducing waste: repair, recondition, remanufacture or recycle? *Sustainable Development,* **14**(4), pp. 257-267.

KLEIN, R., 2011. Material Properties of Plastics. Wiley Online Library, pp. 3-69.

KOCH, H.M. and CALAFAT, A.M., 2009. Human Body Burdens of Chemicals Used in Plastic Manufacture. *Philosophical Transactions: Biological Sciences,* **364**(1526), pp. 2063-2078.

KOERNER, R., 1986. Direct shear/pull-out tests on geogrids. *Report No.l, i Department of Civil Engineering, Drexel University, Philadelphia, Pennsylvania,* .

KOERNER, R.M., 2012. *Designing with geosynthetics.* Xlibris Corporation.

KOERNER, R.M., 2012. *Designing with geosynthetics.* Xlibris Corporation.

KOZLOWSKI, R., 2011. Handbook of natural fibers: processing and applications." vol. 2. *UK: Cambridge,* .

LAIST, D.W., 1997. Impacts of marine debris: entanglement of marine life in marine debris including a comprehensive list of species with entanglement and ingestion records. *Marine Debris.* Springer, pp. 99-139.

LANDTEK DESIGN BUILD INC, 2015-last update, Retaining walls. Available: http://www.landtekdesignbuild.com/?page_id=75.

LANG, I.A., GALLOWAY, T.S., SCARLETT, A., HENLEY, W.E., DEPLEDGE, M., WALLACE, R.B. and MELZER, D., 2008. Association of urinary bisphenol A concentration with medical disorders and laboratory abnormalities in adults. *Jama,* **300**(11), pp. 1303-1310.

LI, C. and ZORNBERG, J.G., 2012. Mobilization of reinforcement forces in fiber-reinforced soil. *Journal of Geotechnical and Geoenvironmental Engineering,* **139**(1), pp. 107-115.

LIBERTY ONESTEEL REINFORCING, 2016-last update, Deformed reinforcing bar. Available: http://www.reinforcing.com/our-products/bar/deformed-reinforcing-bar.

LIN, C., 2005. *Mechanical reponse of fibre-reinforced soil.* PhD edn. University of Texas.

LIN, C., 2005. *Mechanical response of fibre-reinforced soil.* PhD edn. University of Texas.

MAHER, M.H. and GRAY, D.H., 1990. Static response of sands reinforced with randomly distributed fibers. *Journal of Geotechnical Engineering,* **116**(11), pp. 1661-1677.

MALIAKAL, T. and THIYYAKKANDI, S., 2013. Influence of randomly distributed coir fibers on shear strength of clay. *Geotechnical and Geological Engineering,* **31**(2), pp. 425-433.

MARANDI, S., BAGHERIPOUR, M., RAHGOZAR, R. and ZARE, H., 2008. Strength and ductility of randomly distributed palm fibers reinforced silty-sand soils. *American Journal of Applied Sciences,* **5**(3), pp. 209-220.

MCGOWN, A., ANDRAWES, K. and AL-HASANI, M., 1978. Effect of inclusion properties on the behaviour of sand. *Geotechnique,* **28**(3), pp. 327-346.

MEEKER, J.D., SATHYANARAYANA, S. and SWAN, S.H., 2009. Phthalates and other additives in plastics: human exposure and associated health outcomes. *Philosophical transactions of the Royal Society of London.Series B, Biological sciences,* **364**(1526), pp. 2097-2113.

MICHALOWSKI, R.L. and CERMÁK, J., 2003. Triaxial compression of sand reinforced with fibers. *Journal of Geotechnical and Geoenvironmental Engineering,* **129**(2), pp. 125-136.

MIRAFTAB, M. and LICKFOLD, A., 2008. Utilization of carpet waste in reinforcement of substandard soils. *Journal of industrial textiles,* **38**(2), pp. 167-174.

MIRZABABAEI, M., MIRAFTAB, M., MOHAMED, M. and MCMAHON, P., 2012. Unconfined compression strength of reinforced clays with carpet waste fibers. *Journal of Geotechnical and Geoenvironmental Engineering,* **139**(3), pp. 483-493.

MOHANTY, A.K., MISRA, M. and HINRICHSEN, G., 2000. Biofibers, biodegradable polymers and biocomposites: an overview. *Macromolecular materials and Engineering,* **276**(1), pp. 1-24.

MUSTAPHA, A.M., 2008. Bamboo as soil reinforcement: A laboratory trial. *Leonardo Journal of Sciences,* **13**, pp. 69-77.

MYBURG, A., LEV-YADUN, S. and SEDEROFF, R., 2013-last update, Xylem Structure and Function. Available: http://www.els.net [doi: 10.1002/9780470015902.a0001302.pub2].

NATARAJ, M. and MCMANIS, K., 1997. Strength and deformation properties of soils reinforced with fibrillated fibers. *Geosynthetics International,* **4**(1), pp. 65-79.

NGUYEN, M.D., YANG, K.H., LEE, S.H., WU, C.S. and TSAI, M.H., 2013. Behavior of nonwoven-geotextile-reinforced sand and mobilization of reinforcement strain under triaxial compression. *Geosynthetics International,* **20**(3), pp. 207-225.

NICHOLSON, P.G., 2014. *Soil improvement and ground modification methods.* Butterworth-Heinemann.

OCHIAI, H., OTANI, J., HAYASHIC, S. and HIRAI, T., 1996. The pull-out resistance of geogrids in reinforced soil. *Geotextiles and Geomembranes,* **14**(1), pp. 19-42.

OEHLMANN, J., SCHULTE-OEHLMANN, U., KLOAS, W., JAGNYTSCH, O., LUTZ, I., KUSK, K.O., WOLLENBERGER, L., SANTOS, E.M., PAULL, G.C., VAN LOOK, K.J. and TYLER, C.R., 2009. A critical analysis of the biological impacts of plasticizers on wildlife. *Philosophical transactions of the Royal Society of London.Series B, Biological sciences,* **364**(1526), pp. 2047-2062.

O'ROURKE, T.D., DRUSCHEL, S.J. and NETRAVALI, A.N., 1990. Shear strength characteristics of sand-polymer interfaces. *Journal of Geotechnical Engineering,* **116**(3), pp. 451-469.

O'ROURKE, T., DRUSCHEL, S. and NETRAVALI, A., 1990. Shear strength characteristics of sand-polymer interfaces. *Journal of Geotechnical Engineering,* **116**(3), pp. 451-469.

PALMEIRA, E.M. and MILLIGAN, G.W., 1989. Large scale direct shear tests on reinforced soil. *Soils and foundations,* **29**(1), pp. 18-30.

PETERSEN, M., 2009. *Utilizing Consumer Polyethylene bags to reinforce soil.* Bachelor of Science edn. University of Cape Town.

PLASTICS FEDERATION OF SOUTH AFRICA, 2015. *It's all about plastic: Material of choice.*

POKHAREL, G., 1995. *Deformation and ultimate load of reinforced soil structures, theory and experiment.* Doctor of Engineering edn. Nagoya University, Japan.

PRABAKAR, J. and SRIDHAR, R.S., 2002. Effect of random inclusion of sisal fibre on strength behaviour of soil. *Construction and Building Materials,* **16**(2), pp. 123-131.

PRABAKAR, J., DENDORKAR, N. and MORCHHALE, R., 2004. Influence of fly ash on strength behavior of typical soils. *Construction and Building Materials,* **18**(4), pp. 263-267.

PRADHAN, P.K., KAR, R.K.R. and NAIK, A., 2012. Effect of random inclusion of polypropylene fibers on strength characteristics of cohesive soil. *Geotechnical and Geological Engineering,* **30**(1), pp. 15-25.

PROACT, 2013-last update, Tons of plastic bags destined for new product production thanks to growing sort effort by Proact's people with disabilities. Available: http://www.proactinc.org/news-recycling-effort-bags.html.

RANJAN, G., VASAN, R.M. and CHARAN, H.D., 1994. Behaviour of plastic-fibre-reinforced sand. *Geotextiles and Geomembranes,* **13**(8), pp. 555-565.

RAVISHANKAR, U. and RAGHAVAN, S., 2004. Coir stabilised lateritic soil for pavements, *Indian geotech conf, Ahmedabad, India* 2004.

RECYCLING FACTS GUIDE, 2016-last update, Innovative new methods of plastic recycling. Available: https://www.recyclingfactsguide.com/wp-content/uploads/2010/06/methods-plastic-recycling.jpg.

REIS FERREIRA, S.M., CORREIA, A.G. and ROQUE, A.J., 2016. Strength of Non-traditional Granular Materials Assessed from Drained Multistage Triaxial Tests. *Procedia Engineering,* **143**(Supplement C), pp. 67-74.

ROWE, R., HO, S. and FISHER, D., 1985. Determination of soil-geotextile interface strength properties, *Proceedings of the 2nd Canadian Symposium on Geotextile and Geomembranes, Edmonton* 1985, pp. 25.

RYAN, P.G., MOORE, C.J., VAN FRANEKER, J.A. and MOLONEY, C.L., 2009. Monitoring the abundance of plastic debris in the marine environment. *Philosophical transactions of the Royal Society of London.Series B, Biological sciences,* **364**(1526), pp. 1999-2012.

S&P REINFORCEMENT INTERNATIONAL, 1999-last update, S&P C-Sheet 40. Available: http://www.sp-reinforcement.eu/en-CH/products/sheets/sp-c-sheet-240.

SADEK, S., NAJJAR, S.S. and FREIHA, F., 2010. Shear strength of fiber-reinforced sands. *Journal of Geotechnical and Geoenvironmental Engineering,* **136**(3), pp. 490-499.

SAMRIDHI PETROCHEM, 2015-last update, Geosynthetic clayliner. Available: http://www.samridhipetrochem.com/ProductDetail.aspx?catId=5&subCatId=18.

SARAN, S., 2010. *Reinforced soil and its engineering applications.* IK International Pvt Ltd.

SARSBY, R.W., 2007. Use of 'Limited Life Geotextiles'(LLGs) for basal reinforcement of embankments built on soft clay. *Geotextiles and Geomembranes,* **25**(4-5), pp. 302-310.

SCHLOSSER, F. and ELIAS, V., 1978. Friction in reinforced earth, *Symposium on earth reinforcement* 1978, ASCE, pp. 735-763.

SEPE, M., 2014-last update, Performance in Polyethytlene: Density Matters. Available: http://www.ptonline.com/columns/materials-performance-in-polyethylene-density-matters.

SHUKLA, S., SIVAKUGAN, N. and DAS, B., 2009. Fundamental concepts of soil reinforcement—an overview. *International Journal of Geotechnical Engineering,* **3**(3), pp. 329-342.

SIVAKUMAR, B. and VASUDEVAN, A.K., 2008. Strength and stiffness response of coir fiber-reinforced tropical soil. *Journal of Materials in Civil Engineering,* **20**(9), pp. 571-577.

SMITH, A.K.C., 1977. *Experimental and computational investigations of model reinforced earth retaining walls.,* .

SOBHEE, L., 2010. *Soil reinforcement using perforated plastic (polyethylene) waste.* Bachelor of Science edn. University of Cape Town.

SOCIETY FOR PLASTICS INDUSTRY, 2015-last update, SPI resin identification code - Guide to correct use. Available: https://www.plasticsindustry.org/AboutPlastics/content.cfm?ItemNumber=823.

SOUTH AFRICAN INSTITUTION OF CIVIL ENGINEERS,GEOTECHNICAL DIVISION, 1993. *Lateral support in surface excavations : code of practice 1989.* Yeoville: S.A Institute of civil engineers.

SWAMI, S., 2010. *Reinforced Soil and its Engineering Applications.* 1 edn. New Delhi: I.K. International Publishing House Pvt. Ltd.

SWAMY, R.N., 1984. *New reinforced concretes.* Surrey University Press.

SWAN, S.H., 2008. Environmental phthalate exposure in relation to reproductive outcomes and other health endpoints in humans. *Environmental research,* **108**(2), pp. 177-184.

SWAN, S.H., MAIN, K.M., LIU, F., STEWART, S.L., KRUSE, R.L., CALAFAT, A.M., MAO, C.S., REDMON, J.B., TERNAND, C.L., SULLIVAN, S., TEAGUE, J.L. and STUDY FOR FUTURE FAMILIES RESEARCH TEAM, 2005. Decrease in anogenital distance among male infants with prenatal phthalate exposure. *Environmental health perspectives,* **113**(8), pp. 1056-1061.

TALSNESS, C.E., ANDRADE, A.J., KURIYAMA, S.N., TAYLOR, J.A. and VOM SAAL, F.S., 2009. Components of plastic: experimental studies in animals and relevance for human health. *Philosophical transactions of the Royal Society of London.Series B, Biological sciences,* **364**(1526), pp. 2079-2096.

TANG, C., SHI, B., GAO, W., CHEN, F. and CAI, Y., 2007. Strength and mechanical behavior of short polypropylene fiber reinforced and cement stabilized clayey soil. *Geotextiles and Geomembranes,* **25**(3), pp. 194-202.

TESSILBRENTA, 2016-last update, Stopwave - river and marine erosion control. Available: http://www.erosioncontrolmethods.com/.

THOMPSON, R.C., MOORE, C.J., VOM SAAL, F.S. and SWAN, S.H., 2009. Plastics, the Environment and Human Health: Current Consensus and Future Trends. *Philosophical Transactions: Biological Sciences,* **364**(1526), pp. 2153-2166.

TIGERGRID GEOSYNTHETICS, 2015-last update, Geocell - a cost effecive solution for construction. Available: http://www.geogridfabric.com/geogrid/geocell.html.

TIMES FIBREFILL, 2012-last update, Geotouch - Non-woven geotextiles. Available: http://www.timesfiberfill.com/?page_id=123?product_cat=tech.

VAN FRANEKER, J.A., HEUBECK, M., FAIRCLOUGH, K., TURNER, D.M., GRANTHAM, M., STIENEN, E.W.M., GUSE, N., PEDERSEN, J., OLSEN, K.O. and ANDERSSON, P.J., 2005. *'Save the North Sea'Fulmar Study 2002-2004: a regional pilot project for the Fulmar-Litter-EcoQO in the OSPAR area,* .

VIDAL, H., 1969. The principle of reinforced earth. *Highway research record,* (282),.

WANYAMA, P., 2017. *Experimental Investigation on Shear Strength Behaviour of Polyethylene (Plastic) Reinforced Sand Under Triaxial Compression.* MSc Civil Engineering edn. University of Cape Town.

WESTLAKE CHEMICAL CORPORATION, (n.d.). *Linear Low Density Polyethylene: MSDS No. SC74853.* Houston, Texas: .

WILLIAMSON, C., 2012. *Investigation into the use of High Density Polyethylene shopping bag waste as a soil reinforcement material in fine-grained soil.* Bachelor of Science edn. Cape Town: University of Cape Town.

YAMASHITA, R. and TANIMURA, A., 2007. Floating plastic in the Kuroshio current area, western North Pacific Ocean. *Marine pollution bulletin,* **54**(4), pp. 485-488.

YARSLEY, V.E. and COUZENS, E.G., 1945. *Plastics.* Middlesex: Penguin Books LImited.

ZAIMOGLU, A.S. and YETIMOGLU, T., 2012. Strength behavior of fine grained soil reinforced with randomly distributed polypropylene fibers. *Geotechnical and Geological Engineering,* **30**(1), pp. 197-203.

ZORNBERG, J., 2002. Discrete framework for limit equilibrium analysis of fibre-reinforced soil. *Géotechnique,* **52**(8), pp. 593-604.

9 APPENDICES

A. Specific Gravity data

SPECIFIC GRAVITY DATA SHEET		
Pycnometer bottle no.	2	4
W_P = Mass of empty, clean pycnometer (g)	34.678	33.366
W_{PS} = Mass of empty pycnometer + dry soil (g)	46.398	45.395
W_B = Mass of pycnometer +dry soil+ water (g)	93.798	94.798
W_A = Mass of pycnometer +water (g)	86.529	87.309
Specific gravity (G_s)	2.63	2.65
Average specific gravity	2.64	

B. Minimum Density data

MINIMUM DENSITY DATA SHEET		
Sample number	1	2
Volume of mould (m^3)	0.00284	0.00284
Mass of empty mould (kg)	3.038	3.036
Mass of mould + sand (kg)	7.505	7.395
Mass of sand (kg)	4.467	4.359
Density (kg/m^3)	1572.887	1534.859
Average loosest density (kg/m^3)	1553.87	

C. Maximum Density data

MAXIMUM DENSITY DATA SHEET		
Sample number	1	2
Volume of mould (m^3)	0.00251	0.00234
Mass of empty mould (kg)	3.036	3.038
Mass of mould + sand (kg)	7.495	7.284
Mass of sand (kg)	4.459	4.246
Density (kg/m^3)	1776.494	1814.530
Average loosest density (kg/m^3)	1795.51	

D. Relative Density sample data

RELATIVE DENSITY DATA SHEET		
	LCE (15 blows)	HCE (30 blows)
Diameter of sample (mm)	51.47	51.28
Radius of sample (m)	0.03	0.03
Height of sample (m)	0.105	0.103
Volume of sample (m^3)	0.000218468	0.000212727
Mass of sand (kg)	0.36	0.36
Dry density of compacted soil	1669	1686
Maximum density (kg/m^3)	1796	1796
Minimum density (kg/m^3)	1554	1554
Relative density	0.51	0.58

E. Control test shear parameters

Control test							
LE	**HE**						
y=0.6062x+19.902	y=0.6289x+20.527						
					Cohesion	**Friction angle**	
EFFORT						**Radians**	**Degrees**
LE	x=	100	then y=	80.52	19.90	0.54	31.22
HE	x=	100	then y=	83.42	20.53	0.56	32.17

F. Flakes stiffness calculation data

STIFFNESS RATIO			
Confining pressure (kPa)	Concentration (%)	LCE	HCE
75	0.1	34.8	36.8
	0.25	31.9	33.8
	0.5	47.1	50.4
	0.75	33.2	35.5
	1.0	37.3	40.0
150	0.1	66.4	70.3
	0.25	59.6	63.1
	0.5	64.1	62.8
	0.75	39.1	41.4
	1.0	41.0	45.3
300	0.1	96.1	102.0
	0.25	89.7	96.3
	0.5	82.4	89.2
	0.75	61.8	65.2
	1.0	65.6	69.2

G. Pellets stiffness calculation data

STIFFNESS RATIO			
Confining pressure (kPa)	Concentration (%)	LCE	HCE
75	1	34.7	36.2
	2	36.9	39.0
	3	38.6	40.8
	5	38.7	43.3
	7.5	42.4	44.8
150	1	66.2	71.2
	2	56.7	56.7
	3	63.3	67.0
	5	62.2	62.8
	7.5	69.5	72.2
300	1	105.2	110.3
	2	103.1	104.3
	3	100.5	106.5
	5	94.8	101.9
	7.5	115.1	121.8